Guidebook for Rangitoto Island Field Trip, Auckland, 2017

In association with Geoscience Society of New Zealand Annual Conference (28 November−1 December), Auckland
Dynamic New Zealand, Dynamic Earth

Field Trip 3

Led by David Lowe and Peter de Lange

28 November 2017

Captions for cover and title pages:

Front cover: Distinctive profile of Rangitoto viewed across Rangitoto Channel from slopes of Mt Victoria/Takarunga, Devonport.

Title page: View southeastward from Rangitoto's summit over scoria cone (foreground) and a'a lavas and pohutukawa forest towards Islington Bay, just beyond which is southern tip of non-volcanic Motutapu Island. In the distance are Waiheke Island and, to the right, Moutihe Island (both non-volcanic) (photos by D.J. Lowe).

Dynamic New Zealand, Dynamic Earth: Auckland 2017

Annual Conference of the Geoscience Society of New Zealand

Field Trip 3

Tuesday, 28 November 2017

Rangitoto Island

Leaders: David J. Lowe[1] and Peter J. de Lange[2]
with contributions from Phil A.R. Shane[3] and Bruce D. Clarkson[4]

[1]School of Science (Earth Sciences), University of Waikato, Hamilton (david.lowe@waikato.ac.nz)
[2]Department of Natural Sciences, Unitec Institute of Technology, Auckland
[3]School of Environment, University of Auckland, Auckland
[4]Deputy Vice-Chancellor Research, University of Waikato, Hamilton

http://www.gsnz.org.nz/

***Bibliographic reference*:**
Lowe, D.J., Shane, P.A.R., de Lange, P.J., Clarkson, B.D. (2017). Rangitoto Island field trip, Auckland. In: Brook, M. (compiler). Fieldtrip Guides, Geosciences 2017 Conference, Auckland, New Zealand. *Geoscience Society of New Zealand Miscellaneous Publication* 147B, 56 pp.

ISBN: 978-0-9922634-3-0
ISSN (print): 2230-4487
ISSN (online): 2230-4495

Table of contents

Topic	*Page*
Introduction to Rangitoto Island	7
Field trip itinerary, hazard management, outline of guidebook	9
Part 1: Overview of volcanic and other features	11
Volcanic textures	11
Archaeology	14
Soils	15
Flora	16
Vegetation succession	17
Map of summit track route	20
Highlights along track	21
Part 2: Rangitoto volcano and eruption history	26
Using tephra and cryptotephra deposits	27
Rangitoto drilling project	30
Lithology of core	30
Petrography	30
Geochemistry	33
Radiocarbon dating	37
Volcanic history	38
Implications including volcanic risk	39
Part 3: A wider view − Auckland Volcanic Field (AVF)	40
Overview and brief basics	40
Map of volcanoes in AVF	41
Ages of volcanoes in AVF	42
Ar/Ar ages	42
Tephrostratigraphy	44
Palaeoclimatic and other studies involving lake sediments	50
Climate event stratigraphy	50
Acknowledgements	50
References	51

INTRODUCTION TO RANGITOTO ISLAND

Summary of key features of Auckland's largest and youngest volcano

Rangitoto Island is arguably Auckland's most beloved and omnipresent landscape feature. It is a symmetrical, ~6-km wide, basaltic shield volcano that last erupted c. 550–500 calendar/calibrated (cal.) yr BP (c. 1400–1450 AD), not long after arrival and settlement of Polynesians in the Auckland region (c. 1280 AD). It is by far the largest, and the youngest, volcano in the Auckland Volcanic Field (AVF). The AVF consists of ~53 individual eruptive centres, all of which lie within the boundaries of the Auckland urban area. Recent research on deposits in a 150-m-long drill core obtained from Rangitoto Island in February, 2014, and on cryptotephras in sediments from Lake Pupuke on North Shore and on tephras in wetlands on adjacent Motutapu Island, has revealed Rangitoto's complex history, with three main phases (1–3) suggested by Linnell et al. (2016) (but contended by Hayward 2017).

Phase 1: Activity may have commenced as early as c. 6000 cal. yr BP involving minor effusive and pyroclastic volcanism.

Phase 2: A voluminous shield-building phase occurred from c. 650–550 cal. yr BP (c. 1300–1400 AD), forming the main island edifice and erupting isotopically uniform subalkalic basalts (i.e., relatively high SiO_2 content ~50 wt%). Four batches of magma distinguished by trace-element chemistry were erupted sequentially; they lack genetic connection via fractional crystallization or assimilation. In two magmas, trace element abundances and ratios change with age, producing a pattern consistent with cycles of progressive partial melting at the source (Linnell et al. 2016).

Phase 3: The final phase of activity, from c. 550–500 cal. yr BP (c. 1400–1450 AD), was explosive and less voluminous, producing scoria cones at the summit. This phase generated more diversity in magma compositions, including more mafic subalkalic basalt, and alkalic basalt (i.e., relatively low SiO_2 content ~45 wt%), suggesting sourcing of magmas simultaneously from different depths in the mantle (Linnell et al. 2016).

Top of page: Classic profile of Rangitoto Island as seen from Devonport (photo by D.J. Lowe). *Above*: Google Earth image of Rangitoto showing its shield-like character and summit scoria cones, and part of the adjacent (non-volcanic) Motutapu Island. Rangitoto Wharf is on the south coast of Rangitoto Island (bottom of image).

Flora: The flora on Rangitoto is unique among the islands situated in the Hauraki Gulf because of the island's young age, and the fact that technically Rangitoto is an 'oceanic' island. Its flora and fauna are derived entirely from long distance dispersal. The island contains some 582 vascular plant taxa of which 228 (39%) are indigenous. Various other special ecological features, and studies on plant succession and their drivers, make the island a truly fascinating place to visit. At this time of year, we should see some pohutukawa (*Metrosideros excelsa*) and northern rata (*M. robusta*) trees in flower.

Left: Shaded track on lower slopes (photo by D.J. Lowe). *Right*: Pohutukawa flowers, McKenzie Bay (photo by P.J. de Lange).

Name: Rangitoto, Māori for 'blood red sky' (also 'lava, scoria': Ryan 2012), derives from the phrase Ngā Rangi-i-totongia-a Tama-te-kapua (the full name for the island) meaning "the day the blood of Tamatekapua was shed", referring to a battle between Tamatekapua and Hoturoa, commanders of the Arawa and Tainui canoes, respectively, at Islington Bay (Murdoch 1991; Hayward et al. 2011a).

History and tracks: Rangitoto was sold to the Crown by Māori owners in 1854 (for £15 according to Wikipedia) and it became a public domain in 1890 controlled by Devonport Borough Council. The first wharf and track to the summit were made in 1897. Prisoners from Mt Eden jail built the roads, most of the tracks, and the (disused) seawater swimming pool in the 1920s-30s (Wilcox 2007b). The island's distinctive baches (small holiday cottages) are described on p. 25. The island is a Department of Conservation (DOC)-administered reserve in partnership with local iwi and hapū (Tāmaki Collective) under the Ngā Mana Whenua o Tāmaki Makaurau Collective Redress Act (2014). The new wharf at Rangitoto was opened in 2014. It features a carved waharoa or gateway, known as Te Waharoa o Peretu (or the gateway of Peretu, spiritual ancestor of Rangitoto). The post on the left depicts Tangaroa (guardian of the sea); that on the right depicts Tāne Mahuta (guardian spirit of the forest). At the apex, the face looking towards the sea is that of a native parrot, the kākā. On the other side, another bird is sleeping. The two barge boards (maihi) end in kaitiaki, guardians of the gateway.

World War II: Rangitoto hosted military activities before and during World War II (1936-1945), including construction of the causeway between Rangitoto and Motutapu, Yankee Wharf, a fire command post and radar station at the summit, and a gun emplacement at Islington Bay (Wilcox 2007b). Motutapu was also transformed with an army camp in Administration Bay supporting up to c. 1000 personnel, counter-bombardment gun batteries and support including pillboxes and underground complexes, radar, searchlights, US Navy magazines, and engine room for anti-submarine defences (Dodd 2008).

Composition: Basalt lava, scoria, and ash. Broadly bimodal compositionally as noted above: 'high' (subalkalic) and 'low' (alkalic) SiO_2 contents. Further details are reported below.

Volume volcanic material: ~1.8 km^3 (about half the volume of magma erupted from the entire AVF).

Age: Multiple ages, summarised above and described in more detail below.

Hydrology: The island has no appreciable surface runoff of rainwater, even after heavy rain (mean annual rainfall in Auckland is around 1200 mm), with an estimated ~9% of that percolating down into the underyling basaltic deposits to replenish a lens-shaped groundwater aquifer at a depth of ~40-60 m (Merrill 1994; Wilcox 2007b). A bore along Islington Bay Road (drilled in 1977) provides freshwater to facilities at Rangitoto Wharf. A small spring-fed freshwater wetland occurs near the coast north of McKenzie Bay, the only one on the island (Wilcox 2007b).

Field trip itinerary, hazard management, and outline of guidebook

Itinerary and ferry sailing times

The trip is from ~8:45 am to ~4:00 pm, Tuesday, 28 November 2017. Meet at the Downtown Ferry Terminal building (99 Quay St), Auckland, **by 8.45 am**. The **Fullers Ferry will depart (from Pier 2) of the Ferry Terminal at 9.15 am.** Fullers recommend being ready to board about 20 min before sailing (gangway closes 2 min before sailing). The harbour trip from Auckland to Rangitoto takes ~25 minutes; we should be on the island by ~9.45 am. We aim to leave the summit by ~1.30 pm to return (via lava caves) to Rangitoto Wharf. The ferry departs the wharf at **3.30 pm** to return to Auckland (final sailing of the day) and so we should therefore be at Rangitoto Wharf **by ~3.15 pm**. Earlier ferry pick-ups at Rangitoto Wharf are at 12.45 pm and 2.30 pm.

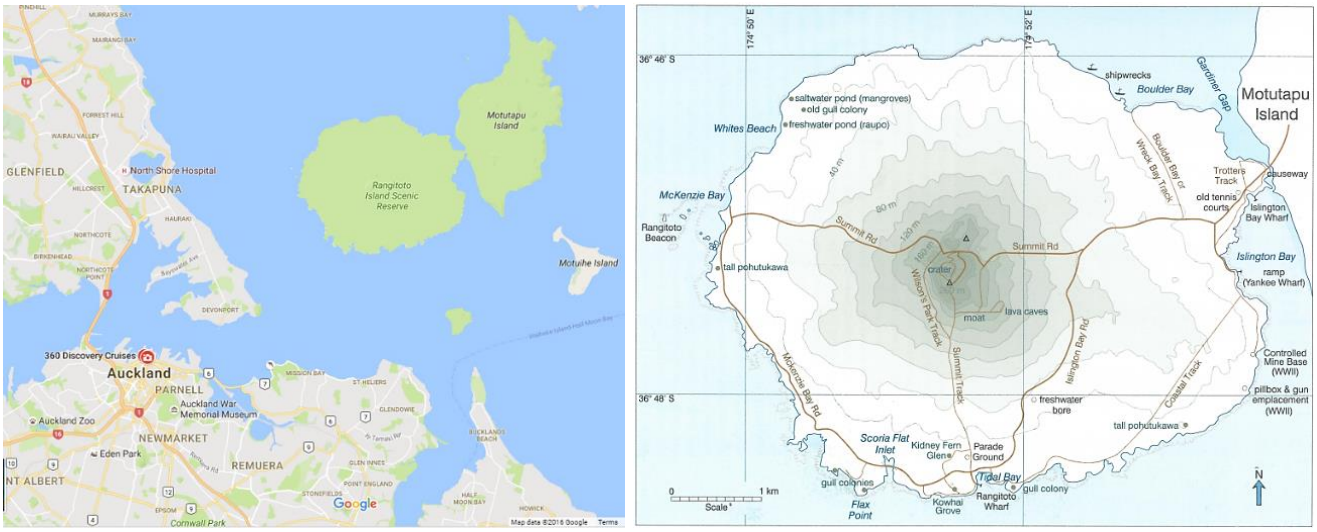

Left: Map of Downtown Auckland showing Ferry Terminal ('360 Discovery Cruises') and location of Rangitoto Island. *Right*: General geography of Rangitoto Island with Rangitoto Wharf (at Tidal Bay on south coast) and Summit track marked, the summit attaining a maximum elevation of 261 m (from Wilxox 2007a, p. 9).

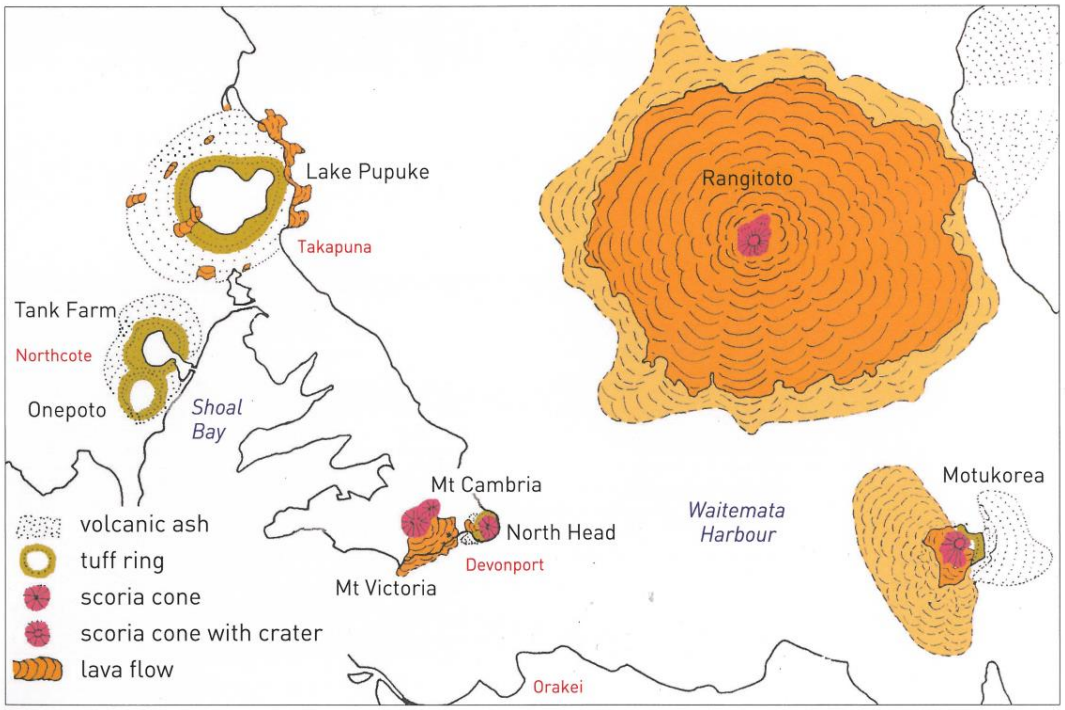

Rangitoto and other volcanoes of Waitemata Harbour and North Shore (land to the west of Rangitoto) (from Hayward et al. 2011a, p.100). Note submerged lava flows.

Hazard management: what to wear and bring, and track conditions

You must wear boots or strong trainers/shoes, a raincoat/windproof is essential, and you need to carry a warm jumper in your backpack in case of bad weather. Remember also that weather conditions can change quickly and so a sunny start to the day may not persist. Showers are always possible but, if sunny, a sun hat and sun block are mandatory. Consider also wearing a long-sleeved shirt. The summit walk is on generally easy, tracks (a bit rougher in places) and requires moderate fitness levels. At the coast the tracks are gentle but they steepen near the summit. Much of the track is sheltered. **Do not go off the track** at any time because the lava is often unstable, loose, with sharp and glassy angular material in many locations, which is dangerous to try to walk over. Be especially cautious on the steeper tracks descending from the summit where loose gravels can be unstable and 'slippery' underfoot. If we have rain, the basalt steps on the track can also become slippery. It is essential, especially if the weather is warm, that you bring plenty to drink to sustain you through the day. No food or water are available on the island. Some food items and drinks are available for purchase on the ferry if you need them.

We have an **optional side-visit** during the descent if conditions and time permit to visit a lava tube/cave with good 'ceiling' height and moderately easy access. **Hard hats** will be mandatory for any who wishes to enter the lava cave, and these will be available for participants to carry individually at the start of the trip (when we board the ferry). Leaders will carry a number of lamps/torches; we would recommend that **you bring your own torch** if you want to go into the lava cave.

Point of contact in Auckland: Dr Martin Brook: (09) 373 7599 Ext 88917 or mobile 021 232 1872
Local emergency agency: Police, fire, ambulance on 111

Outline of guidebook

Following a short introduction and summary, we have arranged the guidebook into three parts (see contents list p. 5). **Part 1** provides a summary of volcanic textures on Rangitoto together with notes about archaeology, soils, and flora (including vegetation succession). Then various geological features at stops along our route on the Summit track are noted in brief (with map). **Part 2** comprises a summary of the volcanic history of Rangitoto Island, including reference to the findings of the Rangitoto drill-core project, and recent work on tephra deposits on Motutapu Island and on tephras and cryptotephras in sediments of Lake Pupuke. Cryptotephras (from Greek *kryptein*, 'to hide'; *tephra*, ash or ashes) are tephra-derived glass shard (and/or crystal) concentrations preserved and 'hidden' in sediments but insufficiently numerous and too fine grained to be visible to the naked eye as a layer (Lowe 2011). **Part 3** takes a wider view by way of short introduction to the AVF, and includes mention of new Ar/Ar and palaeomagnetic dating and tephrostratigraphic work on the deposits in the field, and maar-based palaeoclimatic research.

Note about BP: Regarding ages designated in years (yr) BP, 'BP' represents 'before present', with 'present' being defined as 1950 AD in the radiocarbon (^{14}C) time-scale.

Left: Setting out on summit track near DOC centre, Rangitoto Island wharf, with slopes of volcano rising over lavas and (steeper) scoria cones in far distance at top left. *Right*: View from Tidal Bay (near wharf) towards North Head/Maungauiki and Mt Victoria/Takarunga, Devonport, with city visible beyond (photos by D.J. Lowe).

PART 1: OVERVIEW OF VOLCANIC TEXTURES ON RANGITOTO AND GEOLOGICAL AND VEGETATIONAL FEATURES ON SUMMIT TRACK

Volcanic textures

Rangitoto reveals many interesting volcanic textural features (Fig. 1), most evident alongside the summit track (Balance and Smith 1982; Lindsay et al. 2010). The gentle lower slopes are composed of many overlapping lava flows whose surfaces commonly show good **pahoehoe** textures near to their source (formed when a cooled skin of lava is wrinkled by movement of the lava underneath), and **a'a** textures at their distal (coastal) ends (Fig. 2). The a'a lavas tend to be rough, jagged and with either a **blocky** or a **rubbly/clinkery** surface, both formed essentially by continuous breaking and reworking of the cooled outer surface of a lava flow (Balance and Smith 1982). **Slab lavas/flows**, formed when a somewhat thicker hardened crust is broken by movement of the lava beneath, also occur on Rangitoto (Fig. 2). The a'a type of lava is by far the most common on Rangitoto.

Toward their distal ends, the margins of many flows are defined by prominent **levees** formed by accumulation of chilled lava at the margins of moving flows (Fig. 3).

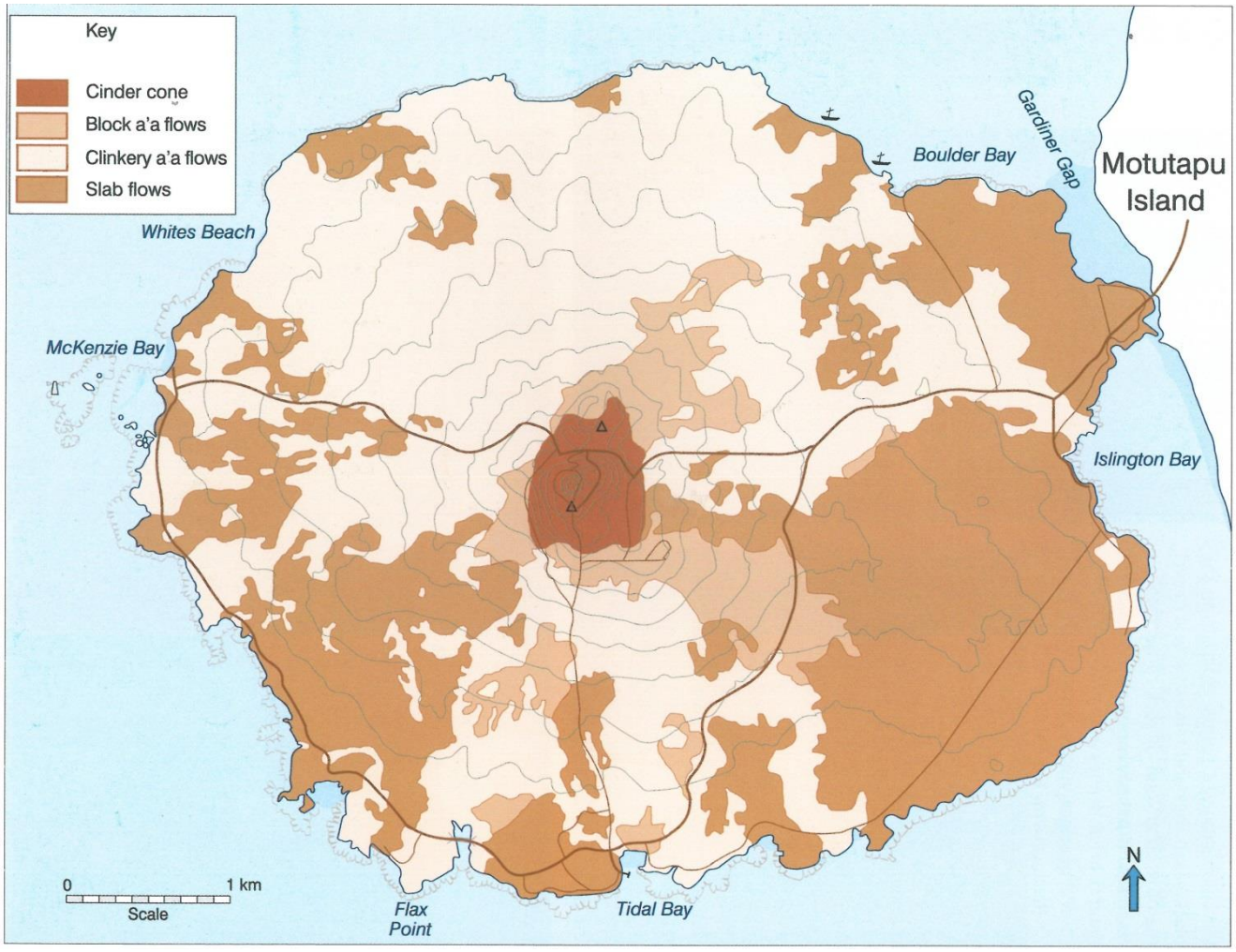

Figure 1. Map showing distribution of different surface textures of lava flows on Rangitoto (from Wilcox 2007b, p. 14). The summit 'cinder' cones are also referred to as scoria cones.

A small but well-developed system of **lava tunnels** linked by **lava trenches** occurs on the south-eastern flanks of Rangitoto Island close to the boundary between the summit **scoria cones** and the surrounding **lava field**. The tunnels formed after still-molten lava withdrew from a channel or 'tube' roofed by chilled lava; the trenches formed in places where the roof was too thin and collapsed as the lava withdrew, or where a roof did not form (e.g. Fig. 3; Hayward et al. 2011a).

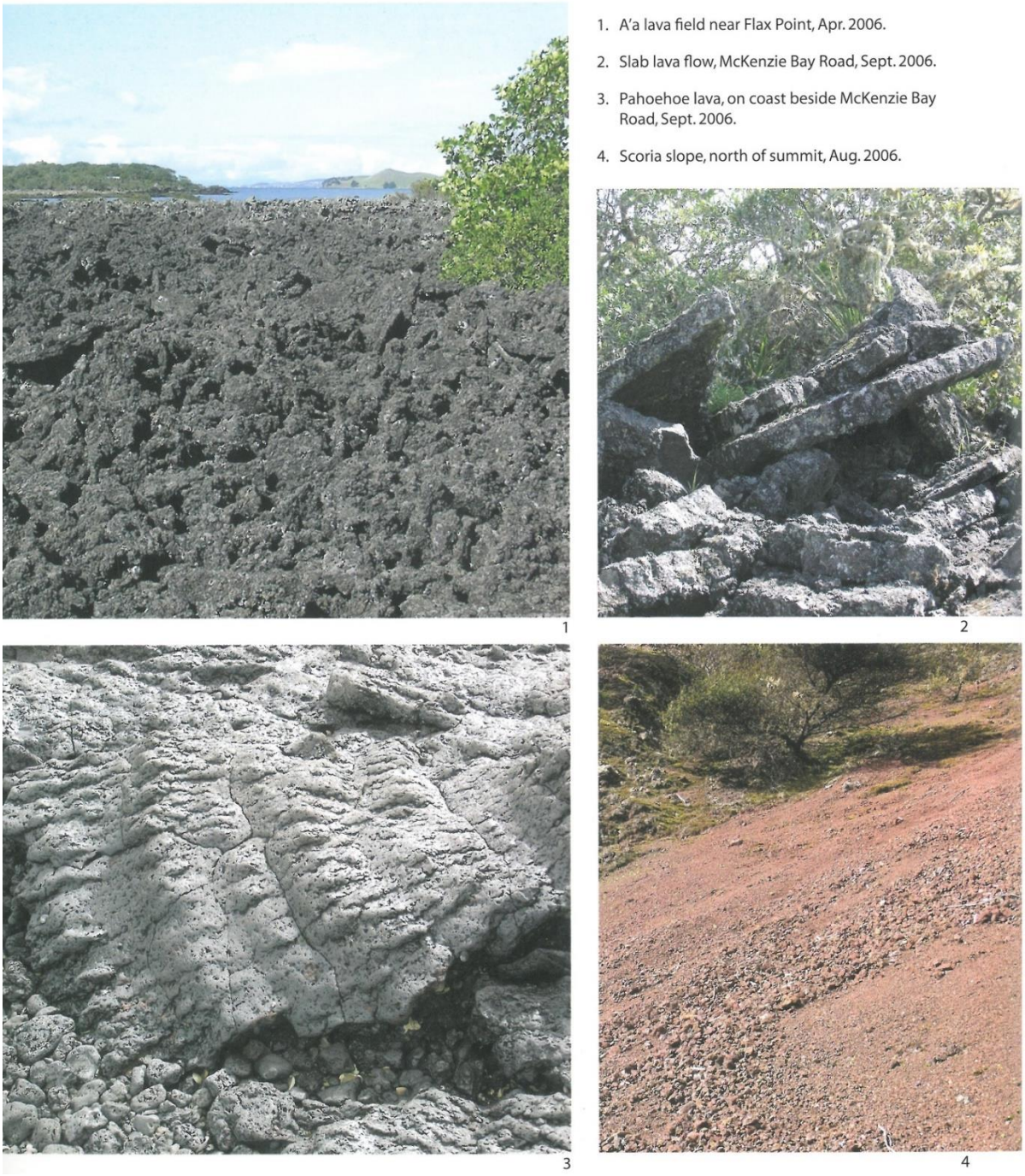

Figure 2. Examples of different surface textures of lava flows (1−3) and scoria (4) (from Wilcox 2007b, p. 12).

Figure 3. Example of rubbly a'a lava in depression or trench ~2−3 m deep flanked by marginal levees comprising heaped-up angular lava blocks formed by the accumulation of chilled lava at the margins of a moving flow. The trench occurs where molten lava inside a flow drained away leaving the collapsed rubbly and blocky roof behind (Balance and Smith 1982) (from Hayward et al. 2011a, p. 105).

The summit **scoria cones** (Fig. 4) rise from the "**moat**" at the top of the lava slopes. As visible from Auckland, the summit cones comprise multiple structures, with two outer cones (North and South) flanking the summit or Central cone and crater (the two outer cones comprise small cone complexes). Good exposures of **scoria** forming the summit area are seen on tracks on the north-eastern side; these formed by episodic **fire fountaining**. When fresh, the scoria is normally dark grey to black but reaction with water percolating through the hot porous scoria soon after the eruption has caused some of the clasts to turn a deep red because of oxidation of the iron in them (Lindsay et al. 2010).

Figure 4. *Top*: Rubbly a'a lava flow surface rucked up into curved ("festoon") ridges as the lava within the flow moved slowly downslope to right. *Left (upper)*: Aerial views of main Central cone (background) and North cone (foreground); (*lower*) summit crater in Central cone and observation platform (from Hayward et al. 2011a, p. 103).

Below: Weathering in a vesicular bomb near summit – the yellowish brown colouration is a hydrous alteration product ("gel-palagonite"), very likely a nanocrystalline variety of smectite(s) (Churchman and Lowe, 2012). Lens cap is 4 cm in diameter (photo by D.J. Lowe).

Archaeology: earliest Polynesian settlement and Māori presence and impact

Although no oral tradition has survived that describes the eruption and formation of Rangitoto (Nichol 1992; Lowe et al. 2002), it is clear that Māori (descendants of the initial Polynesian settlers) were living on adjacent Motutapu Island at the time. (Because it lacked 'garden' soils, Rangitoto was not used for general habitation, but was instead a resource area for fishing, collecting, and hunting, and its clefts and caves were used for burials: Bulmer 1994.) Ash from the latest eruption phases buried wood and shell of a habitation site, Sunde, in Administration Bay on Motutapu (see Fig. 18 below). Excavations at Sunde revealed casts of Māori dog (kurī) and human footprints in the ash (photo at right is from Nichol 1982), together with evidence for gardening activities (Scott 1970; Davidson 1978a; Nichol 1981, 1982; Bulmer 1994; Dodd 2008). Ash at the site has been correlated via glass-shard major element composition with the tephra designated 'Rangitoto 1' (553 ± 7 cal. yr BP) (Needham et al. 2011). This correlation indicates that the latest explosive eruption phases (2) and (3) of Rangitoto were witnessed by early Māori, whose exploitation of local stone and other materials for tool manufacture (e.g. greywacke adzes, chert/jasper hammerstones, bone fishhooks) (Davidson 1978a, 1978b), and then gardening, must have had an impact in the region from at least that time (Lowe et al. 2000).

The timing of earliest Polynesian settlement of New Zealand has been controversial, partly because it has been so recent (Lowe 2011). Radiocarbon age data, potentially questionable because of likely contamination in lake sediments by in-washing of old carbon as a result of Polynesian deforestation, inbuilt age, or dietary effects, effectively resulted in two contradictory models of settlement: 'early' settlement ~1500–2000 years ago (Sutton 1987) versus 'late' settlement ~700 years ago (Anderson 1991, 2013, 2015a). The rhyolitic Kaharoa tephra, erupted ~700 years ago from Mt Tarawera in winter, 1314 ± 12 AD (Hogg et al. 2003; Sahetapy-Engel et al. 2014), is present in Lake Pupuke as a cryptotephra (Newnham et al. 2017). It provides a 'settlement datum' (isochron) in northern New Zealand to help determine which model was correct by tephrochronologically linking and dating palynological (pollen) evidence of initial human impact (derived from analyses of cores from peats and lakes) with archaeological and artefactual evidence to the same point in time (Newnham et al. 1998a; Lowe 2011). No cultural remains are known to occur beneath the Kaharoa except one rat-nibbled seed on Coromandel Peninsula (Wilmshurst and Higham 2004). Palynological evidence for earliest human-induced impact, a sustained deforestation signal comprising a decline in tall trees and a concomitant rise in bracken spores, occurs stratigraphically just before Kaharoa deposition in five pollen profiles at 24 documented sites (Newnham et al. 1998a; Lowe 2011). The use of the Kaharoa isochron, together with evidence from lake- and bog-derived pollen records, bones of the commensal Pacific rat *Rattus exulans*, rat-nibbled seed cases and snail-shells, fire records, ancient DNA, and archaeological and ^{14}C data, all support the 'late' settlement model (Lowe and Pittari 2014). The rat-nibbled seed beneath Kaharoa tephra and the sustained rise in bracken spores starting just below the tephra in pollen profiles are both consistent with earliest settlement in northern and eastern North Island a few decades prior to the c. 1314 AD eruption of Kaharoa (Lowe et al. 2000; Lowe and Pittari 2014) (cf. Jacomb et al. 2014). Earliest Polynesian settlement is now dated at c. 1280 AD (Higham and Hogg 1997; Higham et al. 1999; McGlone and Wilmshurst 1999; Wilmshurst et al. 2008, 2011, 2014; Anderson 2013, 2015a).

Rapid transformation of the landscape, principally by fire, occurred within a few decades of the first human arrivals, with extensive forest being replaced by scrub especially in drier eastern and southern parts of New Zealand (McWethy et al. 2010; Perry et al. 2012, 2014). However, new pollen analyses from Lake Pupuke show an early phase ('step 1') of minor, localised forest clearance around the time of Kaharoa tephra followed by a later, more extensive deforestation phase ('step 2') commencing at around the time of deposition of the two youngest Rangitoto tephras (c. 1400–1450 AD) (Newnham et al. 2017). This pattern is consistent with early Māori settlement patterns and landuse practice (Anderson 2015b, 2016), and concurs with an emerging hypothesis that the Little Ice Age had an impact on pre-European Māori with the onset of harsher conditions causing a consolidation of populations and later environmental impact in northern New Zealand (Newnham et al. 1998b, 2017).

Soils on Rangitoto and Motutapu

The youthfulness of the latest eruptives on Rangitoto Island, and of the ash fallout deposits on adjacent Motutapu and Rakino islands, means that the soils are only weakly developed recent soils at best. Bare lavas are effectively 'nonsoils'.

Rangitoto Island

The soils may be mapped into two groups (1) on lavas, and (2) on the scoria cones. The bare-rock lavas are 'nonsoils' in *Soil Taxonomy* (Soil Survey Staff 2014), and Rocky Raw Soils in *New Zealand Soil Classification* (Hewitt 2010). Sand-sized fragments of rock and partly-decomposed litter can occur in cracks and crevices in the lava. If these sand and organic materials are $\geq$ 5 cm in thickness then such small patches of soil are Lithic Udorthents (= sandy Entisols) or Lithic Udifolists (= shallow organic soil or Histosols) (*ST*), or Rocky Recent Soils (*NZSC*). On the scoria, the soils may qualify as Vitrandic Udorthents (*ST*), or as Typic Tephric Recent Soils (*NZSC*) provided A horizons (including, if present, partly decomposed litter horizons designated F, H) are $\geq$ 5 cm in thickness (Fig. 5).

Motutapu Island

The ash mantle on much of Motutapu Island, generally <1 m in thickness (but reportedly up to ~ 2 m in thickness: Hayward et al. 2011a), provided a new material in which soil could form over the past 500–600 years (Fig. 6). The ash buried a pre-existing soil (Ultisol in *ST*, Ultic Soil in *NZSC*, meaning strongly weathered, clayey, slowly permeable, acid soils) on Tertiary sandstones and mudstones (flysch) (Kermode 1992). The modern soil although fertile is coarse grained (sandy) and has a low water-holding capacity. Where the ash mantle is >50 cm thick, the soil is either a Typic Udorthent or a Vitrandic Udorthent (both being Entisols) in *ST*; where the ash is <50 cm thick, the paleosol is 'recognised' and the soil is possibly an Aquandic Palehumult (needs certain properties). In *NZSC*, the soil is a Tephric Sandy Recent Soil. Away from the ash mantle, the soils on Motutapu on stable landscapes are likely to be mainly Ultisols in *ST*, Ultic Soils in *NZSC*.

Figure 5. *Left:* Section of scoria near the summit and (*right*) associated soil profile of Rangitoto gravelly sand (pocket knife at top for scale). *Far right:* Weak soil profile developed in red (oxidised) scoria (lens cap 4 cm in diameter) (photos by D.J. Lowe).

Figure 6. Soil profile of Rangitoto sandy loam formed on Rangitoto ash (approximately 70 cm in thickness) over a buried, coarse-structured Ultisol/Ultic Soil with pale enleached E horizon on Motutapu Island (scale in inches; photo by H.S. Gibbs).

Flora of Rangitoto

The flora on Rangitoto is unique among the islands situated in the Hauraki Gulf because of the island's young age, and the fact that technically Rangitoto is an 'oceanic' island. This means that as Rangitoto emerged from the sea, and was never connected to the mainland of New Zealand, its flora and fauna are derived entirely from long distance dispersal – an oddity indeed for an island which sits on a continental shelf in such shallow water. The island is home to some 582 vascular plant taxa of which 228 (39%) are indigenous (Wilcox et al. 2007). Although there are no endemic vascular plants, the island is a stronghold for a number of plants that are now 'threatened' or 'at risk', or both, on the adjacent mainland, e.g. the white-flowered kohuorangi or Kirk's tree daisy (*Brachyglottis kirkii* var. *kirkii*), poroporo (*Solanum aviculare* var. *aviculare*), wild carrot (*Daucus glochidiatus*), and plumed greenhood (*Pterostylis tasmanica*) (de Lange et al. 2013). Kirk's tree daisy is declining on the mainland because of possum browse, and the same was happening on Rangitoto until possum and wallabies were eradicated from the island in 1996. Aside from flowering plants, conifers, ferns and clubmosses, Rangitoto is also home to 94 mosses (three naturalised) and 70 hornworts and liverworts (one, *Lunularia cruciata*, is naturalised). Although the mycobiota of the island have yet to be properly studied, 194 lichens (lichenized fungi) have been recorded from the island together with ~170 fungi. The island is the type locality for a number of mosses and liverworts, several of which were long believed endemic to the island, e.g. *Lepidozia elobata*, *Plagiochila bazzanioides*, and *Tortella cirrhata* subsp. *Mooreae*. The occurrence of endemic mosses and liverworts on an island with a flora believed to be c. 600–700 years old or less was always considered anomalous, and it is not a surprise that all of these 'endemics' have since been discovered elsewhere in New Zealand, although, oddly, in the case of some, such as the *Plagiochila*, not so far from the adjacent mainland.

Ecologically what marks Rangitoto is the dominance of pohutukawa (*Metrosideros excelsa*). Rangitoto supports the single largest tract of this forest association in New Zealand, which provides insight into the role that this species has played in the colonisation of bare lava (Fig. 7; see also photo on title page). This is a key process repeated by the genus *Metrosideros* throughout the Pacific where its species all play a critical role in converting bare lava to forest (see next section). On our visit, though, note the dominance of lichens, mosses and at times liverworts, all of which play an important role in converting lava to 'soil' thereby allowing other plants to become established.

Figure 7. Pohutukawa forest growing on a'a lava on Rangitoto. Photo by D.J. Lowe (17 August 2014).

Several other botanical features of Rangitoto are worth noting, namely the occurrence of many vascular plant epiphytes in terrestrial settings, for example Kirk's tree daisy and northern rata, *M. robusta* (Fig. 8), the porous lava providing them with the same conditions found in forest canopies.

Figure 8. *Left*: Flowering northern rata, McKenzie Bay (*M. robusta*). *Right*: Myrtle rust (*Austropuccinia psidii*) is an aggressive fungal disease that has spread across the world from its indigenous haunt in the Amazon Basin. Myrtle rust arrived in New Zealand in May 2017 from Australia. So far its impacts have been minor but it is suspected it could spread rapidly now that winter has passed. **If you see any yellow powder** on the leaves of pohutukawa, rata, manuka (*Leptospermum scoparium*), or rawirinui (*Kunzea robusta*) on the island, **do not touch it**! Please inform the trip leader immediately. Photos by P.J. de Lange.

Also present on Rangitoto are 'weed' species, many of which derive from the distinctive holiday cottages/baches on the island (predating c. 1940). Some of these weed species are components of the Macronesian flora of the Canary Islands, brought to New Zealand as ornamentals and, finding Rangitoto offering a range of habitats similar to those of their distant volcanic home, they have flourished. Whilst most are aggressive weeds, some (such as the species of the genus *Aeonium* and *Echium*) are actually threatened plants in their distant home, and hence present a 'slight' conservation management dilemma. A final matter of botanical interest is the abundance of hybrids between pohutukawa and northern rata (*M. excelsa* × *M. robusta*), a hybrid combination that is less commonly seen on the adjacent mainland.

Now that Rangitoto and nearby Motutapu Island are 'pest-free', both islands afford innumerable opportunities for the restoration of flora and fauna now extirpated or threatened in the wider Hauraki Gulf region. As such, the island has been subjected to a number of indigenous fauna introductions, and a range of plants have also been trialled, including the 'threatened' scurvy grass *Lepidium flexicaule*, last seen on the island in 1906. While this is all good news, the recent arrival of myrtle rust (*Austropuccinia psidii*) (Fig. 8) to New Zealand leaves the future of the *Metrosideros*-dominated forest of Rangitoto Island uncertain. Based on the impact this rust has had on the Raoul Island *M. kermadecensis* forest, there is a very real fear that the pohutukawa forest may be seriously damaged with dire consequences for the island's vegetation succession and indigenous biodiversity.

Pattern and process of vegetation change (succession) on Rangitoto

Using a combination of the chronosequence and direct monitoring methodologies, the pattern and process of vegetation change (succession) across both young volcanic landscapes and long-inactive volcanoes has been much studied (e.g. Clarkson 1990; Walker et al. 2010; Clarkson et al. 2015). As noted above, pohutukawa *(M. excelsa*) is the prime lava colonizer and has coalesced to form continuous forest over large areas of the island (Haines et al. 2007). Clarkson and others have been monitoring *M. excelsa* patch establishment and development between 1980 and the present day on Rangitoto Island. These plots were selected as representative of the most extreme sites of largely un-vegetated a'a lava. The number of vascular species is strongly positively correlated with the size of the *M. excelsa* patch or clump (R^2 = 0.742; n = 80) with 1–4 species recorded in patches of 0.1 m^2 and 16–19 species in patches of 100 m^2 (Fig. 9).

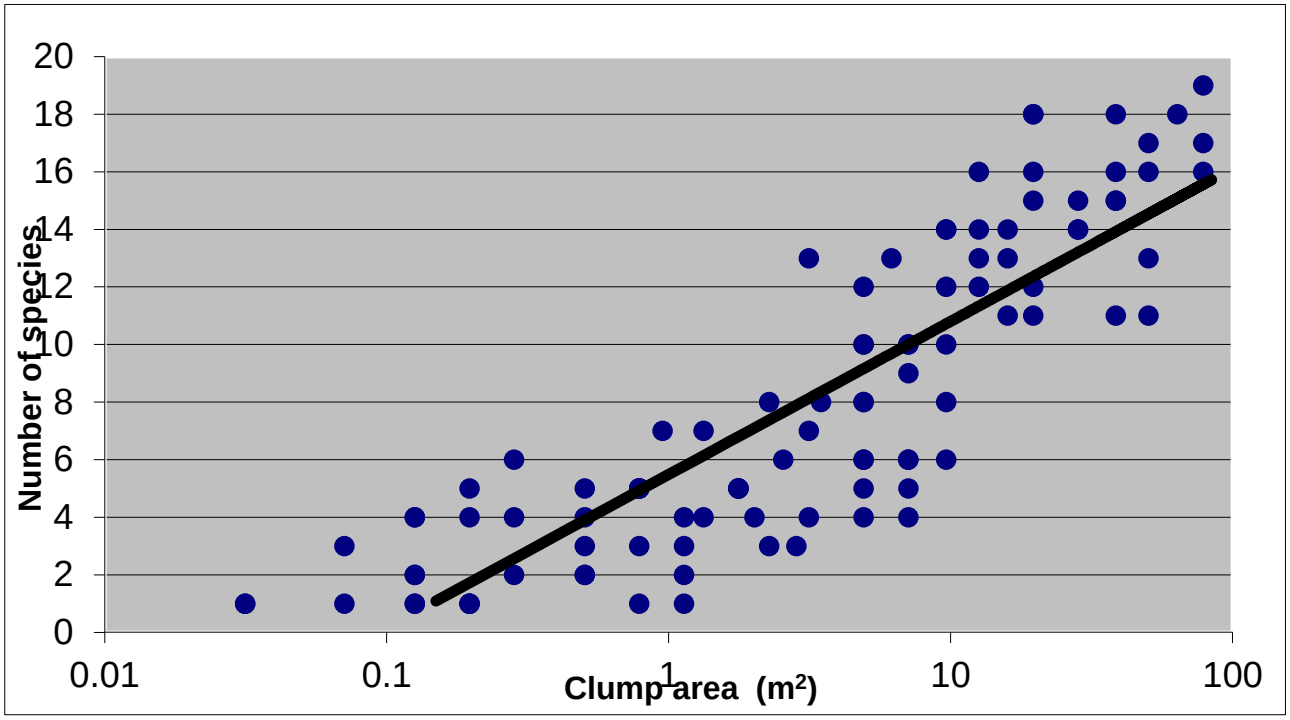

Figure 9. Relationship between numbers of vascular species and size of pohutukawa (*Metrosideros excelsa*) patch on Rangitoto (y = 2.3101 Ln(x) + 5.4827).

Using patch (clump) size in six size classes (midpoints = 1 m^2, 3 m^2, 6 m^2, 12 m^2, 24 m^2, 48 m^2) and frequency of occurrence as a surrogate for age, it is possible to determine the orderly sequential establishment of species (Fig. 10) (Clarkson et al. 2015).

Early establishers (in association with *M. excelsa*) include *Coprosma robusta*, *Myrsine australis* and *Astelia banksii* (Fig. 10A). Middle and late establishers include *Pseudopanax arboreus*, *Astelia hastata* and *Asplenium oblongifolium*. The fern, *Asplenium flaccidum*, which is mostly epiphytic on *M. excelsa*, is one of the last to arrive (Fig. 10B).

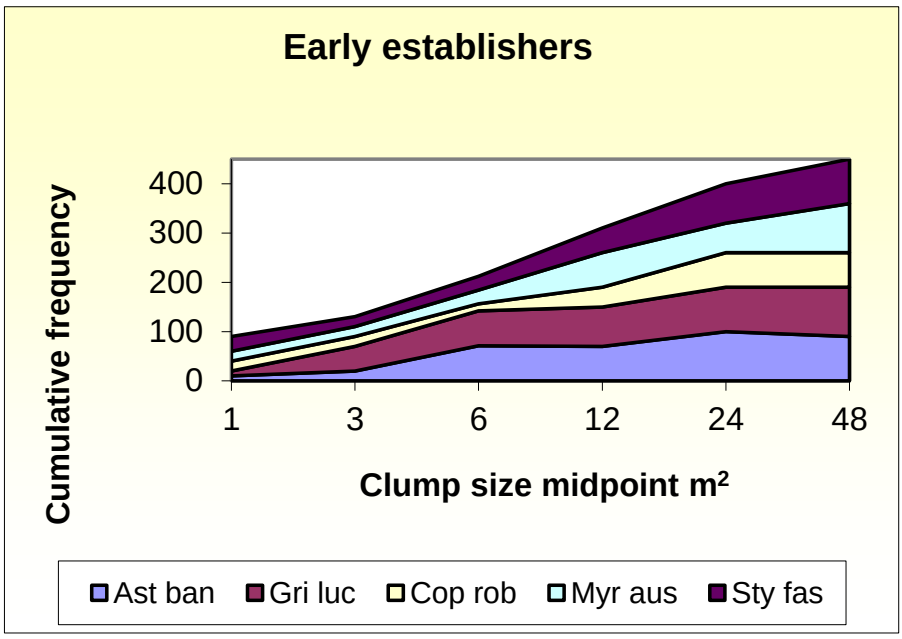

A.

Key

Ast ban: *Astelia banksii*
Gri luc: *Griselinia lucida*
Cop rob: *Coprosma robusta*
Myr aus: *Myrsine australis*
Sty fas: *Leucopogon fasciculatus*

Figure 10A. Use of clump/patch size and frequency of occurrence as surrogates for relative age to determine early establishers.

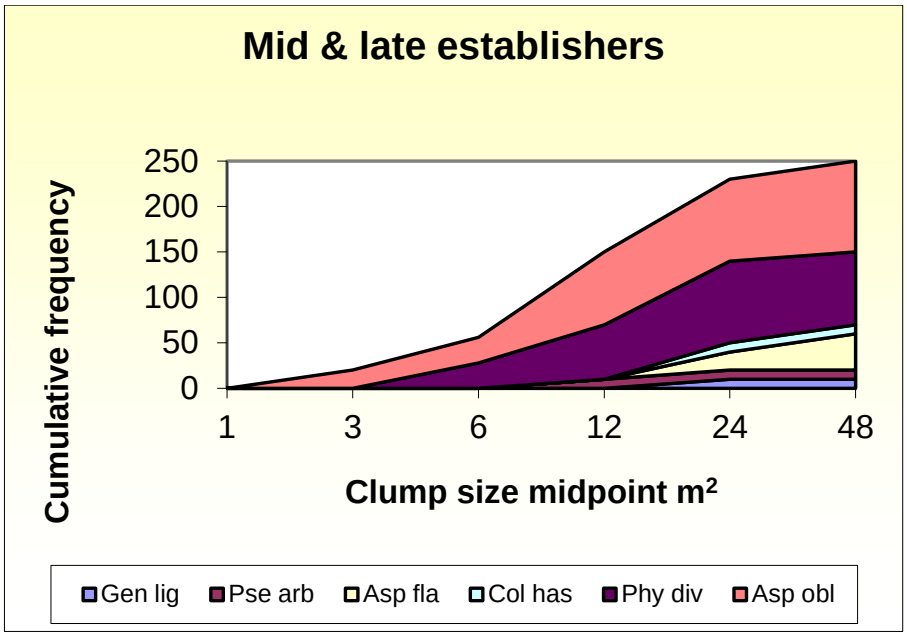

B.

Key

Gen lig: *Geniostoma ligustrifolium*
Pse arb: *Pseudopanax arboreus*
Asp fla: *Asplenium flaccidum*
Col has: *Astelia hastata*
Phy div: *Microsorum pustulatum*
Asp obl: *Asplenium oblongifolium*

Figure 10B. Use of clump/patch size and frequency of occurrence as surrogates for relative age to determine middle and late establishers.

Some species fluctuate in their frequency in relation to patch size, for example, *Brachyglottis kirkii*, *Notogrammitis heterophylla*, and *Asplenium flabellifolium* (Fig. 10C). These are usually patch edge dwellers and are sometimes lost as the *Metrosideros excelsa* canopy expands but may subsequently recolonise the edge of the patch.

Pohutukawa *(M. excelsa*) facilitates this deterministic establishment pattern by influencing the microclimate and light regime of the site. For example, the surface temperature on open lava may exceed 50 °C whereas in the interior of a large patch or extensive forest, it is less than 25 °C. Relative humidity is less than 40% on open lava, exceeds 45% in large patches, and is over 55% in the forest interior (Clarkson et al. 2015).

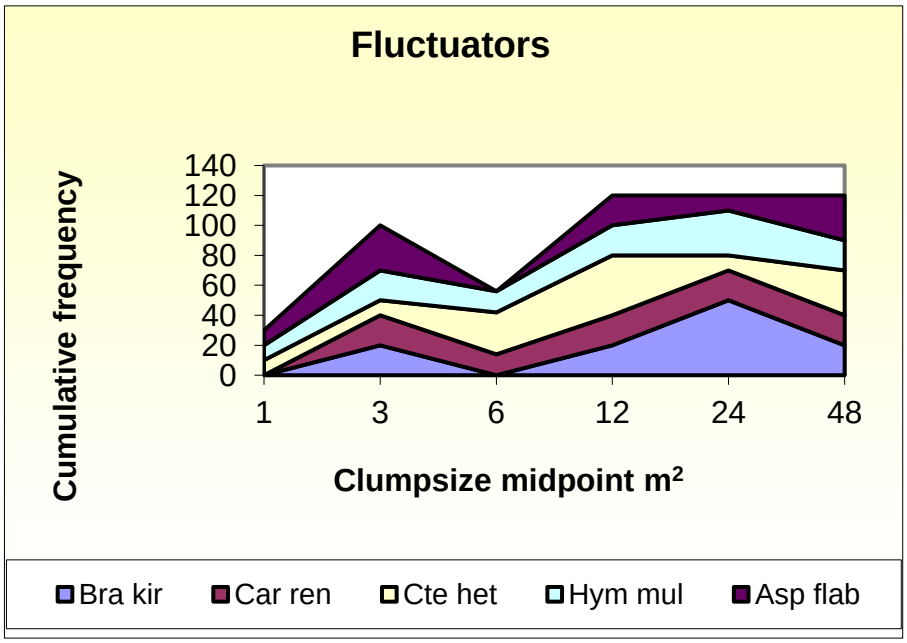

C.

Key

Bra kir: *Brachyglottis kirkii*
Car ren: *Cardiomanes reniforme*
Cte het: *Notogrammitis heterophylla*
Hym mul: *Hymenophyllum multifidum*
Asp flab: *Asplenium flabellifolium*

Figure 10C. Use of clump/patch size and frequency of occurrence as surrogates for relative age to show some species fluctuate in frequency in relation to patch/clump size.

Summary of volcanic features viewable during ascent of Rangitoto via Summit track
(various vegetational features will also be described at appropriate stops)

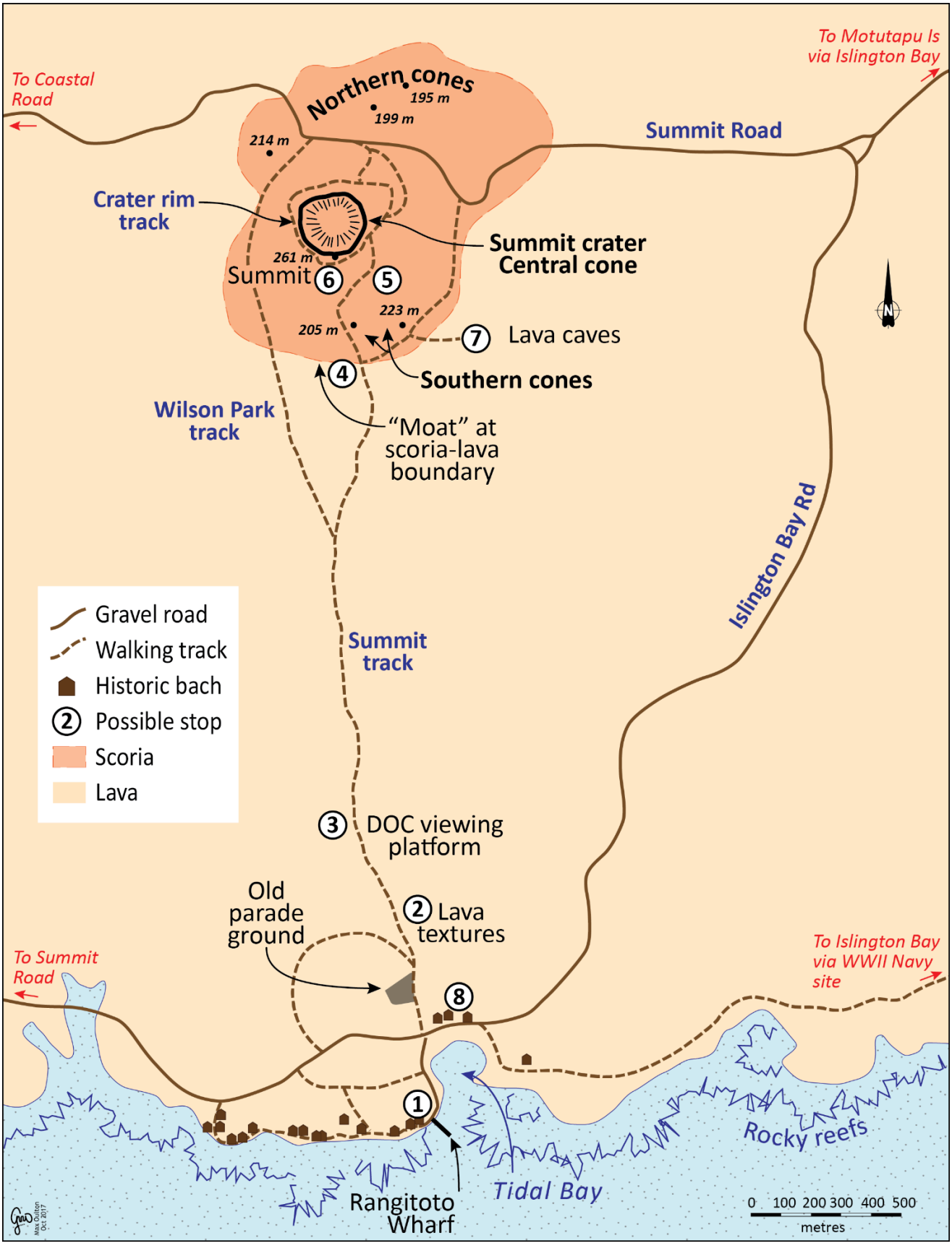

Figure 11. Map showing volcanological and other features including summit cones and lava flows of the southern part of Rangitoto Island, and the route we will take to the summit via Summit track (mainly after Balance and Smith 1982; Lindsay et al. 2010). Possible stopping points are indicated. See also Fig. 15 below.

Some highlights of walk along Summit track (numbers relate to stops marked on Fig. 11).

1. Rangitoto Wharf and information shelter (toilets available)

The ferry arrives at Rangitoto Wharf on the southern coast of Rangitoto Island and at the periphery of the Rangitoto lava field. We may see lava lobes near the wharf if the tide is out. We will start with a briefing and short introductions near the information shelter:

***David Lowe**: volcanic, soil, and archaeological perspectives*
***Peter de Lange**: vegetation perspective*

At low tide, smooth, wrinkly, curved **lava lobes** as described by Hayward (2012) are evident near the wharf. Each lobe is 0.5−1 m across and 3−10 m long, usually curved as it flowed down the steepest gradient (Fig. 12). The lobes have a 0.1−0.2 m wide zone of laminated to flow-banded, more-glassy basalt on either side, whereas interiors may contain ropey styles similar to those on the surface of classic pahoehoe flows (Hayward 2012). The pillow-lava-like lobes are miniature versions of larger lava lobes that flowed into the sea in several other places (Fig. 12). Hayward (2012) suggested that the branching lobate bird's-foot-like form arose possibly as the lavas flowed into water. Cold water may have cooled and stopped the flow at the terminus of each lobe causing the molten lava still inside the lobe to break out as another branch further back up the lobe.

Erosion on the sheltered western and southern shorelines has been minimal, but on the exposed northern coastline, however, the average rate of erosion has been estimated at ~3−6 m per century (Daymond-King and Hayward 2015). This relatively fast rate is partly a result of the wave action efficacy being enhanced by the presence of cooling joints and fractures in the hard lava at irregular spacings of ~0.1−1 m, and partly because loosely cemented breccias of basalt rubble within and between flows provide an easy pathway for wave action to remove such material. Together these attributes allow intertidal crevices, caves, and overhangs to be generated (Fig. 12, bottom right).

Figure 12. *Upper*: Lava flow lobes and other surface features near Rangitoto Wharf, with closer view of small curved lava lobe at right. *Bottom left:* Extensive branching lava flow lobes on southwest margin of Rangitoto Island. *Bottom right*: Caves and arches on the eroding northern coastline. Photos from Hayward (2012, pp. 11-12) and Daymond-King and Hayward (2015, pp. 5-6).

2. A'a lava flows *Brief discussion of the Rangitoto lava field and of lava flow textures*.

As we walk towards the summit we will see the features and textures of the Rangitoto lava field, and some of the key vegetational features of the island. ***Please stay on the track at all times***. Near the source of lava effusion (at the base of the scoria cones near the summit) the lava field is quite thick, up to 50 m, whereas at the coast it is considerably thinner, less than 20 m in thickness (although individual flows themselves are no more than 5 m thick) (Lindsay et al. 2010). The majority of the lava field is comprised of blocky and clinkery (rubbly) a'a lava flows (Fig. 13), with rarer occurrences of smooth, ropey pahoehoe lava flows along the main track to the summit and along coastal areas, e.g. near Islington Bay and the Rangitoto Wharf.

During eruption, the a'a flow tops transported brecciated, broken lava blocks downslope, which sit atop a more massive flow core (Figs. 2, 4, 13). The blocks form at the leading edge of a flow due to instantaneous cooling with the air or water. Blocks generally tumble down the steep flow fronts and are either 'bulldozed' or buried by the advancing flow. Rocks on the outside of the flow tend to be highly vesicular and glassy, whilst those from the flow interior tend to be more massive and crystalline.

Figure 13. Blocky a'a lavas as seen on the lower summit track (photos by D.J. Lowe).

3. DOC information point/lookout *This viewing platform is on the boardwalk, on the left (west) side of the main track, as we ascend. It provides a good opportunity to discuss the structure of the lava field and view to summit, and also a viewpoint southwest towards Auckland city (Fig. 14).*

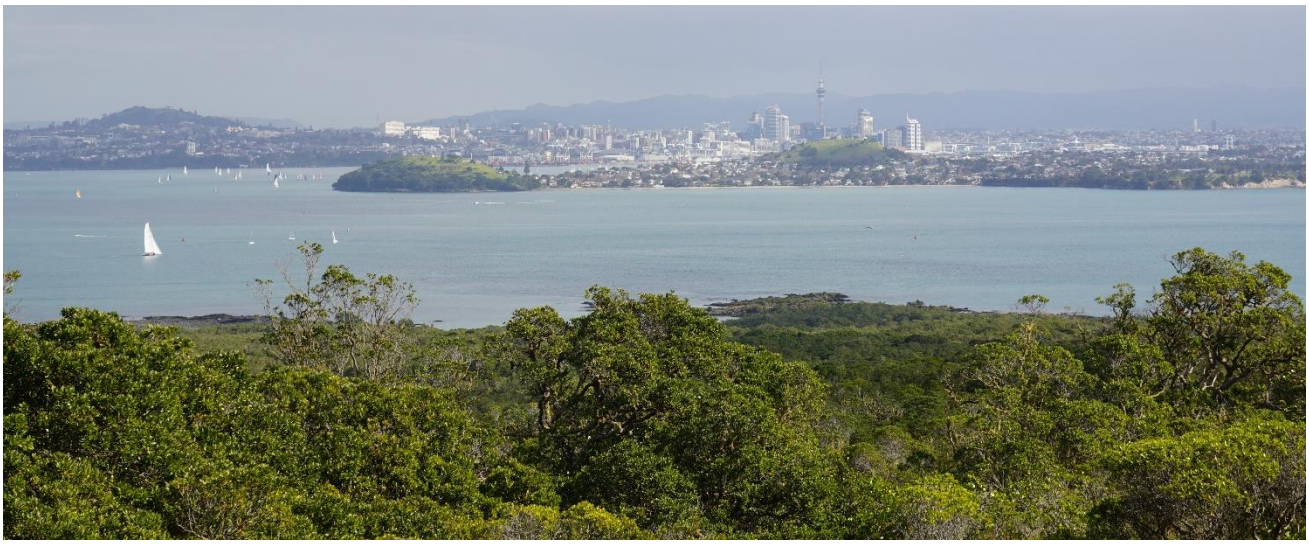

Figure 14. View from DOC lookout towards Devonport on North Shore and Auckland city (photo by D.J. Lowe).

4. Moat between lava field and summit scoria cones *Pause to discuss the two eruptive styles of Rangitoto.*

At an elevation of ~150 m, the southern and eastern flanks of the volcano are dominated by an unusual moat-like structure, which defines the boundary between the lower lava-covered slopes and the scoria crown. It likely formed as a result of a subsidence event following the release of significant volumes of lava from fissures on the upper flanks (Balance and Smith 1982; Lindsay et al. 2010).

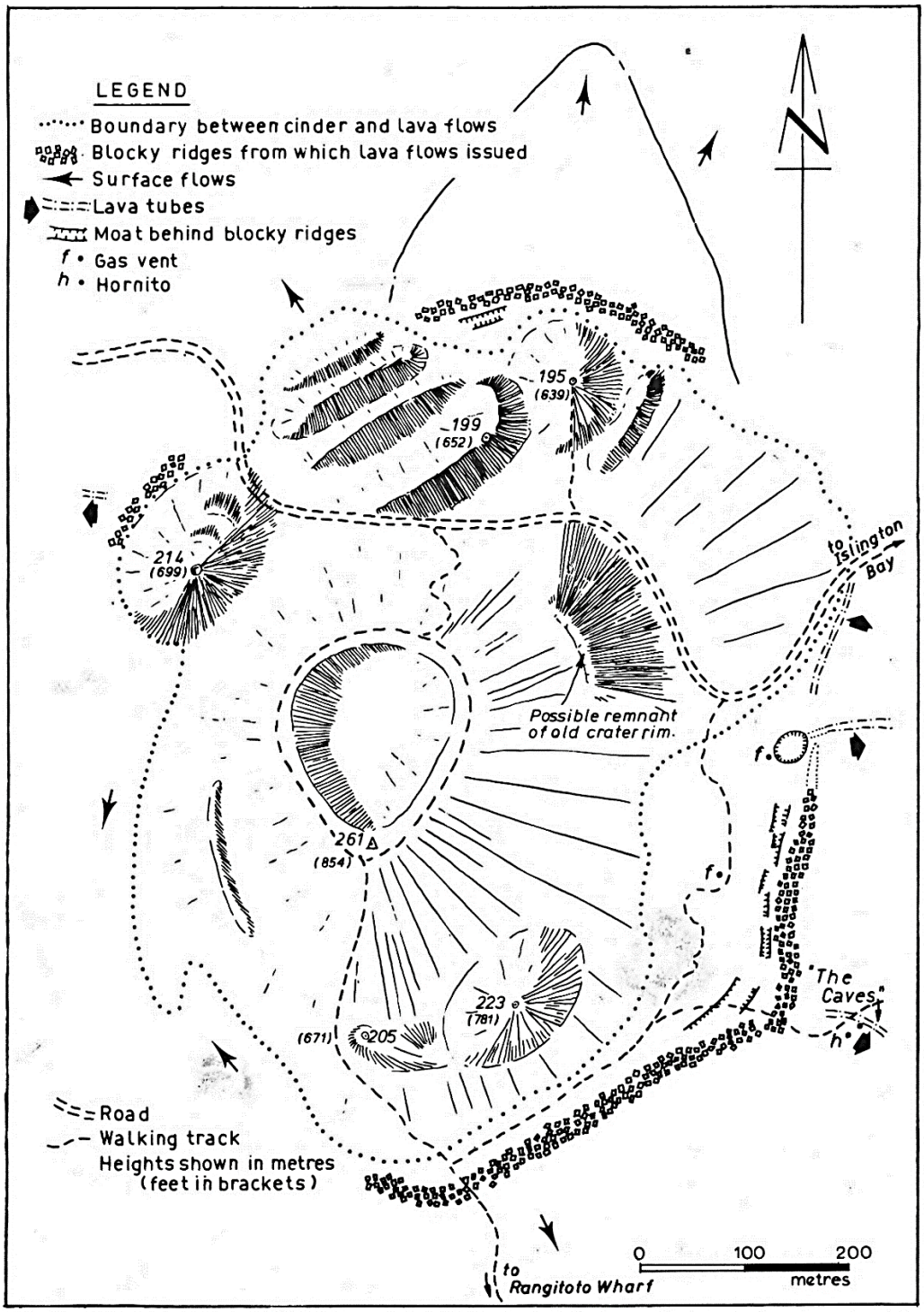

Figure 15. Sketch map of volcanological and pyroclastic features associated with the summit scoria cones. The Central cone (including summit crater, 261 m asl) occupies the main part of the diagram, and is flanked to the north by cones (marked 214, 199, 195 m) collectively referred to as North cone, and to the south by cones (marked 205 and 223 m) that make up the so-called South cone (see Fig. 16) (map from Balance and Smith, p. 11). Central and South cones are subalkalic basalt (typically ~48–50 wt% SiO_2), North cone alkalic basalt (~45–47 wt% SiO_2) in composition (McGee et al. 2011; Needham et al. 2011; Linnell et al. 2016).

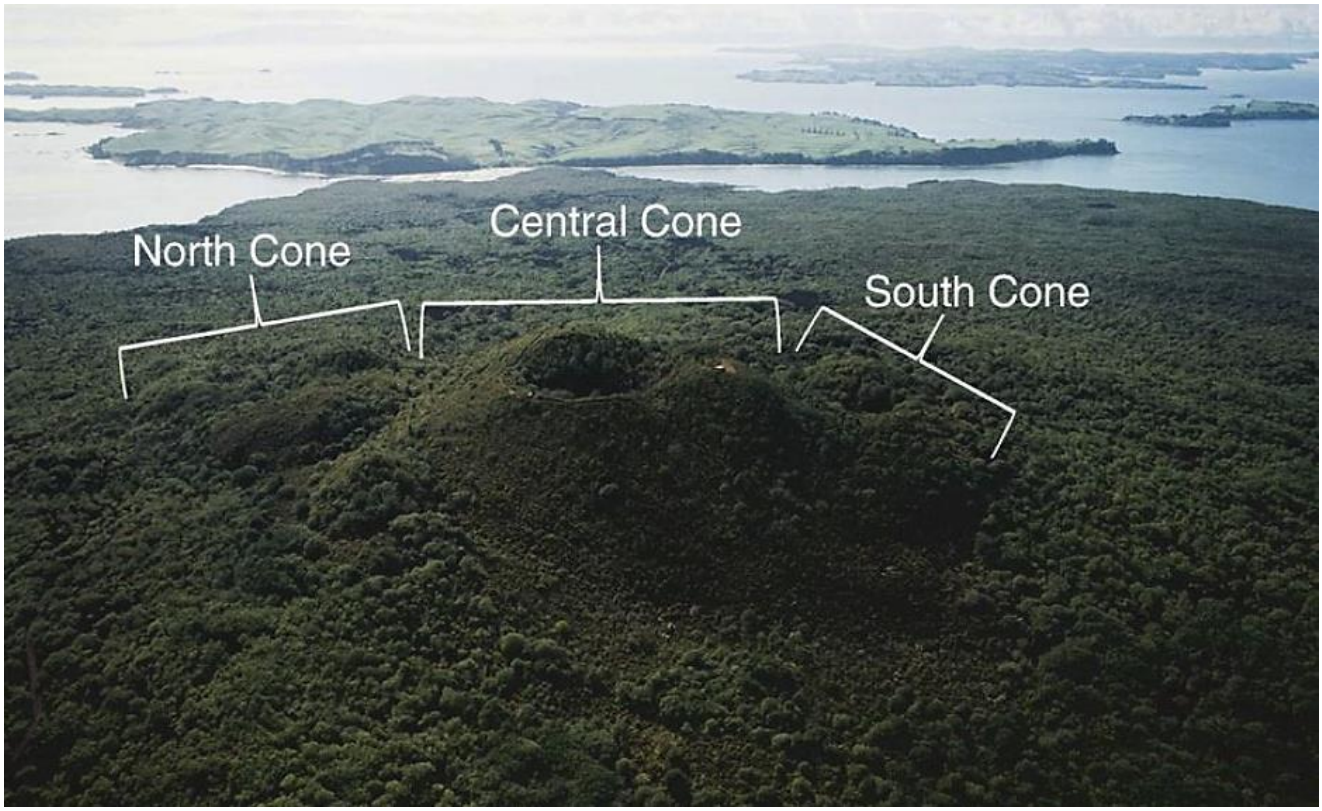

Figure 16. The summit area of Rangitoto (viewed looking ENE), with main cones labelled forming the 'summit scoria cones'. Structure of summit observation deck is just visible on rim of Central cone (on the right). Motutapu Island lies in the background (from Needham et al. 2011, p.129) (cf. Fig. 15).

5. On track immediately before summit crater *Deposits of lapilli/scoriae of the Central cone.*

Exposed in cuttings next to the summit track not far from the main crater of the Central cone are layers of the pyroclastic material (pyroclastic literally means 'fiery fragmental') comprising scoriae of lapilli size (clasts 2–64 mm in diameter; 'lapilli' literally translates as 'little stones') and bombs (rounded, fluidal clasts >64 mm) that make up the Central cone of Rangitoto. These glassy, highly vesicular rock fragments originate from gas-rich molten or semi-molten lava that has been ejected into the air, quickly cooled and deposited close to the vent, frequently still partially molten. The clasts are typically cylindrical, spherical, teardrop, dumbbell or button-like in shape, and generally take their shape when they are airborne. Also common in the pyroclastic deposits of Rangitoto is 'welded' scoria, which forms when semi-molten scoria clasts 'stick' to other clasts when they land. The accumulation of the pyroclastic fragments described above formed the Rangitoto scoria cones. As noted earlier, much of the scoria is dark or black; red scoria indicates Fe-bearing minerals have been oxidised during eruption. Weak soils have developed on the scoria (Fig. 5).

6. Summit crater rim *Summit observation deck located on the rim of the main crater of Central cone of Rangitoto.*

The near circular bowl-shaped crater of Rangitoto is approximately 150 m in diameter and 60 m in depth, and reaches a height of ~261 m (Fig. 15). This is the position of the vent for the latest Rangitoto eruptions c. 550–500 cal. yr BP (c. 1400–1450 AD), which started off as a moderately explosive (Strombolian style) eruption, forming the main scoria cone, and then becoming more effusive (Hawaiian style) towards the latter stages of the eruption. At the summit we are presented with a 360° view of Rangitoto volcano and the surrounding natural and human-made features. To the southwest is the Auckland CBD, situated next to the Waitemata Harbour, and some of the other larger volcanic cones (Mt Wellington, Mt Eden, One Tree Hill, The Domain, Mt Mangere) in the AVF. To the west are the residential suburbs of North Shore and smaller volcanic cones (North Head, Mt Victoria) and slightly larger explosion craters (Lake Pupuke, Tank Farm, Onepoto Basin) (a map of the entire AVF is given below: Fig. 31, p. 41). To the northeast is Motutapu Island, which was covered in significant volumes

of tephra (ash grade) from the Rangitoto eruptions (Figs. 6 and 18). As described below, very thin ash from the latest Rangitoto eruptions has also been found in drill cores from Lake Pupuke. To the south and southeast are the other islands of the Hauraki Gulf, the islands of Waiheke and Motuihe, and volcanic cone(s) of Motukorea (Brown's Island), notable not only for its beautiful cones but also for its unique mineral, motukoreaite (Rodgers et al. 1977).

Leave the summit by ~1.30 pm.

Descent *Please take care on the descent as the scoria/gravel, and wet basalt lava steps, can be unstable or slippery under the feet.*

7. Lava caves (optional and subject to conditions) (Fig. 17) *Please wear hard hat and use torch.*

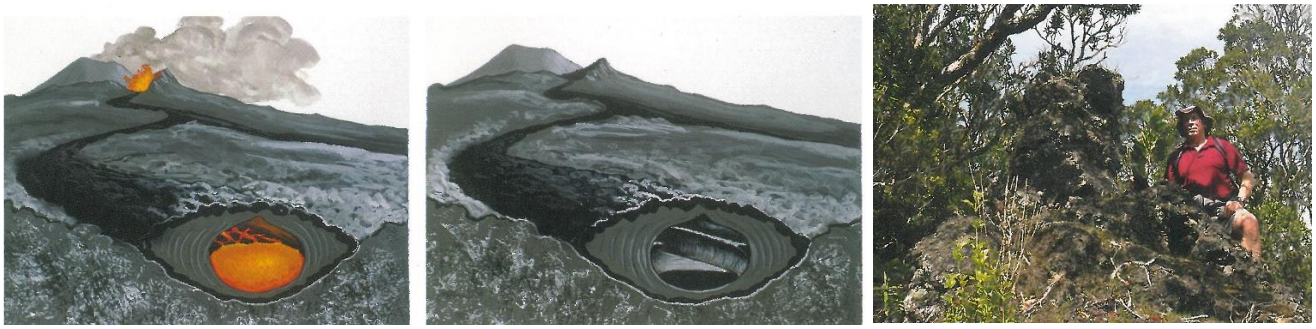

Figure 17. *Left*: Two cross-sections showing lava cave formation. The caves develop inside lava flows: the outside of the flow cools and solidifies to form a crust around an internal tube filled with flowing hot lava. When the supply of lava runs out, the molten liquid drains away leaving an empty tube/cave (paintings by Geoff Cox, from Hayward et al. 2011a, p. 14). *Right*: Small conical tower of basalt spatter near the track to the caves (Fig. 15) known as a *hornito* (Spanish, 'little oven'). The mounds (~3−4 m) high were formed by the accumulation of incandescent lava ejected through holes in the roof of a lava tube (Balance and Smith 1982) (photo from Hayward et al. 2011a, p. 105).

8. Baches in Tidal Bay area

The baches (small holiday cottages) form a still-active community on Rangitoto. They were built in the 1920s and 30s and consist of private holiday dwellings and boatsheds as well as communal facilities such as the swimming pool and the community hall (the hall in Islington Bay was originally built as a stone tennis pavilion). Built by families during the depression era, the "legality of the baches was doubtful from the start", but they demonstrate a do-it-yourself attitude. Since 1937 it has been prohibited to construct new buildings on the island, and in the 1970s and 1980s baches were pulled down as the original leases expired in an effort to diminish human influence on Rangitoto. However, efforts prevailed to preserve the last remaining baches (34 remain from a maximum of 140) as artefacts of New Zealand's architectural and social history (Wilcox 2007b; Hayward et al. 2011a). One bach (#38) near the wharf has been turned into a museum.

Ferry back to Auckland departs from Rangitoto Wharf at 3.30 pm.

PART 2: RANGITOTO VOLCANO AND ITS ERUPTIVE HISTORY

Rangitoto is the youngest and largest of the ~53 volcanoes in the AVF (Hayward et al. 2011a; Fig. 31 below). The estimated volume of basalt in the volcano (1.8 km^3, dense rock equivalent) is about half the volume of all of the basalt in the field. The volcano has a complex structure created during possibly three main phases of eruption, although some details are disputed. The lower lava-covered slopes are relatively gentle (~4° slope angle) although they steepen towards the summit of the island (~12°) where the upper part of the volcano is made up of scoria cones. The three main cones are North, Central, and South (Figs. 11, 15, 16). At the summit there is a central crater. A second smaller crater to the east and a complex series of mounds, ridges and depressions to the north of the main crater show that activity was not confined to a single vent (Fig. 15). Some of these features are remnants of older craters which were destroyed as the eruption progressed (Fig. 15).

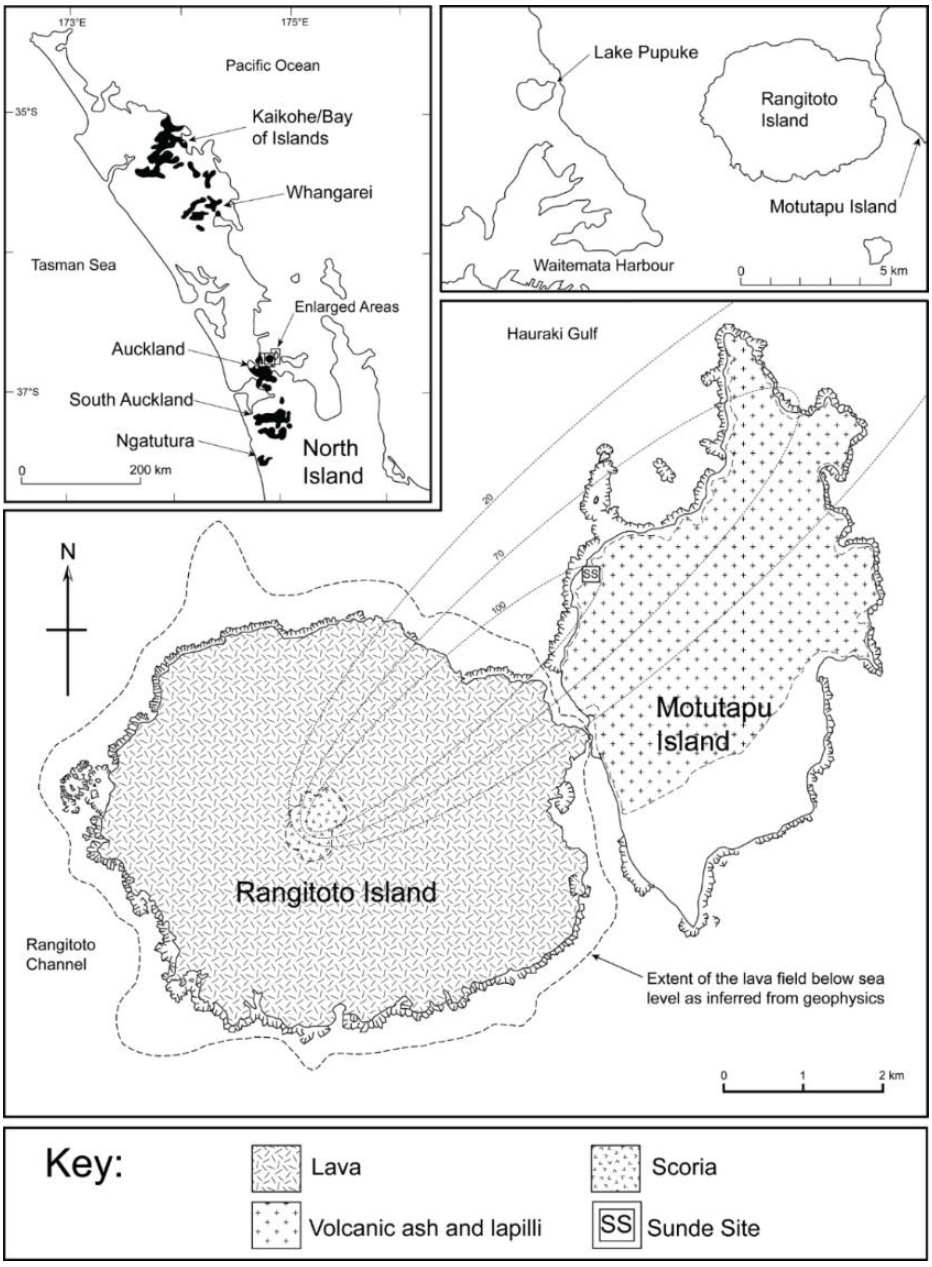

Figure 18. Geological sketch map of Rangitoto volcano and Motutapu Island, showing the main Rangitoto eruptive products (map from Needham et al. 2011, p. 128; partly after Kermode 1992). Ellipses show generalised areas of equal ash thickness (in centimetres) (termed isopachs) representing deposition from the latest phases of the Rangitoto eruptions c. 650–500 cal. yr BP. See text below regarding the 'Rangitoto 1' and Rangitoto 2' tephras that represent (at least in part) this latest phase of eruptions. Insets show (*upper left*) the location of the Auckland Volcanic Field and most other basaltic intraplate volcanic fields in the upper North Island (the Okete field in the Waikato is not shown), and (*upper right*) the position of Lake Pupuke ~5 km to the west of Rangitoto.

Using tephra and cryptotephra deposits in sediments on Motutapu Island and in Lake Pupuke to help determine Rangitoto's eruptive history

As noted previously, multiple eruptions of basaltic tephra occurred during the construction of the main Rangitoto edifice, phase 2 being from c. 650−550 cal. yr BP, and phase 3 from c. 550−500 cal. yr BP (Linnell et al. 2016). These authors suggested that this last phase generated the scoria cones on Rangitito's summit (cf. Hayward 2017) and concomitantly two 'prominent' tephras, designated as 'Rangitoto 1' and 'Rangitoto 2' by McGee et al. (2011) in the first instance, which occur as visible, separate but thin (millimetre- to centimetre-scale depending on location) primary tephra deposits in sediment cores from Motutapu Island and Lake Pupuke (Fig. 19). Rangitoto 1, dated at 553 ± 7 cal yr BP, is compositionally alkalic and characterised by a relatively low SiO_2 content (~45 wt%); Rangitoto 2, dated at 505 ± 6 cal yr BP, is subalkalic and characterised by a relatively high SiO_2 content (~50 wt%) (Horrocks et al. 2005; Needham et al. 2011; Shane et al. 2013; Zawalna-Geer et al. 2016; Hopkins et al. 2017). The ages cited are based on Bayesian models from Shane et al. (2013) derived from dates reported in Needham et al. (2011). The two layers are separated by thin peat on Motutapu and by very thin sediment in Pupuke cores, consistent with a short hiatus between the two depositional events.

Descriptions of the Rangitoto-derived tephra deposits on Motutapu Island include those by Brothers and Golson (1959), Scott (1970), and Needham et al. (2011). All reported abundant (~85–95%) olive brown (green) to brown or black glass shards together with sub-microcrystalline basalt pyroclasts, and minor pyroxene, olivine, plagioclase, and (in some papers) 'ore' (Fe-Ti oxides), either as loose crystals or quench crystals in pyroclasts. Working on tephra deposits from peat cores, Needham et al. (2011, p. 130) described the glass shards as typically smooth skinned, irregular, and vesicular, forming spherical to deformed ovoid shaped droplets; pyroclast textures ranged from irregular open vesicle networks to non-vesicular, and the pyroclasts were described as angular and blocky. In the cores, the tephras contained minor sedimentary lithics (xenoliths) and quartz, plagioclase, and glauconite grains, but at subaerial sites, the grey tephra is compact and massive with no xenoliths reported (Brothers and Golson 1959; Scott 1970). The tephra at the Sunde site was correlated via glass-shard major element composition with the alkalic basalt tephra designated Rangitoto 1 (553 ± 7 cal. yr BP) (Table 1).

Earlier explosively-generated basaltic Rangitoto tephras occur in Pupuke's lake sediments as cryptotephras with up to four identified in cores P06-06 and P08-06 (Fig. 20). These deposits provide evidence of intermittent activity since at least c. 1500 cal. yr BP through to c. 500 cal. yr BP, a longevity of ~1000 years (Shane et al., 2013). The findings were supported by the work of Zawalna-Geer et al. (2016). The fidelity of the cryptotephra research was challenged by Hayward and Grenfell (2013).

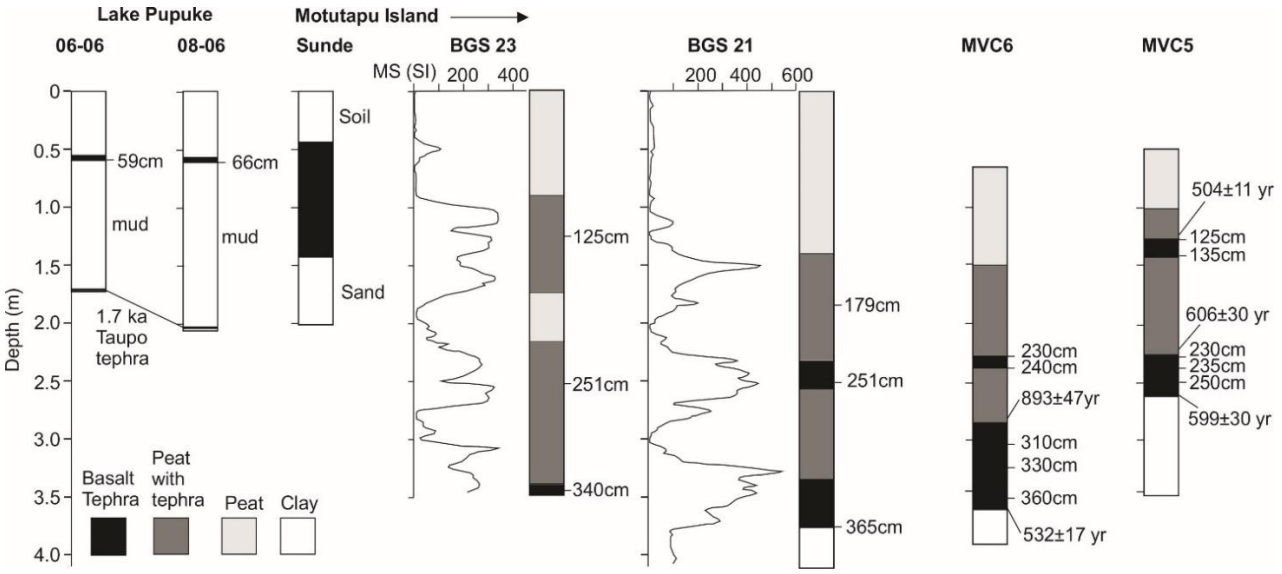

Figure 19. Summary logs of cores from Lake Pupuke containing Rangitoto tephra, with magnetic susceptibility data (MS in dimensionless SI units) in BGS 23 and 21 (from Shane et al. 2013, p. 176). Visible (macroscopic) tephra layer samples used in geochemical studies are marked as depths (in cm, right of log; see also Fig. 20). Ages for MVC5 and 6 are calibrated radiocarbon data from Needham et al. (2011, p. 130). The Sunde site is an archaeological site on the northwest coast of Motutapu Island (Fig. 18; Dodd 2008).

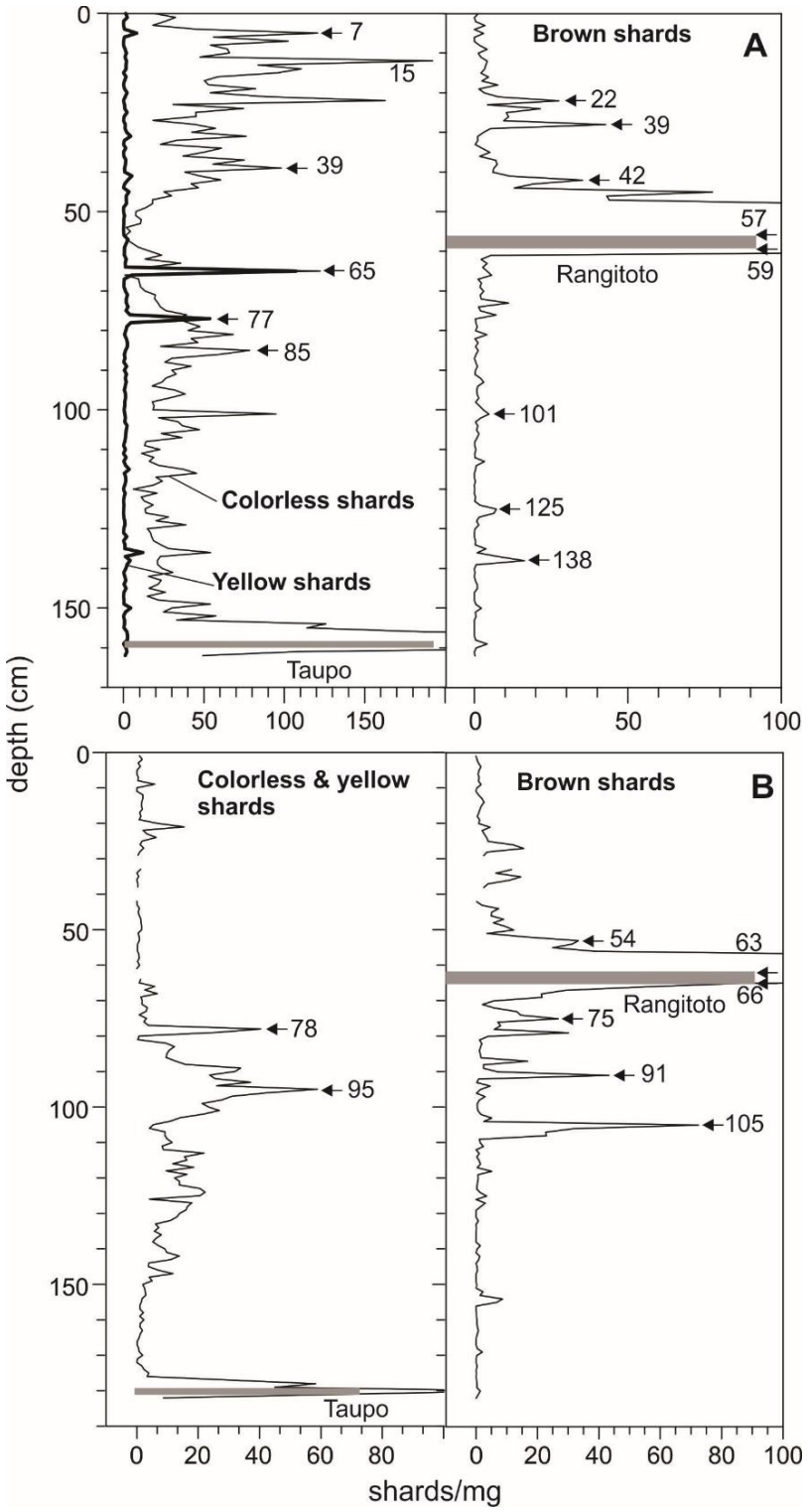

Figure 20. Concentration of shards in sediment samples from Lake Pupuke cores P06-06 (**A**) and P08-06 (**B**). Numbers represent depths (cm) of samples used in geochemical studies. Visible (macroscopic) tephra layers of Rangitoto and Taupo (dated at 1718 ± 10 cal. yr BP, equivalent to 232 ± 10 AD; Hogg et al. 2012) are shown as grey bars, other peaks represent cryptotephras. Brown shards are basaltic shards from Rangitoto; their presence as early as c. 1500 cal. yr BP in the cores suggested Rangitoto had been intermittently active at least since then (Shane et al. 2013) (subsequently supported by drill-core evidence). Colourless and yellow shards are andesites and rhyolites from distant central North Island volcanoes. Rangitoto 1 (called 'lower' Rangitoto by Needham et al., 2011; Shane et al. 2013) occurs as a visible, thin (alkalic basalt) ash layer in P06-06 (at 60 cm depth, age 551 + 7 cal. yr BP), and in P08-06 (at 63 cm depth, 553 + 7 cal. yr BP). Rangitoto 2 ('upper' Rangitoto) occurs as a visible, thin (subalkalic basalt) ash layer in P06-06 (at 57 cm depth, 505 ± 6 cal. yr BP), but in P08-06 it occurs as a cryptotephra (at 54 cm depth, 505 ± 6 cal. yr BP). An equivalent pair of thin basaltic tephras, at 28 and 27 cm depth (separated by thin sediment), were reported for core P5 from Lake Pupuke by Horrocks et al. (2005). Note differences in scaling of shard concentrations (x-axis) (from Shane et al. 2013, p.178).

Table 1. Major element compositions of glass shards in 'Upper' (Rangitoto 2) and 'Lower' (Rangitoto 1) tephras from Lake Pupuke and equivalent analyses of glass from the lower tephra at the Sunde site on Motutapu (from Needham et al. 2011, p. 132). Basaltic shards from (lower) Rangitoto 1 tephra in Pupuke and the lower tephra at Sunde* are correlatives and alkalic, having relatively low SiO_2 and higher Al_2O_3, CaO, Na_2O, and K_2O contents than glass from (upper) Rangitoto 2 tephra in Pupuke, which is subalkalic.

	Upper tephra—Pupuke cores [16 analyses]				Lower tephra—Pupuke cores [20 analyses]				Lower tephra—Sunde Site [20 analyses]			
	Ave.	SD	Max.	Min.	Ave.	SD	Max.	Min.	Ave.	SD	Max.	Min.
SiO_2	50.87	0.48	51.7	49.9	44.64	0.40	45.6	44.0	44.28	1.08	45.7	42.8
TiO_2	3.09	0.25	3.6	2.5	3.25	0.15	3.5	3.0	3.14	0.14	3.4	2.9
Al_2O_3	14.02	1.15	16.6	12.2	15.72	0.34	16.5	15.1	15.76	0.44	16.4	15.1
FeO	12.41	1.02	14.6	10.3	11.96	0.27	12.4	11.3	12.32	0.43	13.0	11.5
MnO	0.18	0.06	0.3	0.1	0.19	0.08	0.3	0.0	0.16	0.05	0.3	0.1
MgO	4.49	0.51	5.4	3.3	4.77	0.45	6.0	3.9	4.85	0.50	5.5	4.0
CaO	9.25	0.62	10.5	7.8	11.39	0.47	12.2	10.3	11.77	0.58	12.8	10.9
Na_2O	4.01	0.36	4.9	3.3	5.25	0.35	6.0	4.8	5.09	0.65	6.3	4.2
K_2O	1.13	0.20	1.5	0.7	1.80	0.18	2.2	1.5	1.66	0.30	2.1	1.3
P_2O_5	0.33	0.32	0.8	0.0	0.58	0.52	1.4	0.0	0.89	0.25	1.3	0.5
Cl	0.22	0.20	0.5	0.0	0.45	0.36	1.2	0.0	0.09	0.04	0.2	0.0
No.	16				20				20			

A number of further observations can be made (Shane et al. 2013):

(1) The well-dated rhyolitic Kaharoa tephra from Mt Tarawera (636 ± 12 cal. yr BP, equivalent to 1314 ± 12 AD) (Hogg et al. 2003) occurs a few centimetres beneath (visible) Rangitoto 1 and 2 tephras in Lake Pupuke (Shane et al. 2013; Zawalna-Geer et al. 2016), and its position is consistent with most of the reported radiocarbon ages for the latter (collected from cores and outcrops on Motutapu Island, e.g. Fig. 19).

(2) The composition of the lower visible tephra layer in Lake Pupuke partly overlaps that of multiple tephra layers deposited on Motutapu Island, where radiocarbon ages have been determined. However, the latter deposits are dominated by geochemically distinct shards. This difference points to multiple tephra eruptions of Rangitoto with different dispersal patterns.

(3) The composition of the upper Lake Pupuke visible layer (Rangitoto 2) matches that of Central and South scoria cones on Rangitoto (i.e. subalkalic basalt, relatively high SiO_2). None of the other visible (macroscopic) tephras matches any of the scoria cones with regard to composition. This finding indicates that the volcanic landforms do not record the entire pyroclastic history of the volcano.

(4) The two tephra layers and zones of tephra-rich peat deposited on Motutapu Island are compositionally identical. They are not considered to result from local reworking because the same stratigraphy is found at several sites. Instead, these tephra occurrences reflect episodic eruptions. The sequences on Motutapu lack visible rhyolitic tephra such as Taupo (1718 ± 10 cal. yr BP), and thus may represent shorter time periods than that recorded in Lake Pupuke. Hence, much of the radiocarbon data for Rangitoto volcano pertains to just one part of the eruption history.

(5) The Lake Pupuke cores contain basaltic cryptotephra layers that pre-date Kaharoa tephra (636 ± 12 cal. yr BP), extending back to 1498 ± 140 cal. yr BP (Fig. 20). These are likely to represent early Rangitoto eruptions and hence demonstrate an extended life-span for the volcano since at least c. 1500 yrs ago (supported by evidence in Linnell et al. 2016 and Zawalna-Geer et al. 2016).

(6) Most of the cryptotephra deposits contain shards that compositionally are similar to those of Central and South scoria cones. This does not imply that the two cones were long-lived. Instead, the cryptotephra deposits could represent periods of earlier volcanism where proximal deposits are now buried beneath the cones.

Another implication of the recognition of Rangitoto 1 and Rangitoto 2 tephras as stratigraphically separate units aged c. 550 and 500 cal. yr BP, both in Lake Pupuke and on Motutapu Island (and irrespective of their relationship to eruptives on Rangitoto Island itself), is that the name "Rangitoto Tephra Formation", which was defined by Froggatt and Lowe (1990) to represent a single eruptive event dated at c. 750 ^{14}C yr BP, should be abandoned (Newnham et al. 2017)

*The Sunde site was named for its discovery by Rudy Sunde in 1958 (Scott 1970, p. 14).

Rangitoto drilling project

The findings were published in detail in Shane and Linnell (2015) and Linnell et al. (2016). The drill site (Fig. 21) was at metric grid north 5927446, east 1765100 (map NZTopo50-BA32, edition 1.02; Land Information New Zealand 2012), ~120 m asl on the western flank of the volcano (Fig. 22). Most of the text and the figures through to p. 39 are from Linnell et al. (2016).

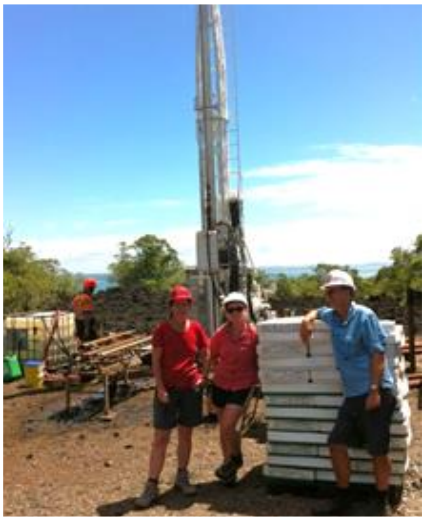

Figure 21. Drill site on Rangitoto Island, February 2014.

Recovery of Miocene sediments at the base of the sequence demonstrates that the entire edifice beneath the drill site was penetrated. The upper 128 m of the sequence comprises massive basaltic lava flow units separated by basaltic breccia (Fig. 24). The breccia consists of highly fractured and angular clasts (<1 cm to 10 cm in size) with very little matrix (<10%). Contacts between the breccia and massive lava are generally gradational, and some contacts display welding of clasts on the flow unit. The breccias are considered to represent autobrecciated zones formed at the top and base of lava flow units during flow emplacement. At least 53 dense lava units are thus recognized; these have thicknesses in the range <0.5 to 7 m (mostly about 1–2 m). They are light to dark grey and generally lack alteration. A few display red oxidation coloration, but there is no systematic pattern in alteration or coloration with depth in the sequence. The lavas range from dense and non-vesicular to highly vesicular (up to 30% vesicles and vugs).

Flow banding is evident in a few units and some dense units display sub-vertical joints. Breccia units (mostly <1 m thick, maximum 5 m) mostly display red-to yellow oxidation colorations. Clasts in the breccia are notably more vesicular than the adjacent flow units.

Lithology of the core sequence

The lava sequence of the upper 128 m of core lacks unambiguous evidence of depositional hiatus such as paleosols, and pyroclastic units are not observed (Fig. 24). One exception is observed clay-filled fractures that developed in the upper 1 m of a lava flow unit at about 95 m depth, which may reflect a period of weathering.

The base of the lava flow sequence at 128.1 m is marked by a sharp contact between lava and fragmented fossil marine shells in ash overlying 20 cm of fossiliferous olive-grey mud (Fig. 24). A basaltic volcaniclastic (pyroclastic?) sequence between 128.3 and ~135 m comprises unconsolidated, poorly-sorted black ash to coarse lapilli. The lapilli are mostly sub-rounded to sub-angular blocky clasts displaying a range of vesicularity. Shell fragments and sedimentary grains occur in the ash-grade fraction. The unconsolidated character of the deposit and disruption from drilling prevents any assessment of stratification. Thin mud layers (10 cm thick at 132.2 m, and 40 cm thick at 133.0–133.4 m), seemingly divide the volcaniclastic unit. The interval 135.4–140.3 m depth is a continuous massive and fossiliferous, olive-grey sandy mud sequence. This unit contains a thin (~60 cm) massive lava flow unit (136.7–137.2 m depth). The sequence beneath 140.3 m is highly weathered Miocene sandstone and mudstone.

Petrography

A set of 13 basalt lava samples was selected from the core sequence for modal mineralogy analysis (Table 2) (Linnell et al. 2016). The basalts are porphyritic and contain ~15%–20% phenocrysts. Olivine crystals are euhedral to subhedral, ~0.5–2 mm in size, and constitute 7%–14% of the rocks. Clinopyroxene crystals are commonly subhedral, 0.5–1.5 mm in size, and represent 2%–8% of the rocks. Glomerocrysts of clinopyroxene also occur in some samples. Lath-shaped plagioclase is a trace phenocryst phase in some samples. The crystalline groundmass contains anhedral clinopyroxene that subophitically encloses laths of euhedral plagioclase. Minor olivine and Fe-Ti oxides also occur. The lava sequence lacks temporal trends in crystal type or abundance (Table 2).

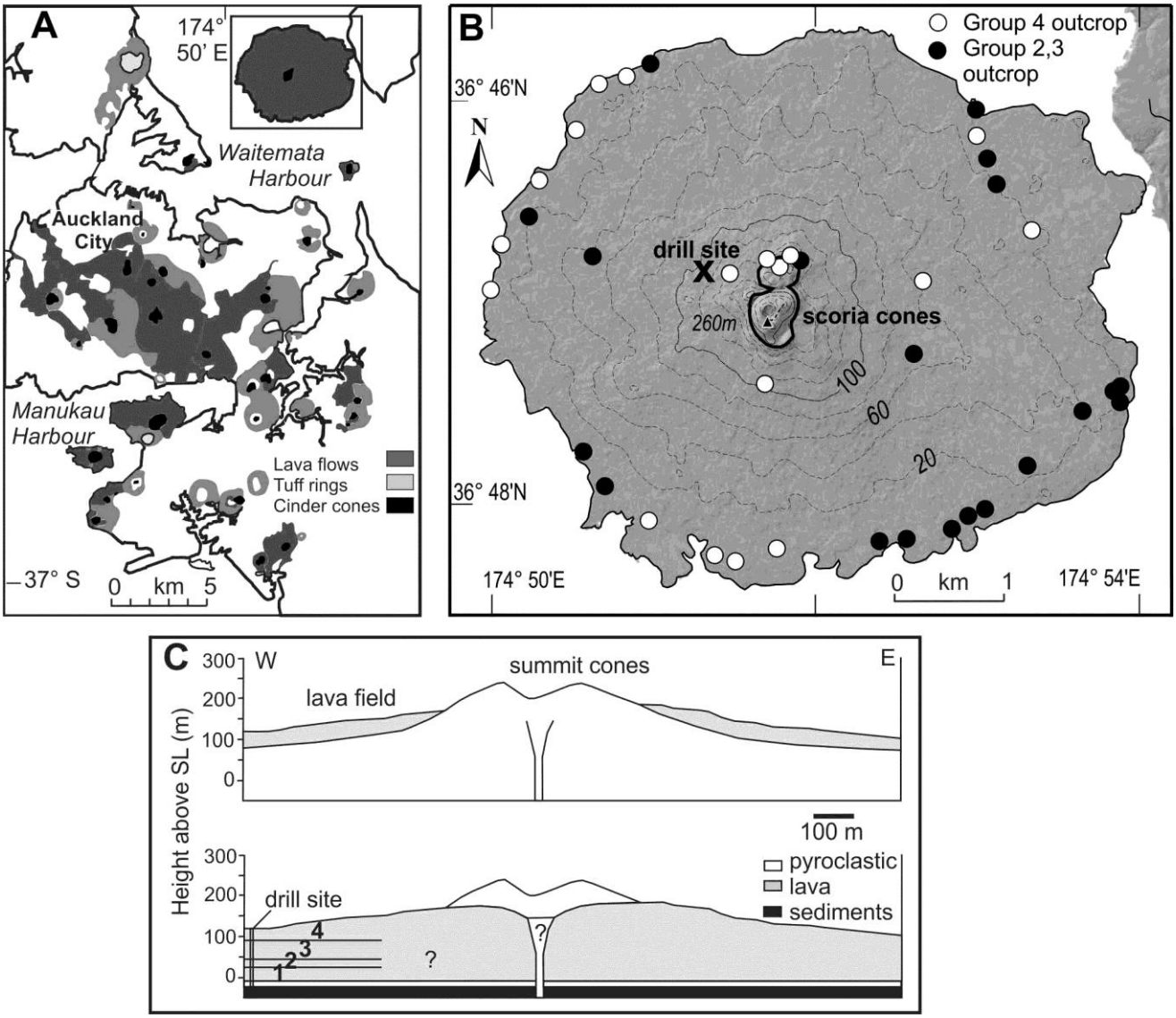

Figure 22. (**A**) Map of the Auckland Volcanic Field, and (**B**) Rangitoto volcano showing the location of the drill site, and outcrops of basalt classified into groups reflecting the geochemistry of sub-surface lava flows (see below and Linnell et al. 2016). Elevation contours in metres. (**C**) Simplified cross sections of Rangitoto volcano from Needham et al. (2011) (*upper*) and based on this study (*lower*) (from Linnell et al. 2016, p.1161; cf. Fig. 23).

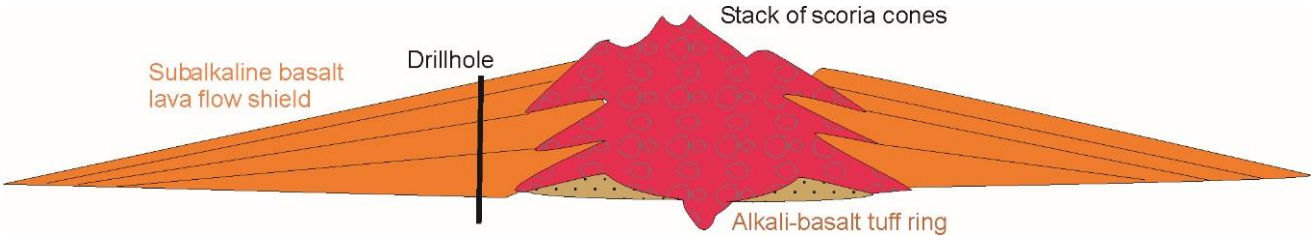

Figure 23. An alternative interpretation of Rangitoto's structure shown in cross-section by Hayward (2017). This interpretation is somewhat similar to that of Balance and Smith (1982) but contrasts with those of Needham et al. (2011) and Linnell et al. (2016), which are shown in Fig. 22C. Hayward (2017) suggested a two-phase model for the eruption of Rangitoto between ~650 and 550 years ago: phase 1, eruption of phreatomagmatic alkalic basalt (resulting in deposition of ash beds on Motutapu) and construction of a tuff ring/cone by dry strombolian eruptions forming North scoria cone; phase 2, eruption of four separate batches of subalkalic magma to build the Central and South scoria cones followed by later issuings of partly degassed lava flows to progressively build the subalkalic basalt lava-flow shield.

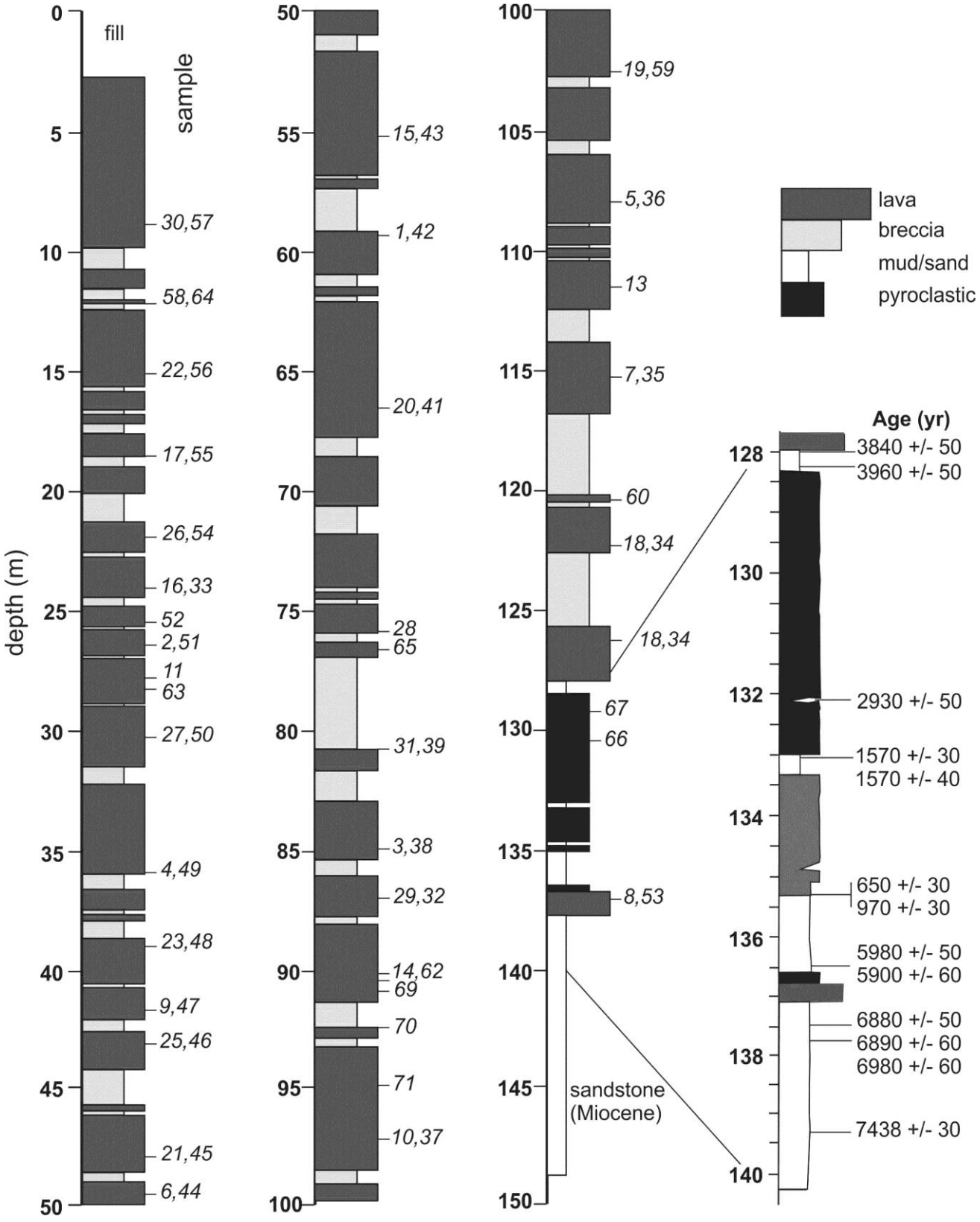

Figure 24. Lithological log of the Rangitoto drill core showing petrological sample locations, and calibrated ages of samples (in cal. yr BP ± 1σ) collected for ^{14}C dating (from Linnell et al. 2016, p.1162).

Table 2. Modal mineralogy of basalt samples from drill core (based on counting 300 phenocrysts) (from Linnell et al. 2016, p. 1164). Sampling points noted on Fig. 24.

Sample	Depth (m)	GM (%)	Ol (%)	Cpx (%)	Plag (%)	Fe-Ti (%)	Cpx gl (%)	Total phen (%)
30	8.92	88	7	3	2	0	0	12
24	25.46	83	13	4	0	0	0	17
2	26.35	81	14	4	1	0	0	19
4	35.96	84	12	4	0	0	0	16
12	42.87	84	12	2	1	1	1	16
1	59.2	85	10	5	0	0	0	15
12	69.44	87	10	2	0	0	1	13
39	80.45	85	11	4	0	0	0	15
3	84.93	84	12	4	0	0	1	16
14	90.13	82	8	8	2	0	0	18
7	115.28	82	10	6	1	0	1	18
18	126.26	86	11	2	0	0	1	14
8	136.93	81	13	4	2	0	1	19

Note: GM—groundmass; Ol—olivine; Cpx—clinopyroxene; Plag—plagioclase; Fe-Ti—Fe-Ti oxide; Cpx gl—clinopyroxene glomerocrysts; Total phen—Total phenocrysts.

Geochemistry

Basalts from the core sequence display a narrow compositional range in major elements (SiO_2 ~48–49 wt%, normalized water-free; Mg# 0.60–0.64) and classify as subalkalic (Fig. 25A). (The Mg-number (Mg#) is defined as 100 x MgO/(MgO + FeO) and is reported in moles.) Because of the narrow range of major elements, compositional trends are poorly defined on variation diagrams. In general, Al_2O_3, TiO_2, CaO, Zr, Hf, and Sr decrease, and Ni and Cr increase with increasing Mg# (examples shown in Fig. 26). Many other elements, including incompatible elements such Nb, Th, Pb, and rare earth elements (REEs), show little systematic variation with Mg#. The relative enrichment in high field strength elements (HFSE) Th, U, Pb, Nb, and Ta on a primitive mantle-normalized multi-element plot and lack of negative Nb and Ta anomalies (Fig. 25B) are characteristic of intraplate basalts as described previously for Rangitoto samples (Needham et al. 2011; McGee et al. 2011). All of the basalts display relative enrichment of light (L) REEs and depletion of heavy (H) REEs (chondrite-normalized) (Linnell et al. 2016).

Clustering of basalt compositions on variation diagrams of nearly all major and trace elements allows four coherent compositional (magmatic) groups in the core to be defined (Fig. 26). The compositional groups relate to stratigraphic order in the core: **group 1** (137–95 m depth), **group 2** (94–69 m depth), **group 3** (68–26 m depth), and **group 4** (26–0 m depth) (Linnell et al. 2016). Features included in group 1 are scoria from the volcaniclastic deposit (128–135 m depth) and the isolated lava flow unit at 137 m depth. Characteristics distinguishing the groups include (1) relative enrichment in Nb, Ta, Ba, U, Th, Rb, and REEs in group 1, and (2) enrichment in Ti, Sr, Zr, and Hf and low Mg# (<0.62) in group 4. Groups 2 and 3 are somewhat similar in composition, but the former is distinguished by lower Mg#, Ni, and Cr (Fig. 26). There is considerable temporal variation within both groups 2 and 3, including prominent upward stratigraphic trends of decreasing incompatible element abundance, e.g. Nb (18.5–12.5 ppm), Sr (326–287 ppm), and most REEs (Fig. 27). Ratios of incompatible elements, such as Zr/Nb (6.2–9.0) and Nd/La (1.2–1.39) in group 2, increase upward in the stratigraphic sequence of both groups (Fig. 27), whereas groups 1 and 4 lack within-group temporal trends (Linnell et al. 2016).

Basalts in the core sequence are compositionally similar to those in surface outcrops of the lava field and Central and South cones, but they are compositionally distinct from the lower SiO_2 and higher Mg# composition of the North cone (Figs. 25A and 28). In addition, the Central cone displays a few higher-Mg# compositions not represented in the subsurface sequence (Linnell et al. 2016).

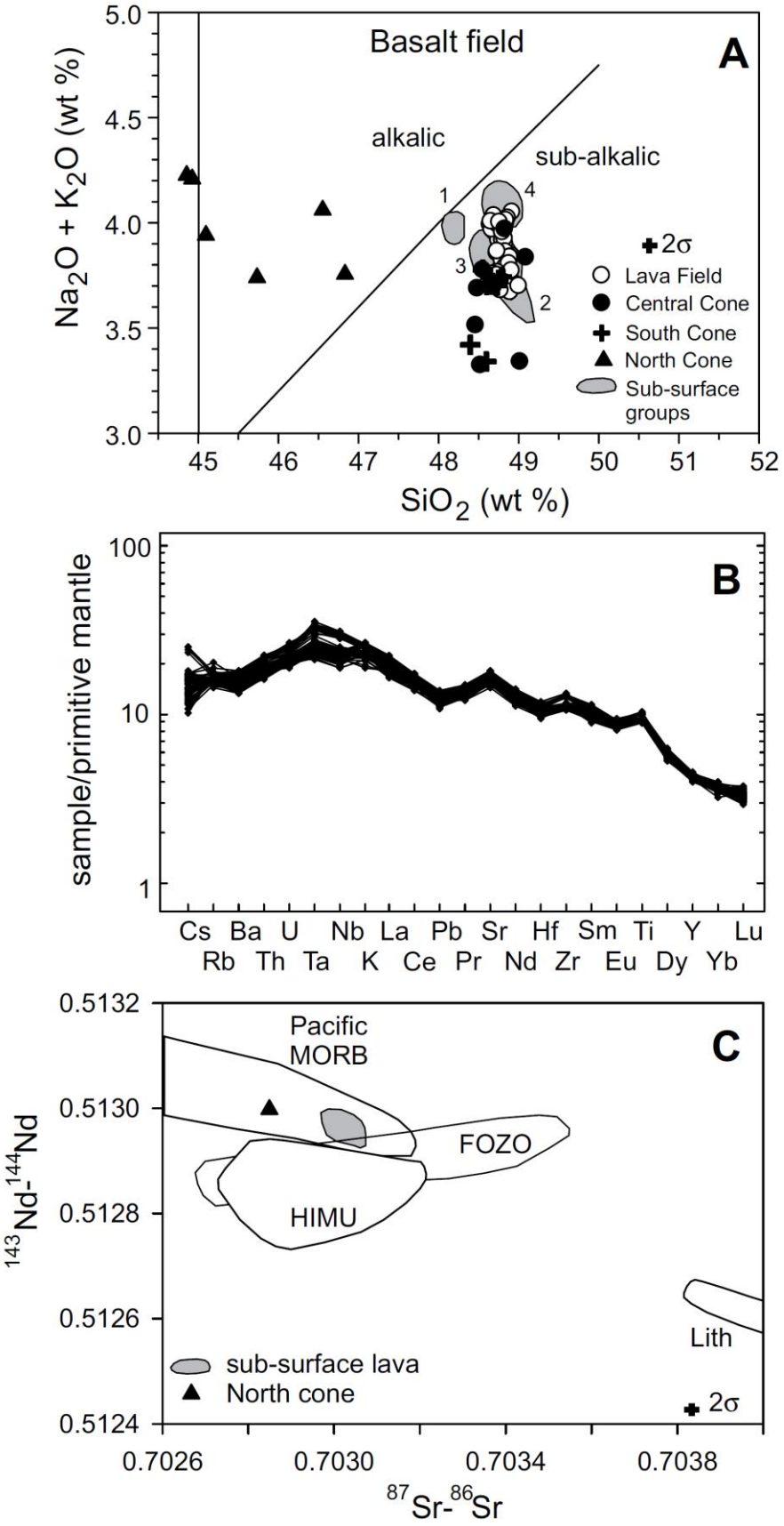

Figure 25. Composition of subsurface basalts from the drill core. (**A**) Classification plot of the basalt field defined by Le Maitre (2002), with alkalic-subalkalic boundary as defined by Irvine and Baragar (1971). (**B**) Incompatible multi-element diagram, normalized to primitive mantle following Sun and McDonough (1989). (**C**) Radiogenic isotope compositions. North cone basalt is shown for comparison. Compositional fields for Pacific mid-ocean-ridge basalt (MORB), HIMU (stands for high μ, where μ = $^{238}U/^{204}Pb$), and Focus Zone (FOZO) are from Stracke et al. (2003, 2005). From Linnell et al. (2016, p. 1165).

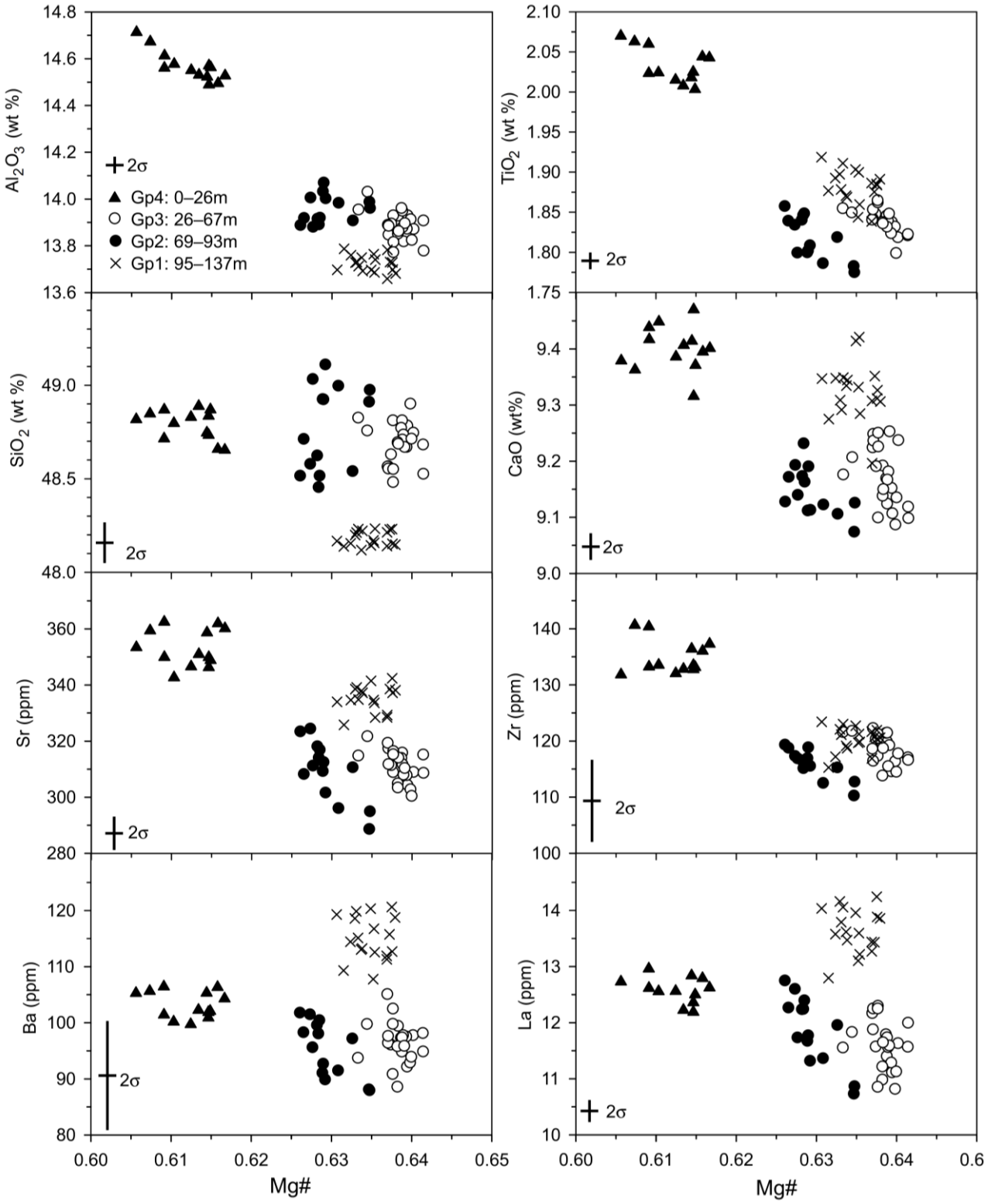

Figure 26. Major- and trace-element chemistry of Rangitoto subsurface basalts plotted against Mg# (= 100MgO/(FeOt + MgO), reported here as mole fraction). Elements were selected to represent the diversity of compositions displayed in the rock suite. From Linnell et al. (2016, p. 1166).

The basalt sequence in the core is isotopically homogeneous, with variation in Sr-Nd-Pb-isotopes barely exceeding analytical error (Fig. 28; Table 3): $^{87}Sr/^{86}Sr$ = 0.702969–0.703069; $^{143}Nd/^{144}Nd$ = 0.512939–0.512983; $^{206}Pb/^{204}Pb$ = 19.037–19.067; $^{207}Pb/^{204}Pb$ = 15.587–15.603; and $^{208}Pb/^{204}Pb$ = 38.729–38.779 (Linnell et al. 2016). These isotopic compositions are in the range previously reported for Rangitoto basalts, and they are similar to basalts from other volcanoes in the AVF (Huang et al., 1997; McGee et al., 2011, 2013). As described by those workers, Sr-Nd isotope signatures plot near the Pacific mid-ocean-ridge basalt (MORB)–HIMU field boundaries (where HIMU represents high μ, and $\mu = {}^{238}U/^{204}Pb$; Fig. 23C), and Pb-isotope ratios place the rocks on the more radiogenic end of the MORB field between Pacific MORB and HIMU, and close to New Zealand lithospheric compositions (Linnell et al. 2016). A sample from the North cone is somewhat distinct, displaying slightly more radiogenic isotopic ratios (Table 3; Fig. 25C).

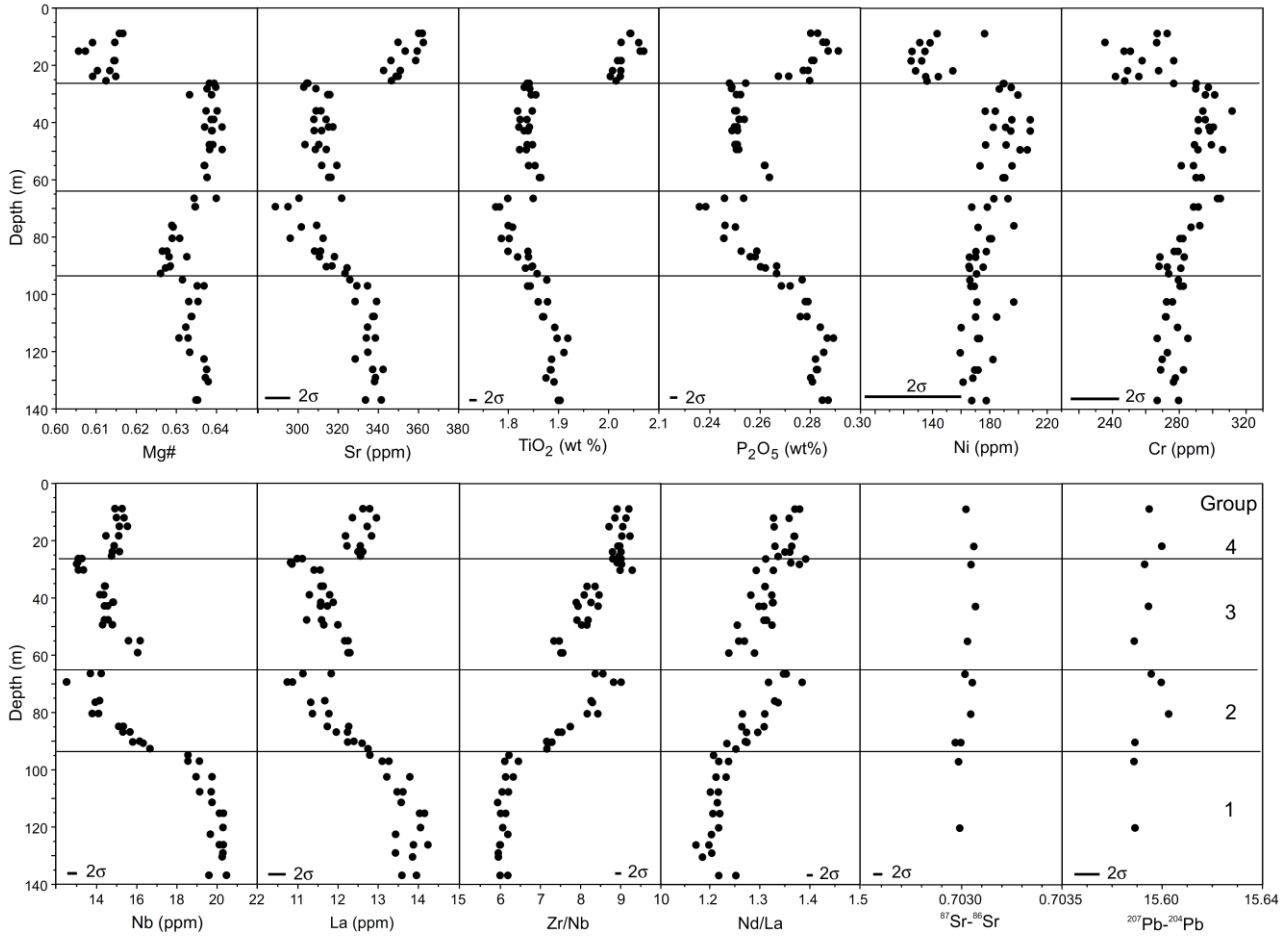

Figure 27. Geochemistry and isotopic composition of Rangitoto subsurface basalts plotted against stratigraphic depth in the drill core. Elements were selected to represent the diversity of compositions displayed in the rock suite (from Linnell et al. 2016, p. 1167).

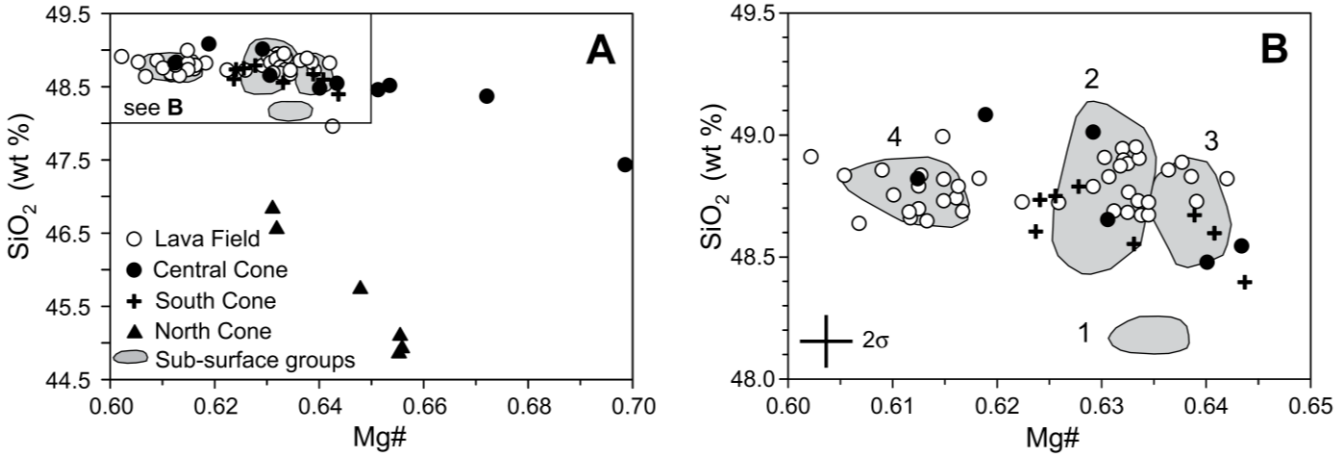

Figure 28. (**A**) Compositional fields of Rangitoto subsurface basalts from drill core compared with analyses of basalts from outcrops studied by Needham et al. (2011). (**B**) Enlargement of the compositional field of subsurface basalts. Refer to Fig. 22B for outcrop distribution. From Linnell et al. (2016, p. 1168).

Table 3. Sr-Nd-Pb isotope composition of basalts in drill core and North cone (NC) (from Linnell et al. 2016, p. 1168).

Depth (m)	Sample	$^{87}Sr/^{86}Sr$ (±0.00004)	$^{143}Nd/^{144}Nd$ (±0.00002)	$^{206}Pb/^{204}Pb$ (±0.05%)	$^{207}Pb/^{204}Pb$ (±0.05%)	$^{208}Pb/^{204}Pb$ (±0.08%)
8.92	57	0.703021	0.512944	19.049	15.595	38.754
21.88	54	0.703061	0.512939	19.055	15.600	38.767
28.22	63	0.703047	0.512947	19.037	15.593	38.737
				19.040	15.597	38.749
42.87	46	0.703069	0.512973	19.045	15.595	38.747
55.02	43	0.703029	0.512968	19.049	15.589	38.729
66.49	41	0.703017	0.512959	19.046	15.596	38.749
69.44	40	0.703053	0.512963	19.051	15.600	38.762
80.45	39	0.703045	0.512972	19.067	15.603	38.779
90.38	62	0.702996	0.512977	19.059	15.589	38.736
		0.702969				
97.07	37	0.702985	0.512983	19.064	15.589	38.739
120.24	60	0.702990	0.512962	19.058	15.589	38.735
NC	59319	0.702857	0.512998	19.174	15.589	38.813
		0.702788				

Note: See text for analytical details and uncertainty estimates.

Radiocarbon ages and core chronology

Thirteen samples were selected from the interval containing organic material (128–139 m depth) for dating via the AMS ^{14}C technique. Organic material provides a concordant sequence of ages from c. 7400 to 5900 cal. yr BP for the estuarine muds at ~139.5–136.5 m depth that contain the oldest lava (137 m depth) in the core (Fig. 24). These stratigraphically concordant ages include both terrestrial (wood) and marine (shell) materials, and non-abraded, whole gastropod shells with delicate morphology. Both argue against reworking of the sediments. The massive mud sequence lacks depositional features that could be interpreted as secondary transport, and is indicative of sedimentation in a low-energy environment. There is no evidence for magma-sediment interaction such as glassy chilled-margins on the lava or breccia formation (peperite) that would point to magma intrusion into shallow, water-saturated sediments. In addition, there is no evidence of soft-sediment deformation. Thus, Linnell et al. (2016) considered the lava to be an *in situ* flow unit rather than a dike or a transported block.

Discordant ages of components from the same stratigraphic level at 135.4 m depth (foraminifera = 650 ± 30 cal. yr BP; shell fragments = 970 ± 30 cal. yr BP) indicate reworking has occurred. Linnell et al. (2016) suggested one possible explanation for the age sequence at ~135.5–128 m depth is that the volcaniclastic deposits and associated mud layers represent mass-flow units, emplaced by slumping from a sub-marine pyroclastic structure. The growth of the lava shield could have loaded and destabilized a pre-existing edifice. Catastrophic failure of a pyroclastic edifice and its marine-mud substrate is likely to have produced a chaotic/random series of dates in the resulting deposit. Instead, the inverted age sequence found could reflect a progressive 'top-down' incision of a nearby pyroclastic edifice with intercalated mud, built between c. 4000 to c. 650 cal. yr BP. This hypothesis suggests that shield growth was preceded by intermittent pyroclastic activity, which lends support to the findings of Shane et al. (2013) who reported cryptotephra deposits from Rangitoto volcano preserved in lake sediments extending back to 1498 ± 140 cal. yr BP, suggesting an extended time-span for the volcano's activity (Figs. 19 and 20).

Regardless of the depositional history of the volcaniclastic deposits, the youngest age in the sequence (c. 650 cal. yr BP) provides a maximum age for the shield-building stage represented by the overlying lava flows. A previous paleomagnetic investigation of the lava field revealed scatter in the demagnetized remnant directions (Robertson 1986), but much of the data are within wide error limits thereby preventing reliable interpretation of eruption duration. The only previous radiocarbon determinations associated with lava flows produced widely disparate ages of 214 ± 129 cal. yr BP for wood beneath a flow unit and 1161 ± 72 cal. yr BP for marine shells in mud baked by a (different) lava flow. These were dismissed by some workers as representing young tree roots penetrating the lava flow (e.g. Nichol 1992), and relict shells pre-dating the eruption, respectively. However, the age of marine shells is within the range of ages obtained from the sub-surface sequence. Age estimates not based on ^{14}C dating for the most recent eruptions of Rangitoto were summarised by Lowe et al. (2000), who reported an error-weighted mean obsidian hydration age of c. 1385 ± 35 AD on artefacts from middens beneath the ash at the Sunde site on Motutapu Island (Stevenson et al. 1996) (see also review by Lindsay et al. 2011).

If the tephra layers downwind of the volcano reflect pyroclastic activity associated with summit scoria cones rather than the main shield-building stage, they then provide an upper age limit (c. 550–500 cal. yr BP) for shield development. This gives a maximum duration of about 100 years for shield growth. Continuity of the eruption during the shield-building stage is suggested by the lack of intercalated sediments and paleosols. However, four composition groups erupted and the surface intercalation of lavas show that the shield was built in a series of closely spaced episodes (Linnell et al., 2016), with one compositional change coinciding with a horizon of clay-filled fractures (at 95 m depth between groups 1 and 2), which may indicate a pause of a few years to decades.

Volcanic history

Linnell et al. (2016) divided the construction of Rangitoto volcano into three major magmatic and eruptive phases.

Phase 1 includes the oldest lava flow (c. 6000 cal. yr BP) and overlying volcaniclastic deposits. These units are compositionally indistinguishable from the lowermost shield-building lava flows (group 1) that post-date c. 650 cal. yr BP. Two alterative explanations for the sequence are possible.

(1) The deposits represent a phase of prolonged and/or periodic tapping a common magma source. The sub-alkalic basalts are unique to Rangitoto volcano and differ from the more alkalic compositions at other AVF volcanoes. Under this scenario, magmatic output was low until the beginning of the shield-building lava flow phase. The ages in the volcaniclastic deposits, albeit lacking stratigraphic order, reflect reworking of a pyroclastic edifice built during the interval c. 4000 to 650 cal. yr BP.

(2) The oldest lava flow and the volcaniclastic deposits are part of a separate volcano (or several volcanoes) buried beneath the Rangitoto shield. Based on the high aerial density of volcanic centres in the AVF, the width of the shield could easily cover older edifices. However, close proximity of AVF volcanoes does not equate to similarity in age. Thus, Holocene ages for all deposits in the Rangitoto core point to a volcanic complex rather than coincidental spacing of volcanoes.

Phase 2 comprises the main lava shield-building stage of Rangitoto when magma production significantly increased for a short period at c. 650–550 cal. yr BP. Cycles of increasing degree of melting at the mantle source occurred (group 2 and 3 magma), presumably representing thermal perturbations.

Phase 3 represents a change to pyroclastic volcanism and the construction of summit scoria cones at c. 550–500 cal. yr BP. At this time, the magmatic system was compositionally more diverse, but volumetrically less productive. Although Central and South cones are compositionally similar to the shield-building lava flows (subalkalic basalt), they also erupted lower-Mg# magma. In contrast, North cone is distinctly alkalic magma, reflecting a deep mantle source.

The eruption of multiple magma batches both sequentially and simultaneously has been reported at other small basaltic volcanoes, in particular in the Newer Volcanics Province in southern Australia. Changes in magmatic compositions at these and other small volcanoes often accompany changes in eruption style, such as effusive versus explosive. However, no overriding temporal trends are evident. Of the few AVF volcanoes for which temporally-controlled data is available, there is a lack of common compositional evolution. This finding points to the localized influence of mantle heterogeneity and conduit systems (Linnell et al. 2016).

Implications including volcanic risk

Regardless of whether Rangitoto was a long-lived volcano (c. 6000 years) or was the site of separate eruptive episodes from edifices now buried, the new insights from drilling raise the possibility of future eruptions from that part of the AVF. Rangitoto may be better described as a complex that has experienced periods of activity (Linnell et al. 2016). Previous studies have implied that the edifice represents an amalgamation of scoria cones, overlain by a thin veneer of late-stage lava flows (e.g. Balance and Smith 1982; Needham et al. 2011; Fig. 22C). In contrast, Linnell et al. (2016) have inferred from the drill-core evidence that the edifice mostly consists of a lava shield (Fig. 22C), consistent with Walker's (1993) interpretation of Rangitoto as a scutulum-type lava shield. Hayward (2017) provided a hybrid model (Fig. 23), which he "based on landform and new drillhole data, consistent with traditional understanding".

In addition, AVF volcanism in the Holocene was more frequent than previously known. The prolonged and varied pattern of behavior of Rangitoto volcano is consistent with other recently investigated volcanoes in monogenetic basaltic fields (e.g. Newer Volcanics Province), and may require a change in emphasis in hazard scenario modelling. By inference, other AVF volcanoes with large lava fields (e.g. One Tree Hill, Mt. Eden) could conceal earlier phases of eruption, but little is known about their sub-surface deposits. Future eruptions in the AVF could last for decades and involve large-volume outpourings of sub-alkalic basalt as the case of Rangitoto volcano. It is uncertain how long a mantle magma source for small intra-plate basalt volcanoes may be productive and generate eruptions, but the Rangitoto drill core chronology of Linnell et al. (2016) indicates a minimum duration of c. 6000 years.

Figure 29. Borehole seismometer on Rangitoto.

In a further effort to understand the origins of the island, including existing faults and possible seismic activity, University of Auckland and the DEVORA (Determining Volcanic Risk in Auckland) project installed a specialized borehole seismometer into the hole left by the coring (Fig. 29). This records any seismicity that occurs under Rangitoto as well as the surrounding area. Most interest is directed to the question whether small earthquakes occur under Rangitoto that are too small to be seen on seismic recordings from the rest of the Auckland seismic network, and whether faults can be located based on the occurrence of these small events.

Articles on the volcanic risks and potential impacts posed by Auckland volcanoes – covering volcanic petrology to modelling to communication to engineering aspects – are listed on the DEVORA website (e.g. Ashenden et al. 2011; Bebbington and Cronin 2011; Brand et al. 2014; Potter et al. 2014; Tomsen et al. 2014; Bebbington 2015; Blake et al. 2017).

PART 3: A WIDER VIEW − THE AUCKLAND VOLCANIC FIELD (AVF)

Overview

A volcanic field comprises an area where magma production rates are low and numerous eruptions occur at the land surface at widely spaced vents over a period of thousands to hundreds of thousands of years. The AVF (Fig. 31) is an excellent example of such a field, and consists of around 53 volcanoes within a 20-km radius of central Auckland (Kermode 1992; Edbrooke 2001; Hayward et al. 2011a, 2011b, 2017). With the exception of Rangitoto, each volcano likely erupted only once over a period of possibly weeks to several years in a single eruption episode (possibly with multiple phases), and with each eruption episode in a different place so that a new volcanic crater or cone is produced. Hence the term 'monogenetic' is usually applied to such volcanic fields, although the viability of that term has been questioned in light of the work at Rangitoto and elsewhere, as already described in part 2 of the guide. The AVF has been active since c. 200,000 years ago, the oldest known volcano being Pupuke at 193,200 ± 2800 yr BP (Leonard et al. 2017). Rangitoto's latest activity (generating the summit scoria cones) was only about 600 to 550 years ago (c. 1400 to 1450 AD) and the field is considered to be still active and likely to erupt again (summaries of ages of other volcanoes in the AVF are given below).

Some brief basics

The basaltic magma generating Auckland volcanoes derives from the mantle 70–90 km beneath the land surface (Hayward et al. 2011a). Magmas contain almost all of Earth's known chemical elements, but typically they comprise just nine: silicon, oxygen, aluminium, magnesium, iron, calcium, sodium, potassium and titanium. Oxygen and silicon together are the most abundant elements, making up 48–76% by weight of most magmas. The chemistry of magma, especially silicon content, is important for influencing the way it erupts. Three main magma types, and resulting volcanic rocks, are identified on the basis of their chemical composition: andesite, basalt, and rhyolite (Smith et al. 2006).

- Andesite magma is intermediate in composition and physical properties. Erupting at around 800–1,000 °C it is more viscous than basalt, but much less viscous than rhyolite. Andesite magma cools to form dark grey lava if gas-poor, or scoria if gas-rich.
- Basalt is rich in iron and magnesium, but has less silicon than other magmas. It erupts at very high temperatures (around 1100–1200 °C) as a very fluid magma. Basalt magma with little gas cools to form black, dense lava, but where magma erupts with lots of gas it cools to form ragged scoria.
- Rhyolite magma is rich in silicon, potassium and sodium and erupts at temperatures between 700°C and 850 °C as an extremely viscous (sticky) magma. Rhyolite magma containing lots of gas bubbles cools to form pumice. Because it is low in iron, rhyolite is normally light-coloured – it may vary from white to pink or brown. Obsidian is a type of rhyolite produced when lava is chilled to form glass (notes from Smith et al. 2006).

The shape of an Auckland volcano depends on the styles of eruptions that formed it, and its size depends on the volume of magma erupted and the duration of the eruption phases (Hayward et al. 2011a). Three different styles of eruptions in the AVF have resulted in three different types of volcanic rock and three distinct landforms: (1) lava flows, (2) scoria cones (sometimes called cinder cones), and (3) explosion craters or tuff cones/rings (Figs. 30 and 31).

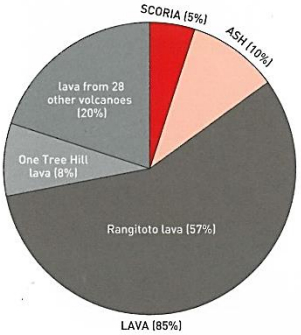

The styles of eruption, types of rock produced and the resulting landforms in Auckland's Volcanic Field

ERUPTION STYLE	SCIENTIFIC TERM	ROCK PRODUCED	LANDFORM
Wet explosive	Phreatomagmatic, Surtseyan	Tuff (hardened volcanic ash)	Explosion crater (maar), tuff cone or tuff ring
Fire-fountaining & fiery explosive	Hawaiian & Strombolian	Scoria (lapilli, cinders), spatter, volcanic bombs	Scoria cone (cinder cone)
Lava outpouring	Strombolian & Hawaiian	Basalt lava	Lava flow, lava field or small lava shield

Figure 30. *Left*: Proportions of lava, scoria, and ash erupted from Auckland volcanoes. *Right*: Relationships between eruption style and landforms in AVF (both from Hayward et al. 2011a, pp.3 and 5).

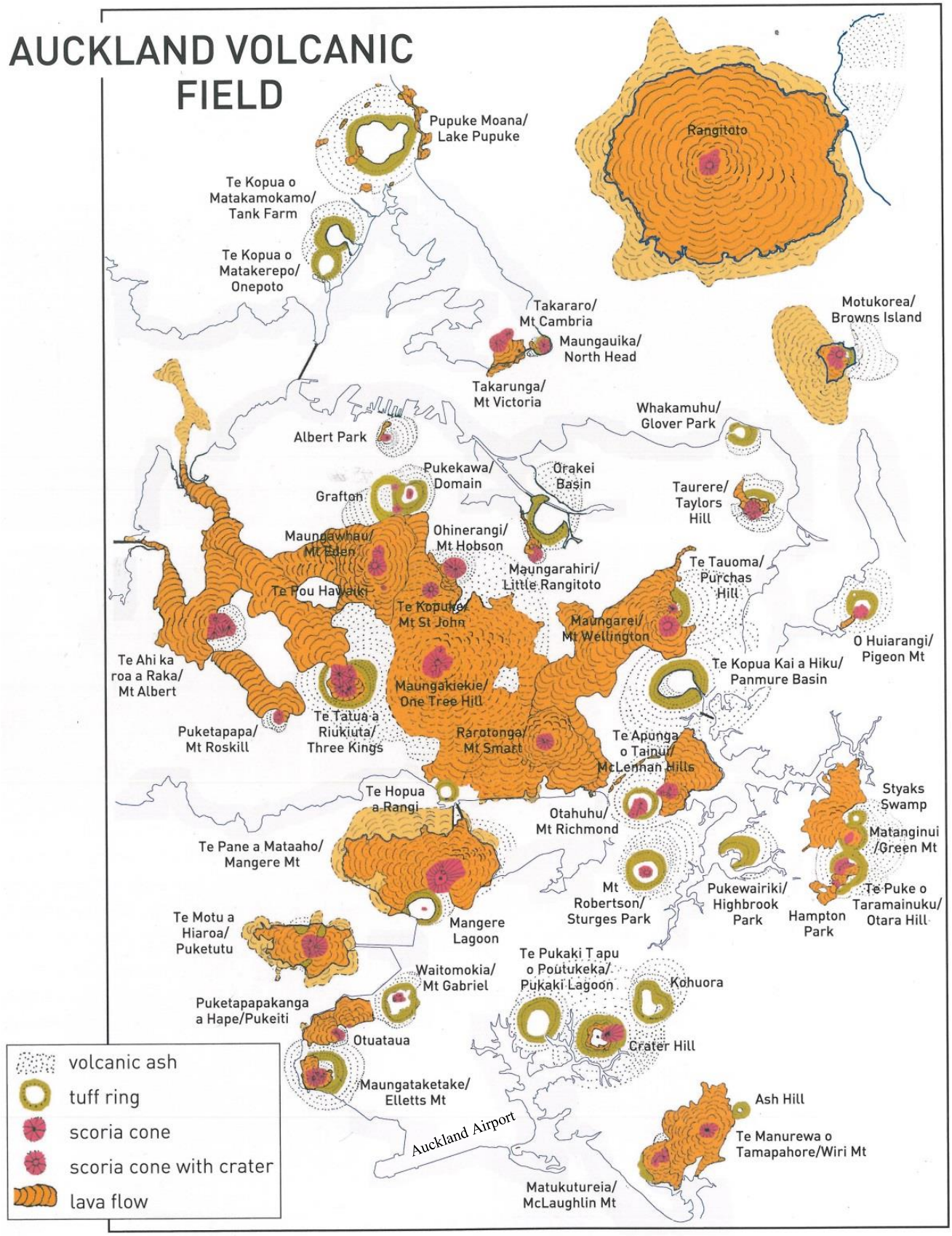

Figure 31. Map of volcanoes making up the AVF, and their eruptive products (from Hayward et al. 2011a, p. 4).

Ages of deposits in the AVF

Dating the individual volcanoes (centres) in the AVF has been problematic for various reasons for a long time (e.g. Nichol 1992; Allen and Smith 1994; Lindsay et al. 2011; Green et al. 2014), but great strides have been made very recently using (1) new $^{40}Ar/^{39}Ar$ dating of lavas (Table 4; Figs. 32 and 33) together with paleomagnetic measurements (Leonard et al. 2017), and (2) further analyses of interfingering basaltic, andesitic, and rhyolitic tephra deposits in cores from maar lakes (tephrostratigraphy) (see below).

Ar/Ar ages

Table 4. Newly published $^{40}Ar/^{39}Ar$ ages for eruptives of AVF (from Leonard et al. 2017, p. 62). Samples dated comprised processed groundmass of dense crystalline lava samples with low glass concentrations (<10%) and feldspar crystals >10 μm wide; mean K_2O content was 1−3 wt%. Named volcano locations are shown in Figs. 31 and 33.

$^{40}Ar/^{39}Ar$ results (in ka) for newly dated Auckland Volcanic Field samples. The interpreted age is given in bold; this is the Weighted Mean Plateau Age (WMPA) for all samples other than Mt. Richmond, for which the isochron age is preferred. See text for details.

Volcano	Experiment	Steps	$^{40}Ar/^{39}Ar$ Weighted mean plateau age				$^{40}Ar/^{39}Ar$ Isochron age					$^{40}Ar/^{39}Ar$ total gas Age (ka)
			Age (ka, ±1 s.d.)	% ^{39}Ar	[#steps: temperaure range(°C)]	MSWD	Age (ka, ±1 s.d.)	% ^{39}Ar	[#steps, temperaure range(°C)]	MSWD	$^{40}Ar/^{36}Ar$	
Pukeiti	11Z0326	10	**11.4 ± 3.6**	96.4	9: 600–1100	1.71	30.9 ± 9.0	96.4	9, 600–1100	1.17	290.5 ± 5.3	6.5 ± 3.0
Motukorea	10Z0238	10	**14.3 ± 6.0**	71.6	8: 600–1000	0.41	26.6 ± 11.7	71.6	8, 600–1000	0.39	294.0 ± 3.1	32.3 ± 8.9
Mt Smart	11Z0322	9	**16.4 ± 1.8**	86.4	6: 600–925	1.02	15.4 ± 4.6	86.4	6, 600–925	1.21	296.0 ± 5.5	15.4 ± 2.0
Green Mtn	11Z0325	9	**19.6 ± 3.3**	84.1	7: 600–925	1.52	24.2 ± 12.8	84.1	7, 600–925	1.77	294.2 ± 7.9	12.4 ± 2.7
Little Rangitoto	10Z0239	11	**20.7 ± 2.2**	78.6	9: 600–1025	0.59	23.6 ± 7.8	78.6	9, 600–1025	0.72	294.1 ± 8.3	24.6 ± 2.9
Mt Eden	11Z0317	9	**21.2 ± 3.3**	86.5	8: 600–975	0.86	19.6 ± 8.3	86.5	8, 600–975	0.99	295.8 ± 4.2	17.9 ± 3.4
Taylors Hill	11Z0321	10	**27.4 ± 1.6**	93.9	9: 600–1100	1.17	23.8 ± 3.0	93.9	9, 600–1100	1.08	297.8 ± 4.2	27.8 ± 1.7
Mt Richmond	10Z0243	10	24.2 ± 2.7	68.1	7: 600–950	1.11	**34.3 ± 4.8**	68.1	7, 600–950	0.42	291.5 ± 3.8	9.7 ± 4.8
McLennan Hills	11Z0335	10	**34.7 ± 2.4**	93.2	9: 600–1100	0.5	39.5 ± 5.4	93.2	9, 600–1100	0.43	293.5 ± 4.8	32.7 ± 2.3
Mt Cambria	10Z0235	11	**42.3 ± 11.1**	95	10: 600–1100	1.65	63.5 ± 23.9	95	10, 600–1100	2.24	294.2 ± 3.2	47.2 ± 10.3
McLaughlins Hill	11Z0328	10	**48.2 ± 3.2**	94.4	9: 600–1100	1.76	53.4 ± 6.1	94.4	9, 600–1100	1.75	293.7 ± 4.1	47.7 ± 2.6
Hopua	11Z0323	10	**51.6 ± 3.2**	89.6	9: 600–1100	0.35	59.7 ± 7.0	89.6	9, 600–1100	0.15	292.2 ± 6.0	49.5 ± 3.1
One Tree Hill	12Z0235	11	**52.8 ± 3.8**	87.5	8: 650–1075	0.66	52.6 ± 8.0	87.5	8, 650–1075	0.77	295.5 ± 6.5	50.3 ± 4.3
Mt Victoria	08Z0260	14	**57.6 ± 7.4**	96	13:600–1250	2.88	54.9 ± 13.8	96	13,600–1250	3.18	295.2 ± 6.4	57.2 ± 6.4
Mt Hobson	11Z0329	10	**56.9 ± 5.8**	98.9	9: 600–1100	1.44	93.9 ± 27.8	98.9	9, 600–1100	1.3	285.7 ± 17.0	56.5 ± 4.9
Mangere	11Z0327	10	**70.3 ± 3.6**	89.3	9: 600–1100	1.11	73.1 ± 7.2	89.3	9, 600–1100	1.23	294.3 ± 5.5	71.6 ± 3.2
Mt St John	11Z0319	10	**75.3 ± 1.7**	92.1	9: 600–1100	1.17	78.9 ± 3.3	92.1	9, 600–1100	1.08	293.4 ± 3.9	74.7 ± 1.7
North Head	10Z0229	13	**87.5 ± 7.6**	96.4	9: 600–1050	1.32	94.9 ± 13.8	96.4	9, 600–1050	2.08	294.7 ± 2.2	102.3 ± 6.9
Maungataketake	10Z0242	10	**88.9 ± 2.4**	70.3	5: 600–800	0.38	82.7 ± 17.0	70.3	5, 600–800	0.55	298.2 ± 17.4	80.2 ± 5.5
Mt Roskill	11Z0330	10	**105.3 ± 3.1**	91.8	9: 600–1100	1.34	114.1 ± 10.2	91.8	9, 600–1100	1.37	291.9 ± 9.2	105.9 ± 2.6
Mt Albert	11Z0324	10	**119.2 ± 2.8**	76.3	7: 600–925	1.24	128.9 ± 5.3	76.3	7, 600–925	0.66	290.6 ± 5.6	110.0 ± 2.5
Albert Park	11Z0320	10	**146.9 ± 2.8**	75.6	5: 600–800	1.21	162.3 ± 10.6	75.6	5, 600–800	0.93	286.1 ± 15.2	139.1 ± 2.7
Pupuke	11Z0331	10	**193.2 ± 2.8**	94.9	9: 600–1100	0.63	199.4 ± 5.4	94.9	9, 600–1100	0.47	291.9 ± 6.3	192.2 ± 3.0

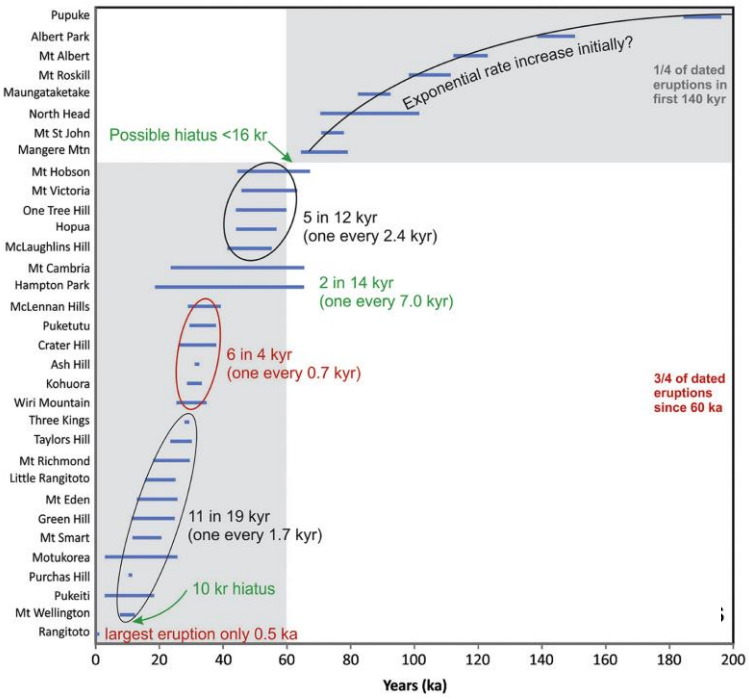

Figure 32. Radiometrically-dated volcanoes of AVF arranged in eruptive sequence (oldest at top) on vertical axis (data from Table 2). Interpretations of eruption tempos over time are indicated on the broad curves (based on radiometrically-dated volcanoes only, remainder omitted). From Leonard et al. (2017, p. 67).

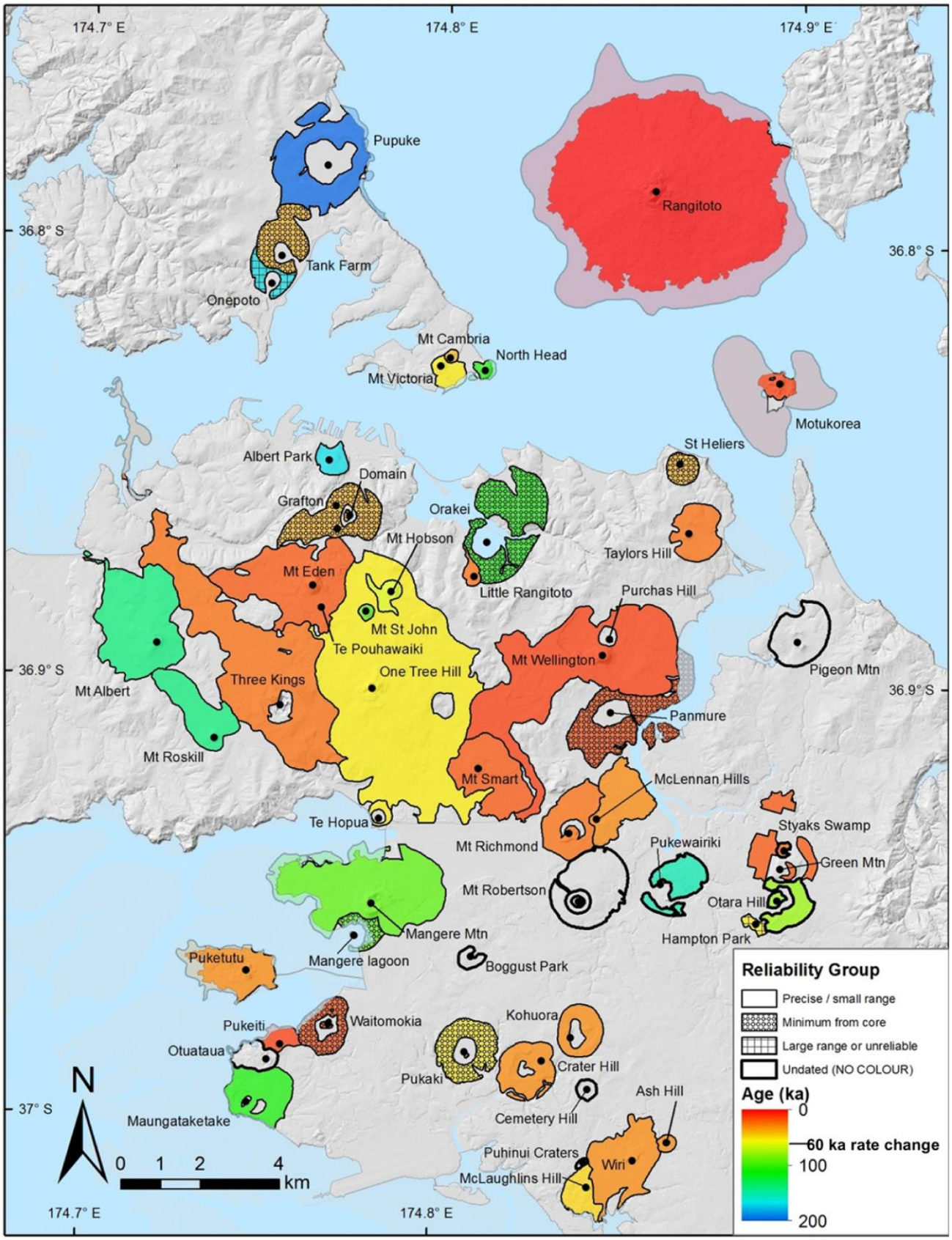

Figure 33. Map of volcanic products of the volcanic centres of AVF coloured by interpreted ages. Hatching indicates broad reliability of age. Bold outline indicates no direct control on age, but colour has been assigned where age can be inferred. From Leonard et al. (2017, p. 69).

Tephrostratigraphy

Tephrostratigraphy involves the use of layers of tephra (Greek, *tephra*, 'ash' or 'ashes') – explosively erupted, loose fragmental volcanic material including volcanic ash (particles <2 mm in diameter) (Lowe 2011) – preserved in lake sediments to help date local basaltic ash layers using stratigraphic relationships (order of occurrence in the sedimentary sequences) and rhyolitic marker tephras of known age (e.g. Newnham and Lowe 1991; Newnham et al. 1999). The tephras also provide isochronous tie points to connect cores from different lakes or peatlands and help to synchronise their time scales, an important role because local radiocarbon dating on lake sediments in Auckland maars has been problematic because of hardwater effects arising from the incorporation of Tertiary-aged fossil shells (i.e. calcareous xenoliths) in basaltic eruptives (e.g. Sandiford et al. 2001). Shane and Smith (2000) were the first to systematically analyse basaltic tephra deposits in the AVF. Despite extensive weathering (in subaerial sections), many of the tephras contained basaltic glass that could be used to geochemically fingerprint the volcanic source and individual eruptive events. They showed the glasses to be predominantly basanites with SiO_2 contents in the range 42-50 wt%. Many individual emplacement units were compositionally homogeneous on the basis of electron microprobe analysis (SiO_2 ± 0.5 wt%), and could be distinguished using TiO_2, CaO, K_2O, and P_2O_5 contents. Although individual tephra beds therefore could be characterised, some deposits displayed a significant compositional range (SiO_2 45–50 wt%) within short stratigraphic sequences that showed no evidence of hiatuses, increasing the difficulty in these cases of matching basaltic tephra deposits to their source (Shane and Smith 2000). Research on the eruptives of Mt Wellington (Maungarei) volcano, including those in nearby Panmure Basin (Te Kōpua Kai a Hiku) (Fig. 31) and other lakes and peats by Shane and Zawalna-Geer (2011) provides a case study of proximal–distal connections able to be achieved through tephrostratigraphy.

Subsequent studies on the basaltic and other tephras (and on cryptotephras since 2013) in sediment cores have been many (e.g. Shane and Hoverd 2002; Shane 2005; Molloy et al. 2009; Shane et al. 2013; Zawalna-Geer et al. 2016). In addition, new methodologies have been developed for the detection and verification of tephras as primary rather than secondary (reworked) deposits in sediments. Hopkins et al. (2015) combined major and trace element glass-shard signatures of basaltic tephras (e.g. Fig. 34) with X-ray density scanning coupled with magnetic susceptibility analysis to identify basaltic glass-shard-bearing layers in lacustrine sediments, all these parameters being used together to distinguish primary from reworked layers (Fig. 35).

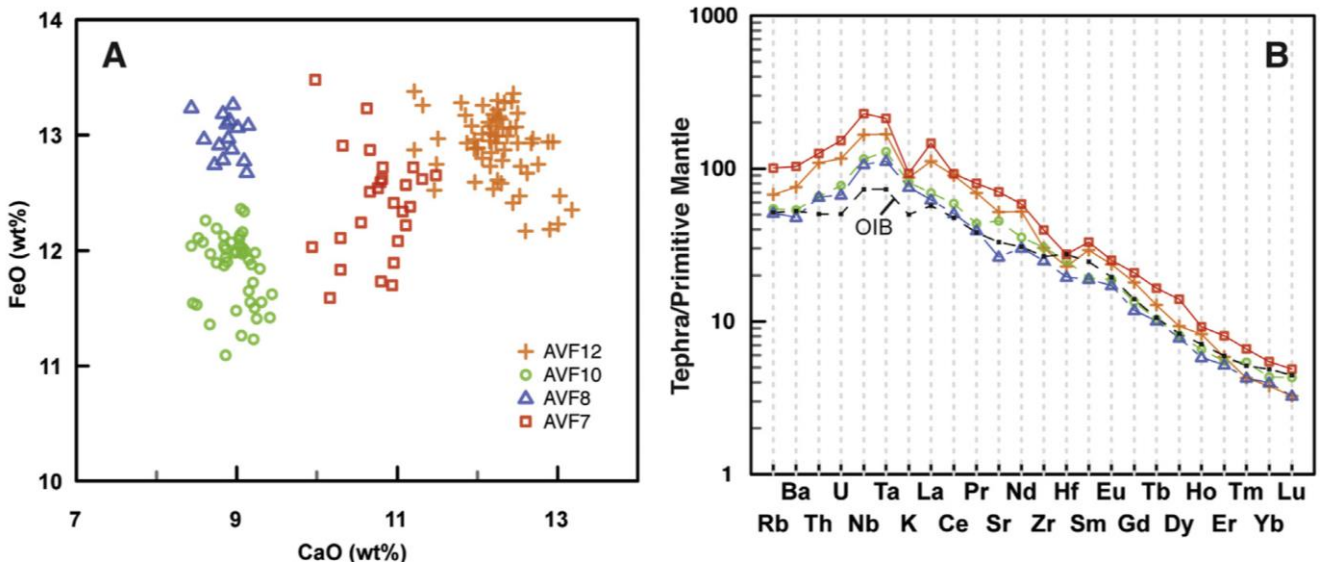

Figure 34. Analyses of glass shards from selected successive basaltic tephra deposits (AVF*n*) from a core from Orakei Basin showing major and trace element variability (from Hopkins et al. 2015, p.64). (**A**) CaO vs. FeO (wt%). (**B**) Primitive mantle-normalized trace element patterns, with OIB (ocean-island basalt) values and normalisation values from Sun and McDonough (1989).

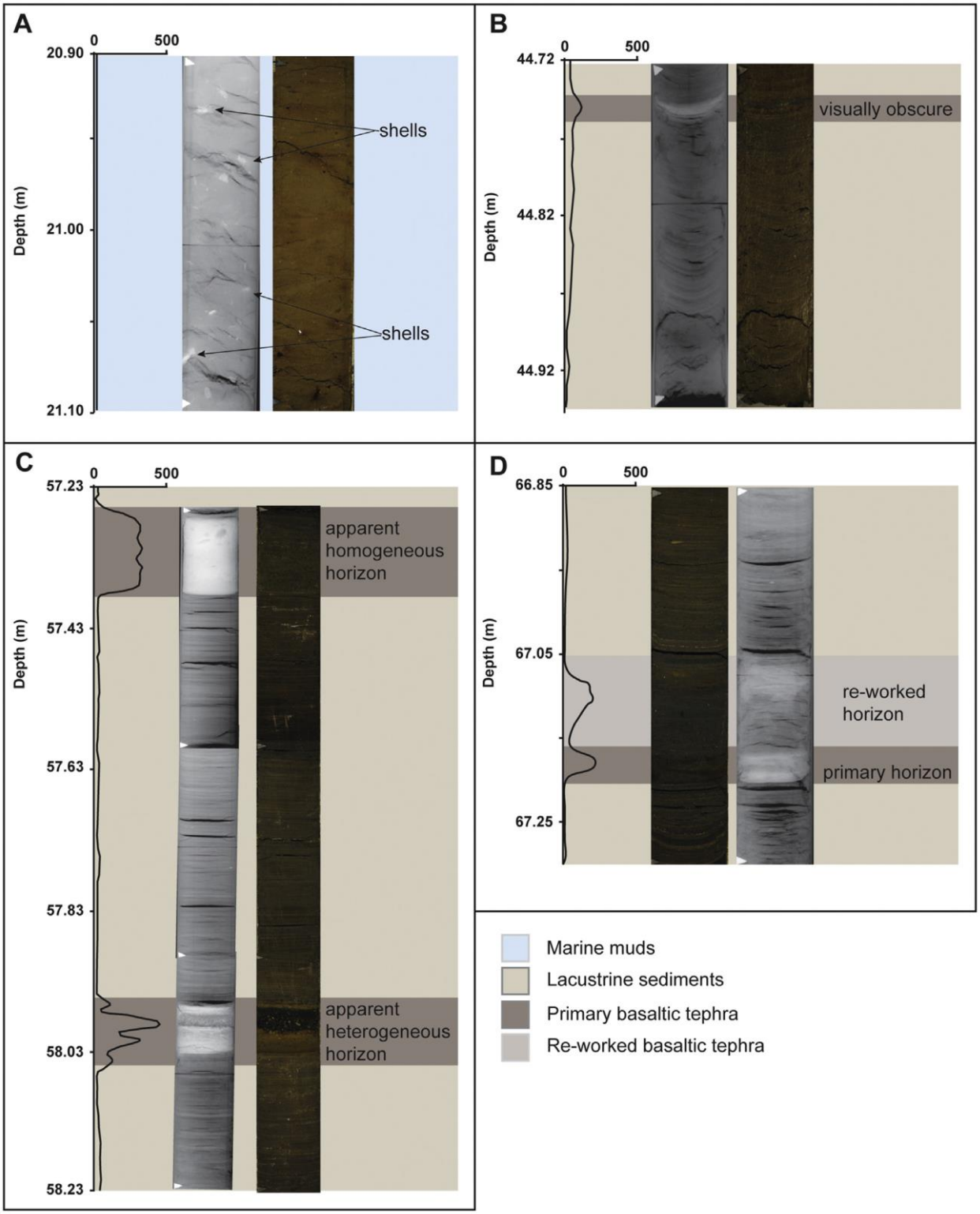

Figure 35. Examples of features evident within a core from Orakei Basin using magnetic susceptibility (curve at left in dimensionless SI units), X-ray density scan (middle image), and photograph (image at right) (from Hopkins et al. 2015, p. 66). (**A**) Intermittent bright signals on the X-ray image picking up shells within marine muds. (**B**) A thin basaltic deposit showing sharp upper and basal contacts in X-ray and magnetic susceptibility but ambiguity in visual observation. (**C**) Two contrasting primary tephra deposits: the upper deposit appears mostly homogeneous, as indicated by uniform X-ray contrast and corresponding magnetic susceptibility peak; in contrast, the lower deposit is more heterogeneous in shard size, as indicated by peaks and troughs in magnetic susceptibility and variable grey-tones in the X-ray imagery. (**D**) Primary and re-worked deposit. The lower labelled band is a primary deposit with a sharp basal contact with a marked sharp contrast in grey scale on the X-ray image and a sharp peak in magnetic susceptibility. The upper-labelled band has a blurred upper and basal contact, a lower contrast in grey scale on X-ray imagery, and more variable magnetic susceptibility levels (Hopkins et al. 2015).

Table 5. Summary of modelled ages for basaltic tephras (denoted AVF*n*) recorded in cores from six maars (Pupuke, Onepoto, Orakei Basin, Glover Park, Hopua, Pukaki) (Fig. 31), together with ages on intercalated distal rhyolitic marker tephras, as determined by Hopkins et al. (2017, p. 11).

Source	abv.	Age	error	ref	interpreted age (yr)	error	95% confidence limits	
AVF24 [P48]*	Ra2	504	5	a				
AVF24 [P49]*	Ra1	553	7	a				
Taupo	Tp	1,718	30	b				
Tuhua	Tu	6,577	547	b				
Mamaku	Ma	7,940	257	b				
Rotoma	Ro	9,423	120	b				
AVF23					9,950	300	9,650	10,240
Opepe	Op	9,991	160	b				
Waiohau	Wh	14,009	155	b				
AVF22					15,310	650	14,660	15,960
Rotorua	Rr	15,635	412	b				
Rerewhakaiaitu	Rk	17,496	462	b				
AVF21					20,080	100	19,080	21,070
AVF20					20,310	142	18,890	21,740
Okareka	Ok	21,858	290	b				
AVF19					24,200	880	23,320	25,090
AVF18					24,260	400	23,860	24,650
AVF17					23,350	350	23,000	23,700
AVF15					24,410	290	24,120	24,700
AVF14					24,550	290	24,270	24,840
Te Rere	Tr	25,171	964	b				
AVF16					25,230	860	24,370	26,090
AVF13					25,230	310	24,920	25,540
Kawakawa/Oruanui	Kk	25,358	162	b				
AVF12					28,030	260	27,760	28,290
Okaia	O	28,621	1428	b				
AVF11					29,770	2240	27,530	32,010
AVF10					30,200	120	30,080	30,320
AVF9					30,200	2080	28,120	32,280
AVF8					30,400	400	30,000	30,810
AVF7					31,040	900	30,140	31,940
AVF6					33,710	1160	32,550	34,870
AVF5					34,200	860	33,340	35,070
AVF4					34,780	2000	32,780	36,780
Maketu	Mk	36,320	575	c				
Tahuna	Ta	39,268	1193	c				
Rotoehu	Re	52,000	7000	d				
AVF3					*59,230*	*10,230*	*49,000*	*69,460*
AVF2					*67,200*	*6,250*	*60,950*	*73,450*
AVF1					*106,170*	*4,300*	*101,870*	*110,470*
AVFa					*126,150*	*3,320*	*122,830*	*129,470*
AVFb					*144,870*	*2,400*	*142,470*	*147,270*
AVFc					*181,430*	*580*	*180,850*	*182,010*
AVFd		193,200	2,800	e				

References: (a) Needham et al. (2011); (b) Lowe et al. (2013); (c) Molloy (2008); (d) D.J. Lowe, *pers. comm* (2016); and (e) Leonard et al. (2017). AVF24 is split into Rangitoto (Ra)1 and 2 identified and dated (^{14}C in cal. yr. BP) by Needham et al. (2011). The ages for the rhyolitic marker horizons (shaded grey) are outlined in cal. yr. BP. The age of AVF17 is shown in grey text as an outlier, and the position of AVF16 also shown in grey text as out of sequence; both of these are discussed in the text. The age of deposit AVFd in the base of the Onepoto core is taken from the minimum ^{40}Ar/^{39}Ar age estimation for Pupuke centre, see text for details. All errors are reported as 2s.d., and the 95% confidence limits are also reported

[a] Nomenclature from Molloy et al. (2009) for the tephra horizons found in the Pupuke core

Most recently, Hopkins et al. (2017) obtained major and trace element glass compositions for distal basaltic tephras from six maar craters (Pupuke, Onepoto, Glover Park, Orakei, Hopua, and Pukaki) and compared these with published and newly obtained whole-rock geochemical data for proximal eruptives in the AVF. The correlations obtained enabled Hopkins et al. (2017) to transfer the newly-acquired Ar/Ar ages obtained on lavas at the source volcanoes to many of the distal basaltic tephra deposits (Table 5). (This chronostratigraphic transfer method is the fundamental basis of tephrochronology, i.e. an age-equivalent dating tool: Lowe et al. 2017.)

The results showed (like Shane and Smith 2000) that not every volcanic centre in the AVF has a unique geochemical signature, thus preventing unambiguous correlation of tephras to source using geochemistry alone (Hopkins et al. 2017). Additional criteria were thus combined to further constrain the sources of the basaltic tephras including age, eruption scale, and location (of centres and lake/maar sites where tephras were sampled). The combination of tephrostratigraphy, $^{40}Ar/^{39}Ar$ dating, and morphostratigraphic features allowed, for the first time, the ordering of 48 of 53 volcanic centres of AVF to be resolved (Fig. 36; Tables 6 and 7).

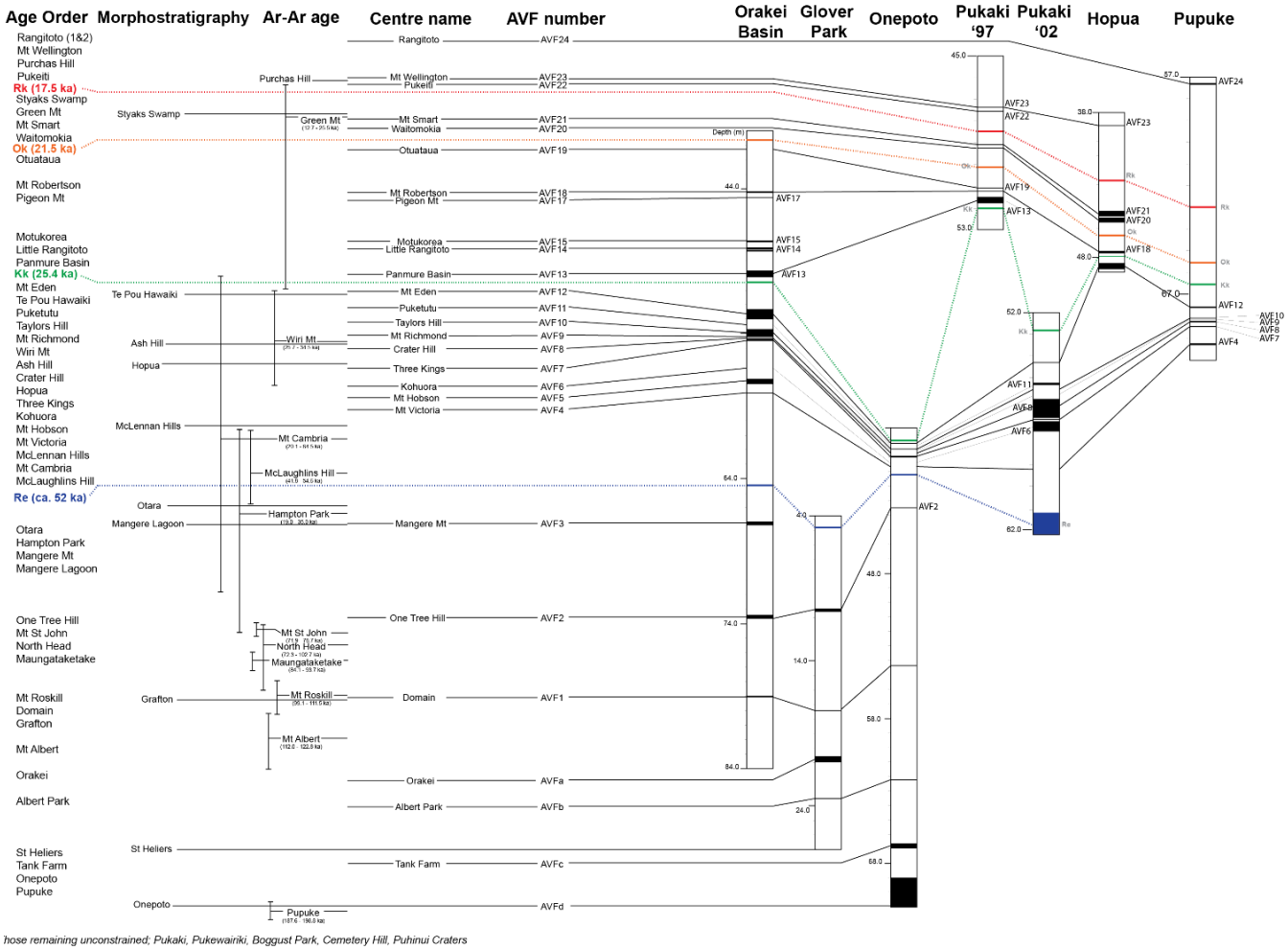

Figure 36. Sequence of eruptives of each centre of the AVF arranged in stratigraphic order and integrated using a combination of tephrostratigraphy, $^{40}Ar/^{39}Ar$ dating, and morphostratigraphic constraints. Key rhyolitic marker horizons are shown in colours, and highlight the chronostratigraphic age limits for the basaltic horizons (AVF numbers). Age ranges depicted by error bars are not to scale. From Hopkins et al. (2017, p. 28).

Table 6. Summary of various features of all 53 volcanic centres in the AVF: name, eruption type, age and method by which it was estimated, relative age relationships (superpositioning), and morphological evidence (from Hopkins et al. 2017, pp. 7-8).

Centre name	Eruption types[a]	Age estimate (ka)			Method	Method reference	Relative ages and relationships based on morphology	DRE volumes $\times 10^6$ m^3			
		Min 2sd	Mean	Max 2sd				Total	Tuff	Scoria cone	Tephra
Albert Park	A, B, C	141.3	146.9	152.5	Ar–Ar	Leonard et al. 2017		27.8	0.82	0.01	0.43
Ash Hill	A	31.4	31.8	32.2	14C	Hayward 2008	Older than Wiri Mt.[b]	0.076	0.05	0.00	0.03
Boggust Park	A? (new)							0.32	0.18	0.00	0.09
Cemetery Hill	(new)							0.24	0.14	0.00	0.07
Crater Hill	A, B, C	26.7	32.1	37.5	Ar–Ar	Cassata et al. 2008	Mono Lake' p.mag excursion[j], younger than Kohuora[a]	24.5	5.88	0.76	4.09
Domain	A, B	52.0			Rotoehu tephra in drill core		Younger than Grafton Park[a], one of the older centres in the AVF[g]	11.4	4.06	0.06	2.11
Grafton Park	A, B	52.0			Morphostratigraphy		Older than Domain[a], one of the older centres in the AVF[g]	11.4	4.06	0.06	2.11
Green Mt.	A, B, C	13.0	19.6	26.2	Ar–Ar	Leonard et al. 2017	Older than Styaks Swamp[a]	12.2	0.36	1.50	2.43
Hampton Park	A, B, C	37.0	55.0	73.0	Ar-Ar	Cassata et al. 2008	Unusual p.mag orientation[j], just older than Otara[a]	2.41	0.11	0.40	0.65
Hopua	A	45.2	51.6	58.0	Ar–Ar	Leonard et al. 2017	Younger than One Tree Hill[a]	0.86	0.31	0.00	0.15
Kohuora	A	32.0	33.0	34.0	14C	Lindsay et al. 2011	Older than Crater Hill[a], contains Kawakawa/Oruanui tephra (>25.4 ka)[h]	7.24	5.10	0.00	2.55
Little Rangitoto	B, C	16.3	20.7	25.1	Ar–Ar	Leonard et al. 2017	Younger than Orakei[a]	1.71	0.00	0.50	0.75
Mangere Lagoon	A, B	63.1			Morphostratigraphy		Just older than Mangere Mt[k]	2.04	0.71	0.01	0.37
Mangere Mt	B, C	63.1	70.3	77.5	Ar–Ar	Leonard et al. 2017	Just younger than Mangere Lagoon[k], younger than One Tree Hill[a]	46.2	0.00	15.01	22.51
Maungataketake	A, B, C	84.1	88.9	93.7	Ar–Ar	Leonard et al. 2017	Sea cut platform from last interglacial[a]	33.6	4.40	0.87	3.51
McLaughlins Hill	A, B, C	41.8	48.2	54.6	Ar–Ar	Leonard et al. 2017	Older than Wiri Mt[a,b]	7.58	0.51	0.43	0.90
McLennan Hills	A, B, C	29.9	34.7	39.5	Ar–Ar	Leonard et al. 2017	Laschamp p.mag excursion[j], older than Mt. Richmond[a]	21.9	0.42	3.79	5.90
Motukorea	A, B, C	2.3	14.3	26.3	Ar–Ar	Leonard et al. 2017		4.56	0.66	1.31	2.30
Mt. Albert	A, B, C	113.6	119.2	124.8	Ar–Ar	Leonard et al. 2017	Older than Mt. Eden and Mt. Roskill[a]	22.9	0.35	3.03	4.72
Mt. Cambria	B, C	20.1	42.3	64.5	Ar–Ar	Leonard et al. 2017		0.29	0.00	0.29	0.44
Mt. Eden	B, C	14.6	21.2	27.8	Ar–Ar	Leonard et al. 2017	Much younger than Mt. St John, younger than Three Kings, Mt. Hobson[a], One Tree Hill, and Domain[g]	89.8	0.00	5.94	8.92
Mt. Hobson	B, C	45.3	56.9	68.5	Ar–Ar	Leonard et al. 2017	Older than Three Kings[a]	6.68	0.00	1.20	1.80
Mt. Richmond	A, B	24.7	34.3	43.9	Ar–Ar	Leonard et al. 2017	Mono Lake' p.mag excursion[j], younger than McLennan Hills[a], older than Okaia tephra (28.6 ka)[d]	5.67	1.17	3.04	5.14
Mt. Robertson	A, B							2.72	1.01	0.24	0.87
Mt. Roskill	A, B, C	99.1	105.3	111.5	Ar–Ar	Leonard et al. 2017	Post–Blake p.mag excursion[j], younger than Mt. Albert[a]	14.4	0.02	1.37	2.07
Mt. Smart	A, B, C	12.8	16.4	20.0	Ar–Ar	Leonard et al. 2017	Younger than One Tree Hill[a]	13.4	0.00	2.34	3.52
Mt. St John	B, C	71.9	75.3	78.7	Ar–Ar	Leonard et al. 2017	Much older than Mt. Eden and Three Kings[a]	28.1	0.00	0.40	0.60
Mt. Victoria	B, C	42.8	57.6	72.4	Ar–Ar	Leonard et al. 2017		4.81	0.00	2.58	3.87
Mt. Wellington	B, C	9.3	10.3	11.3	14C	Lindsay et al. 2011	Just younger than Purchas Hill[a]	82.3	1.93	3.02	5.49
North Head	A, B	72.3	87.5	102.7	Ar–Ar	Leonard et al. 2017	Raised sea levels ca. 128–116 ka[i]	2.65	1.12	0.04	0.61
One Tree Hill	B, C	45.2	52.8	60.4	Ar–Ar	Leonard et al. 2017	Older than Hopua, Mt. Hobson, Mt. Eden, Mt. Smart, Three Kings, One Tree Hill[a]	260	0.00	5.70	8.56
Onepoto	A	52.0			Rotoehu tephra in drill core		Similar age to Pupuke and Tank Farm[a]	2.62	1.54	0.00	0.77
Orakei	A	85.0		130.0	sed. rate ages of tephra horizons	Molloy et al. 2009	Not breached in last interglacial, older than Little Rangitoto[a]	6.70	3.77	0.00	1.89
Otara	A, B, C	0.0		73.0	Morphostratigraphy		Unusual p.mag orientation, just younger than Hampton Park[a]	2.30	0.11	0.70	1.10
Ouataua	A, B, C							6.30	0.00	0.99	1.49
Panmure Basin	A, B	17.5			Rerewhakaaitu tephra in drill core		Older than Rerewhakaaitu (17 ka[c])	7.44	4.65	0.30	2.77
Pigeon Mt	A, B, C							3.31	1.33	0.28	1.08
Puhinui Craters	A? (new)						–	–	–	–	
Pukaki	A	52.0			Core extent			9.19	7.10	0.00	3.55
Pukeiti	B, C	4.2	11.4	18.6	Ar–Ar	Leonard et al. 2017	Younger than Otuataua[a]	3.70	0.00	0.44	0.66
Puketutu	B, C	29.8	33.6	37.4	Ar–Ar	Cassata et al. 2008	Paleomag excursion (32.4 ± 0.3 ka)	11.0	3.00	2.15	4.72
Pukewairiki	A, C	130.0			Morphostratigraphy		Sea cut platform from last interglacial[a]	17.5	2.29	0.00	1.15
Pupuke	C, B, A	187.6	193.2	198.8	Ar–Ar	Leonard et al. 2017	Similar age to Tank Farm and Onepoto[a]	46.7	20.11	0.00	10.06
Purchas Hill	A, B	10.7	10.9	11.1	14C	Lindsay et al. 2011	Just older than Mt. Wellington[a]	1.68	0.21	0.03	0.14
Rangitoto 2	A, B, C	0.494	0.504	0.514	14C	Needham et al. 2011	Youngest in the field[a]	699	4.65	41.60	64.73
Rangitoto 1	A, B, C	0.539	0.553	0.567	14C; Needham et al. 2011	Needham et al. 2011					
St Heliers	A	52.0			Rotoehu tephra in drill core			2.20	1.23	0.00	0.62
Styaks Swamp	A	0.0		24.5	Morphostratigraphy		Just younger than Green Mt[a]	0.37	0.25	0.00	0.12
Tank Farm	A	52.0			Morphostratigraphy		Similar age to Onepoto and Pupuke[a]	5.87	4.13	0.00	2.06
Taylors Hill	A, B, C	24.2	27.4	30.6	Ar–Ar	Leonard et al. 2017	Mono Lake' p.mag excursion[j]	5.07	0.47	0.18	0.51
Te Pou Hawaiki	B	14.6			Morphostratigraphy		Older than Mt. Eden [c]	28.1	0.00	0.08	0.12
Three Kings	A, B, C	27.7	28.7	29.7	14C	Lindsay et al. 2011	Younger than One Tree Hill, Mt. St John, Mt. Hobson, older than Mt. Eden[a]	69.3	0.00	3.00	4.51
Waitomokia	A, B	15.6			Morphostratigraphy		Core contains Rotorua tephra, older than Pukeiti[a]	9.79	2.30	0.11	1.31
Wiri	A, B, C	25.6	30.2	34.8	Ar–Ar	Cassata et al. 2008	Mono Lake' p.mag excursion[j], younger than Ash Hill[b]	16.4	0.08	0.86	1.34

Sources are (a) Hayward et al. (2011); (b) Allen and Smith (1994); (c) Affleck et al. (2001); (d) Sandiford et al. (2002); (e) Lowe et al. (2013); (f) Lindsay et al. (2011); (g) Kermode (1992); (h) Newnham et al. (2007); (i) Agustín-Flores et al. (2015); (j) Leonard et al. (2017); (k) Hayward et al. (2016); the estimated dense rock equivalent (DRE) volumes for the total, tuff ring, and scoria cone from Kereszturi et al. (2013); and the calculated tephra volumes using the equation reported in Kawabata et al. (2015). For the eruption types, (A) phreatomagmatic wet explosive eruption which produces maar craters and tuff rings, (B) dry magmatic eruptions including fire fountaining creating scoria cones, and (C) effusive eruptions resulting in lava flows, and shield building

Table 7. Ages of volcanoes of AVF (from Leonard et al. 2017, p. 65).

Age ranges for Auckland Volcanic Field eruptions including all studies; this study in bold. Age sources: a = summarised in Lindsay et al. (2011); b = Cassata et al. (2008); c = Needham et al. (2011); d = Hayward et al. (2011b). Pukeiti is listed out of mean age order (see text). Centres highlighted with a (#) have their ages assigned as composite mean ages with 1 σ error based on two previously reported dates. Styaks Swamp and Otara Hill (*) are assigned ages based on stratigraphic restrictions; Styaks Swamp is younger than Green Mtn (Hayward et al., 2011a), therefore the maximum age for Green Mtn is assigned. Similarly Otara Hill is younger than Hampton Park (Hayward et al., 2011a), therefore the maximum age for Hampton Park (H. Park) is assigned. For age limits assigned based on tephra horizons found within cores, ages for Rotorua, Rerewhakaaitu, Okaia and Kawakawa are from Lowe et al. (2013); and for Rotoehu from Danišík et al. (2012) reported as a minimum age. For paleomagnetic data; α_{95} = radius cone of confidence for mean direction at 95% probability; Ref. = references as follows: s = Shibuya et al. (1992); c = Cassidy (2006); Or. = paleomagnetic orientation, colour coded and labelled where established as: N = Normal polarity; H = Hilina Pali excursion (orange); A = Mono Lake excursion (pink); L = Laschamp excursion (beige); ? = uncertain ages with unusual inclinations and declinations (peach); B = post-Blake excursion (yellow). ^{14}C ages are cal BP (i.e. before 1950).

Name	Age (ka, 1 σ)	Age control	Age source	Paleomagnetic Details					
				Inclination	Declination	α_{95}	Colatitude	Ref.	Or.
Rangitoto 2	0.504 ± 0.005	^{14}C	c						
Rangitoto 1	0.553 ± 0.007	^{14}C	c	−58.7°	358.6°	0.9°	2.9°	s	N
				−61.3°	2.9°	1.5°	6.0°	s	N
Mt Wellington#	10.3 ±0.5	^{14}C	a	−51.9°	9.9°	4.8°	9.2°	s	N
Purchas Hill	10.9± 0.1	^{14}C	a						
Pukeiti	**11.4 ± 3.6**	**$^{40}Ar/^{39}Ar$**	**This study**						
Motukorea	**14.3 ± 6.0**	**$^{40}Ar/^{39}Ar$**	**This study**	−57.3°	0.1°	3.6°	1.1°	s	N
Mt Smart	**16.4 ± 1.8**	**$^{40}Ar/^{39}Ar$**	**This study**	−60.1°	28.9°	2.3°	22.8°	s	H?
Styaks Swamp*	<19.6 (<Grn Mt)	Max	a (stratigraphy)						
Green Mtn	**19.6 ± 3.3**	**$^{40}Ar/^{39}Ar$**	**This study**	−48.7°	343.3°	1.7°	15.7°	s	N
Little Rangitoto	**20.7 ± 2.2**	**$^{40}Ar/^{39}Ar$**	**This study**						
Mt Eden	**21.2 ± 3.3**	**$^{40}Ar/^{39}Ar$**	**This study**	−74.7°	329.1°	2.5°	31.0°	s	H?
				−72.9°	328.4°	3.8°	29.7°	s	H?
Taylors Hill	**27.4 ± 1.6**	**$^{40}Ar/^{39}Ar$**	**This study**	58°	342°	4°	78°	c	A
Wiri Mountain#	30.1 ± 2.2	$^{40}Ar/^{39}Ar$	b (Wiri B)	62°	355°	2°	80°	s	A
	31.0 ± 1.4	$^{40}Ar/^{39}Ar$	b (Wiri A)						
Crater Hill	32.1 ± 2.7	$^{40}Ar/^{39}Ar$	b	63°	352°	5°	82°	s	A
Puketutu	33.6 ± 1.9	$^{40}Ar/^{39}Ar$	b	62°	3°	4°	80°	s	A
Mt Richmond	**34.3 ± 4.8**	**$^{40}Ar/^{39}Ar$**	**This study**	62°	345°	7°	81°	s	A
Three Kings#	28.7 ± 0.5	^{14}C	a	−50.3°	3.3°	1.9°	6.4°	s	N
Ash Hill	31.8 ± 0.2	^{14}C	a						
Kohuora#	34.4 ± 2.1	^{14}C	a						
McLennan Hills	**34.7 ± 2.4**	**$^{40}Ar/^{39}Ar$**	**This study**	−22.4°	165.8°	5.0°	129.6°	s	L?
	39.1 ± 2.1	$^{40}Ar/^{39}Ar$	b						
Otara Hill*	<37.5 (<H. Park)	Max	a (stratigraphy)	−43.8°	248.6°	4.1°	90.2°	s	?
Hampton Park	37.5 ± 3.0	$^{40}Ar/^{39}Ar$	b	−36.0°	263.6°	3.4°	83.0°	s	?
Mt Cambria	**42.3 ± 11.1**	**$^{40}Ar/^{39}Ar$**	**This study**						
McLaughlins Hill	**48.2 ± 3.2**	**$^{40}Ar/^{39}Ar$**	**This study**	−49.7°	7.5°	5.6°	9.0°	s	N
Hopua	**51.6 ± 3.2**	**$^{40}Ar/^{39}Ar$**	**This study**						
One Tree Hill	**52.8 ± 3.8**	**$^{40}Ar/^{39}Ar$**	**This study**	−50.1°	21.7°	4.6°	18.9°	s	N
Mt Victoria	**57.6 ± 7.4**	**$^{40}Ar/^{39}Ar$**	**This study**	−49.7°	356.2°	3.1°	7.1°	s	N
Mt Hobson	**56.9 ± 5.8**	**$^{40}Ar/^{39}Ar$**	**This study**						
Mangere	**70.3 ± 3.6**	**$^{40}Ar/^{39}Ar$**	**This study**	−45.9°	357.5°	3.3°	9.9°	s	N
Mt St John	**75.3 ± 1.7**	**$^{40}Ar/^{39}Ar$**	**This study**						
North Head	**87.5 ± 7.6**	**$^{40}Ar/^{39}Ar$**	**This study**						
Maungataketake	**88.9 ± 2.4**	**$^{40}Ar/^{39}Ar$**	**This study**	−51.4°	1.9°	2.6°	5.1°	s	N
Mt Roskill	**105.3 ± 3.1**	**$^{40}Ar/^{39}Ar$**	**This study**	−68.2°	352.7°	6.2°	25.3°	s	B?
Mt Albert	**119.2 ± 2.8**	**$^{40}Ar/^{39}Ar$**	**This study**						
Albert Park	**146.9 ± 2.8**	**$^{40}Ar/^{39}Ar$**	**This study**						
Pupuke	**193.2 ± 2.8**	**$^{40}Ar/^{39}Ar$**	**This study**	−65.3°	357.8°	2.4°	10.6°	s	N
Waitomokia	>15.2	Min	a (stratigraphy; core contains Rotorua tephra)						
Panmure Basin	>17.0	Min	a (stratigraphy; core contains Rerewhakaiitu tephra)						
St Heliers	>45	Min	a (stratigraphy; core contains Rotoehu tephra)						
Tank Farm	>45	Min	a (stratigraphy)						
Domain	>45	Min	a (stratigraphy; contains Rotoehu tephra)						
Grafton Park	>45	Min	a (stratigraphy; older than the Domain)						
Pukaki	>52	Min	a (core length)						
Mangere Lagoon	>70.3 ± 3.6	Min	a (stratigraphy; older than Mangere)						
Orakei Basin	>85	Min	a (core length)						
Pukewairiki	>130	Min	a (shore cut platform)						
Onepoto	>150	Min	Unpublished $^{40}Ar/^{39}Ar$						

Table 7 contd

Boggust Park	>130	Min	d (Breached by Last Interglacial sea–level highstand)
Te Pou Hawaiki			No data
Otuataua			No data
Puhinui Craters			No data
Mt Robertson			No data
Cemetery Hill			No data
Pigeon Mountain			No data

Palaeoclimatic and other studies involving lake sediments

The sediments deposited in crater lakes provide a gold-mine of environmental change as well as a record of volcanic activity, and more than 10 lakes and lagoons have now been drilled or cored in the AVF (Hayward et al. 2011a; Augustinus 2016). In some lakes, the sediments are laminated. Various components including pollen have been extracted from the sediments and analysed by groups of specialist scientists in multidisciplinary palaeolimnological or geochronological projects (e.g. Newnham et al. 2007; Augustinus et al. 2008, 2011, 2012; Nilsson et al. 2011; Stephens et al. 2012a, 2012b; Striewski et al. 2013; Hopkins et al. 2015), and volcanic history and hazards assessment projects (e.g. Newnham et al. 1999; Shane and Hoverd 2002; Molloy et al. 2009; McGee and Smith 2016; Zawalna-Geer et al. 2016; Hopkins et al. 2017). Most studies relate to the pre-Holocene because, except for Lake Pupuke, the Auckland maars were breached by postglacial marine transgression and associated marine sediment flux that terminated lacustrine deposition (Hayward et al. 2011a). Studies of the Holocene, and of human impacts, from lake sediment or peat analysis include those of Newnham and Lowe (1991), Horrocks et al. (2001, 2002, 2005), Augustinus et al. (2006), Striewski et al. (2009), Heyng et al. (2014), and Newnham et al. (2017).

Climate event stratigraphy

A review of past climates of New Zealand since 30,000 years ago was developed by Barrell et al. (2013) for the NZ INTIMATE project (INTegration of Ice core, MArine, and TErrestrial records). They identified a sequence of climatic events, spanning the onset of cold conditions marking the final phase of the Last Glaciation, through to the emergence to full interglacial conditions in the early Holocene. To facilitate more detailed assessments of climate variability, a composite stratotype was proposed as a climate event stratigraphy for New Zealand. It was based on terrestrial stratigraphic records. The type records were selected on the basis of having very good numerical age control and a clear proxy record. In all cases the proxy of the type record is pollen. The type record for the emergence from glacial conditions following the termination of the Last Glaciation (post-Termination amelioration) is in a core of lake sediments from Pukaki crater near Auckland International Airport (Fig. 31), and spans the period from c. 18,000 to 15,600 cal. years ago (Barrell et al. 2013). Further palaeoclimatic research currently being undertaken in New Zealand includes work under the aegis of the International Focus Group “Southern Hemisphere Assessment of PalaeoEnvironments” (SHAPE), which replaced the NZ INTIMATE project.

Acknowledgements

We thank Martin Brook (field trip coordinator) and Stephanie Szmurlo (conference event manager) for their help with logistical and administrative support for this trip. At the time of writing, around 45 participants were booked on the excursion. Jenni Hopkins provided several ‘top copies’ of figures from Hopkins et al. (2017), and Bruce Hayward provided a preprint of Hayward (2107). Max Oulton is thanked for preparing Fig. 11, and Waikato print (University of Waikato) for expertly printing the guides. The guide is a much-revised and expanded version of earlier guides by Lindsay et al. (2010), Smith et al. (2012), and Lowe et al. (2016). Further information on Auckland and its volcanoes, including Rangitoto, is provided by Hayward et al. (2011a, 2017). Another colourful book on the area is that of Homer et al. (2000). Wilcox (2007a) comprehensively covers the natural history of the island. Research on “Reconstructing Rangitoto” based on analyses of drill core obtained in February 2014, described in the guide, was supported by the Earthquake Commission (EQC project 14/U684). The leaders/authors acknowledge support of the Universities of Waikato and Auckland, and Unitec Institute of Technology, in developing and running the trip and preparing the guide. The guidebook is an output of the EXTRAS project “EXTending TephRAS as a global geoscientific research tool stratigraphically, spatially, analytically, and temporally within the Quaternary”, an initiative of the International Focus Group of Tephrochronology and Volcanism (INTAV) (http://www.comp.tmu.ac.jp/tephra/intavtmu/pg772.html) supported by the Stratigraphy and Chronology Commission (SACCOM) of the International Union for Quaternary Research (INQUA).

References

Affleck, D.K., Cassidy, J., Locke, C.A. 2001. Te Pou Hawaiki volcano and pre-volcanic topography in central Auckland: volcanological and hydrogeological implications. *New Zealand Journal of Geology and Geophysics* 44, 313-321.

Agustín-Flores, J., Németh, K., Cronin, S.J., Lindsay, J.M., Kereszturi, G. 2015. Construction of the North Head (Maungauika) tuff cone: a product of Surtseyan volcanism, rare in the Auckland Volcanic Field, New Zealand. *Bulletin of Volcanology* 77, 11.

Allen, S.R., Smith, I.E.M., 1994. Eruption styles and volcanic hazard in the Auckland Volcanic Field, New Zealand. *Geoscience Reports of Shizuoka University* 20, 5-14.

Anderson, A.J. 1991. The chronology of colonization in New Zealand. *Antiquity* 65, 767-695.

Anderson, A.J. 2013. A fragile plenty: pre-European Māori and the New Zealand environment. *In*: Pawson, E., Brooking, T. (editors) Making a New Land: Environmental Histories of New Zealand, new edition. Otago University Press, Dunedin, pp. 35-51.

Anderson, A. 2015a. Speaking of migration AD 1150-1450*. In*: Anderson, A., Harris, A., Williams, B. (editors), Tangata Whenua – An Illustrated History. Bridget Williams Books, Auckland, pp. 42-69.

Anderson, A.J. 2015b. Emerging Societies AD 1500-1800*. In*: Anderson, A., Harris, A., Williams, B. (editors), Tangata Whenua – An Illustrated History. Bridget Williams Books, Auckland, pp. 120-130.

Anderson, A.J. 2016.The making of the Māori Middle Ages. J.D. Stout Lecture 2016. *Journal of New Zealand Studie*s NS23, 2-18.

Ashenden, C.L., Lindsay, J.M., Sherburn, S., Smith, I.E.M., Miller, C., Malin, P. 2011. Some challenges of monitoring a potentially active volcanic field in a large urban area: Auckland Volcanic Field, New Zealand. *Natural Hazards* 59, 507-528.

Augustinus, P.C. 2016. Probing the history of New Zealand's Orakei maar. *Eos* 97*,* https://eos.org/project-updates/probing-the-history-of-new-zealands-orakei-maar.

Augustinus, P.C., Reid, M., Andersson, S., Deng Y., Horrocks, M. 2006. Biological and geochemical record of anthropogenic impacts in recent sediments from Lake Pupuke, Auckland City, New Zealand. *Journal of Paleolimnology* 35, 789-805.

Augustinus, P., Bleakley, N., Deng, Y., Shane, P., Cochrane, U. 2008. Rapid change in early Holocene environments inferred from Lake Pupuke, Auckland City, New Zealand. *Journal of Quaternary Science* 23, 435-447.

Augustinus, P., D'Costa, D., Deng, Y., Hagg, J., Shane, P. 2011. A multi-proxy record of changing environments from ca. 30 000 to 9000 cal. a BP: Onepoto maar palaeolake, Auckland, New Zealand. *Journal of Quaternary Science* 26, 389-401.

Augustinus, P., Cochrane, U., Kattel, G., D'Costa, D., Shane, P., 2012. Late Quaternary paleolimnology of Onepoto maar, Auckland, New Zealand: implications for the drivers of regional paleoclimate. *Quaternary International* 253, 18-31.

Balance, P.F., Smith, I.E.M. 1982. Walks through Auckland's geological past: a guide to the geological formations of Rangitoto, Motutapu, and Motuihe islands. *Geological Society of New Zealand Guidebook* 5, 24 pp.

Barrell, D.J.A., Almond, P.C., Vandergoes, M.J., Lowe, D.J., Newnham, R.M., NZ-INTIMATE members 2013. A composite pollen-based stratotype for inter-regional evaluation of climatic events in New Zealand over the past 30,000 years (NZ-INTIMATE project). *Quaternary Science Reviews* 74, 4-20.

Bebbington, M. 2015. Spatio-volumetric hazard estimation in the Auckland Volcanic Field. *Bulletin of Volcanology* 77, 39.

Bebbington, M.S., Cronin, S.J. 2011. Spatio-temporal hazard estimation in the Auckland Volcanic Field, New Zealand, with a new event-order model. *Bulletin of Volcanology* 73, 55-72.

Blake, D.I.M., Deligne, N.I., Wilson, T.M., Lindsay, J.M., Woods, R. 2017. Investigating the consequences of urban volcanism using a scenario approach II: Insights into transportation network damage and functionality. *Journal of Volcanology and Geothermal Research* 340, 92-116.

Brand, B.D., Gravley, D., Clarke, A., Lindsay, J., Boomberg, S.H., Agustin-Flores, J., Németh, K. 2014. Combined field and numerical approach to understanding dilute pyroclastic density current dynamics and hazard potential: Auckland Volcanic Field, New Zealand. *Journal of Volcanology and Geothermal Research* 276, 215-232.

Brothers, R.N., Golson, J. 1959. Geological and archaeological interpretation of a section in Rangitoto ash on Motutapu Island, Auckland. *New Zealand Journal of Geology and Geophysics* 2, 569-577.

Bulmer, S. 1994. Sources for the archaeology of the Maaori settlement of the Taamaki volcanic district. *New Zealand Department of Conservation Science and Research Series* 63, 1-33.

Cassata, W.S., Singer, B.S., Cassidy, J. 2008. Laschamp and Mono Lake geomagnetic excursions recorded in New Zealand. *Earth and Planetary Science Letters* 268, 76-88.

Cassidy, J., 2006. Geomagnetic excursion captured by multiple volcanoes in a monogenetic field. *Geophysical Research Letters* 33, L21310.
Churchman, G.J., Lowe, D.J. 2012. Alteration, formation, and occurrence of minerals in soils. *In*: Huang, P.M., Li, Y., Sumner, M.E. (editors) Handbook of Soil Sciences, 2nd edition. Vol. 1: Properties and Processes. CRC Press, Boca Raton, FL, pp.20.1-20.72.
Clarkson, B.D. 1990. A review of vegetation development following recent (<450 years) volcanic disturbance in North Island, New Zealand. *New Zealand Journal of Ecology* 14, 59-71.
Clarkson, B.D., Clarkson, B.R., Juvik, J.O. 2015. Pattern and process of vegetation change (succession) on two northern New Zealand island volcanoes. *Surtsey Research* 13, 45-48.
Davidson, J. M. 1978a. The prehistory of Motutapu Island, New Zealand: five centuries of Polynesian occupation in a changing landscape. *Journal of the Polynesian Society* 87**,** 327-337.
Davidson, J.M. 1978b. Auckland prehistory: a review. *Records of the Auckland Institute and Museum* 15, 1-14.
Daly, M., Johnston D. 2015**.** The genesis of volcanic risk assessment for the Auckland engineering lifelines project: 1996–2000. *Journal of Applied Volcanology* 4, 1-17.
Danisík, M., Schmitt, A.K., Lovera, O.M., Dunkl, I., Evans, N.J. 2017. Application of the combined U-Th-disequilibrium/U-Pb and (U-Th)/He zircon dating to tephrochronology. *Quaternary Geochronology* 40, 23-32.
Daymond-King, P., Hayward, B.W. 2015. Just 600 years of erosion on Rangitoto's coast. *Geocene (Auckland GeoClub Magazine)* 12, 5-7.
de Lange, P.J., Rolfe, J.R., Champion, P.D., Courtney, S.P., Heenan, P.B., Barkla, J.W., Cameron, E.K., Norton, D.A., Hitchmough, R.A. 2013. Conservation status of New Zealand indigenous vascular plants, 2012. *New Zealand Threat Classification Series 3*. New Zealand Department of Conservation. Available at: http://www.doc.govt.nz/publications/science-and-technical/products/series/new-zealand-threat-classification-series/
Dodd, A. 2008. Motutapu Archaeological and Historic Landscapes: Heritage Assessment. Department of Conservation, Auckland, 36 pp. http://www.doc.govt.nz/Documents/conservation/historic/by-region/auckland/motutapu-island/motutapu-archaeooglical-and-historic-landscapes-heritageassessment-full.pdf
Edbrooke, S.W. (compiler) 2001. Geology of the Auckland area. Institute of Geological and Nuclear Sciences 1: 250 000 Geological Map 3. 1 sheet + 74 pp, Institute of Geological and Nuclear Sciences, Lower Hutt.
Froggatt, P.C., Lowe, D.J. 1990. A review of late Quaternary silicic and some other tephra formations from New Zealand: their stratigraphy, nomenclature, distribution, volume, and age. *New Zealand Journal of Geology and Geophysics* 33, 89-109.
Green, R.M., Bebbington, M.S., Cronin, S.J., Jones, G. 2014. Automated statistical matching of multiple tephra records exemplified using five long maar sequences younger than 75 ka, Auckland, New Zealand. *Quaternary Research* 82, 405-419.
Haines, L., Julian, A., Wilcox, M.D. 2007. Vegetation patterns. *In*: Wilcox, M.D. (editor), Natural History of Rangitoto Island. Auckland Botanical Society, Epsom, Auckland, pp. 41-58.
Hayward, B.W. 2008. Ash Hill volcano, Wiri. *Geocene (Auckland GeoClub Magazine)* 3, 8-9.
Hayward, B.W. 2012. Rangitoto branching lava lobes. *Geocene (Auckland GeoClub Magazine)* 7, 11-12.
Hayward, B.W. 2017. Eruption sequence of Rangitoto volcano, Auckland. *Geoscience Society of New Zealand Newsletter* 23, 4-10.
Hayward, B.W., Grenfell, H. 2013. Did Rangitoto erupt many times? *Geoscience Society of New Zealand Newsletter* 11, 5-8.
Hayward, B.W., Murdoch, G., Maitland, G. 2011a. Volcanoes of Auckland: the Essential Guide. Auckland University Press, 234 pp.
Hayward, B.W., Kenny, J.A., Grenfell, H.R. 2011b. More volcanoes recognised in Auckland Volcanic Field. *Geoscience Society of New Zealand Newsletter* 5, 11-16.
Hayward, B.W., Hopkins, J.L., Smid, E.R. 2016. Mangere Lagoon predated Mangere Mt. *Geocene (Auckland GeoClub Magazine)* 14, 4-5.
Hayward, B.W., Jamieson, A., Morley, M.S. 2017. Out of the Ocean, Into the Fire. History of the Rocks, Fossils and Landforms of Auckland, Northland, and Coromandel. *Geoscience Society of New Zealand Miscellaneous Publication* 146, 336 pp.
Hewitt, A.E. 2010. New Zealand Soil Classification, 3rd edition. *Landcare Research Science Series* 1, 1-136.
Heyng, A.M., Mayr, C., Lücke, A., Wissel, H., Striewski, B. 2014. Late Holocene hydrologic changes in northern New Zealand inferred from stable isotope values of aquatic cellulose in sediments from Lake Pupuke. *Journal of Paleolimnology* 51, 485-497.

Higham, T.F.G., Hogg, A.G. 1997. Evidence for late Polynesian colonisation of New Zealand: University of Waikato radiocarbon measurements. *Radiocarbon* 39, 149-192.
Higham, T.F.G., Anderson, A.J., Jacomb, C. 1999. Dating the first New Zealanders: the chronology of Wairau Bar. *Antiquity* 73, 420-427.
Hogg, A.G., Higham, T.F.G., Lowe, D.J., Palmer, J., Reimer, P., Newnham, R.M. 2003. A wiggle-match date for Polynesian settlement of New Zealand. *Antiquity* 77, 116-125.
Hogg, A.G., Lowe, D.J., Palmer, J.G., Boswijk, G., Bronk Ramsey, C.J. 2012. Revised calendar date for the Taupo eruption derived by ^{14}C wiggle-matching using a New Zealand kauri ^{14}C calibration data set. *The Holocene* 22, 439-449.
Homer, L., Moore, P., Kermode, L. 2000. Lava and Strata: a Guide to the Volcanoes and Rock Formations of Auckland. Landscape Publications with Institute of Geological and Nuclear Sciences, Wellington, 96 pp.
Hopkins, J., Millet, M.A., Timm, C., Wilson, C.J.N., Leonard, G.S., Palin, M.J., Neil, H. 2015. Tools and techniques for developing tephra stratigraphies in lake cores: a case study from the basaltic Auckland Volcanic Field, New Zealand**.** *Quaternary Science Reviews* 123, 58-75.
Hopkins, J.L., Wilson, C.J.N., Millet, M-A., Leonard, G.S., Timm, C., McGee, L.E., Smith, I.E.M., Smith, E.G.C. 2017. Multi-criteria correlation of tephra deposits to source centres applied in the Auckland Volcanic Field. New Zealand. *Bulletin of Volcanology* 79, 55.
Horrocks, M., Deng, Y., Ogden, J., Alloway, B.V., Nichol, S., Sutton, D.G. 2001. High spatial resolution of pollen and charcoal in relation to the c. 600 year BP Kaharoa Tephra: implications for Polynesian settlement of Great Barrier Island New Zealand. *Journal of Archaeological Science* 28, 153-168.
Horrocks, M., Deng, Y., Nichol, S.L., Shane, P.A., Ogden, J. 2002. A palaeo-environmental record of natural and human change from the Auckland Isthmus, New Zealand, during the Late Holocene. *Journal of the Royal Society of New Zealand* 32, 337-353.
Horrocks, M., Augustinus, P.C., Deng, Y., Shane, P., Andersson, S. 2005. Holocene vegetation, environment and tephra recorded from Lake Pupuke, Auckland, New Zealand. *New Zealand Journal of Geology and Geophysics* 48, 85-94.
Huang, Y.M., Hawkesworth, C., van Calsteren, P., Smith, I.E.M., Black, P. 1997. Melt generation models for the Auckland volcanic field, New Zealand: constraints from U-Th isotopes. *Earth and Planetary Science Letters* 149, 67-84.
Irvine, T.N., Baragar, W.R.A. 1971. A guide to the chemical classification of the common volcanic rocks. *Canadian Journal of Earth Sciences* 8, 523-548.
Jacomb, A., Holdaway, R.N., Allentoft, M.E., Bunce, M., Oskam, C.L., Walter, R., Brooks, E. 2014. High-precision dating and ancient DNA profiling of moa (Aves: Dinornithiformes) eggshell documents a complex feature at Wairau Bar and refines the chronology of New Zealand settlement by Polynesians. *Journal of Archaeological Science* 50, 24-30.
Kawabata, E., Cronin, S., Bebbington, M., Moufti, M., El-Masry, N., Wang, T. 2015. Identifying multiple eruption phases from a compound tephra blanket: an example of the AD1256 Al-Madinah eruption, Saudi Arabia. *Bulletin of Volcanology* 77, 6.
Kereszturi, G., Németh, K., Cronin, S.J., Agustín-Flores, J., Smith, I.E.M., Lindsay, J. 2013. A model for calculating eruptive volumes for monogenetic volcanoes – implication for the Quaternary Auckland Volcanic field, New Zealand. *Journal of Volcanology and Geothermal Research* 266, 16-33.
Kereszturi, G., Németh, K., Cronin, S.J., Procter, J., Agustín-Flores, J. 2014. Influences on the variability of eruption sequences and style transitions in the Auckland Volcanic Field, New Zealand. *Journal of Volcanology and Geothermal Research* 286, 101–115
Kermode, L. 1992. Geology of the Auckland urban area. Scale 1: 50,000. Institute of Geological and Nuclear Sciences Geological Map 2. 1 sheet + 63 pp. Institute of Geological and Nuclear Sciences, Lower Hutt.
Le Maitre, R.W. 2002, Igneous Rocks: a Classification and Glossary of Terms. Cambridge University Press, Cambridge, 236 pp.
Leonard, G.S., Calvert, A.T., Hopkins, J.L., Wilson, C.J.N., Smid, E.R., Lindsay, J.M., Champion, D.E. 2017. High-precision $^{40}Ar/^{39}Ar$ dating of Quaternary basalts from Auckland Volcanic Field, New Zealand, with implications for eruption rates and paleomagnetic correlations. *Journal of Volcanology and Geothermal Research* 343, 60-74.
Lindsay, J.M. 2010. Volcanoes in the big smoke: a review of hazard and risk in the Auckland Volcanic Field. *In*: Williams, A.L., Pinches, G.M., Chin, C.Y. McMorran, T.J., Massey, C.I. (editors). Geologically Active. 11th Congress of the International Association for Engineering Geology and the Environment (IAEG). Taylor & Francis, London.
Lindsay, J.M., Needham, A.J., Smith, I.E.M. 2010. Rangitoto re-visited: new insights to an old friend. GeoNZ Conference 2010 – pre-conference field trip 3, The University of Auckland. *Geoscience Society of New Zealand Miscellaneous Publication* 129B, 8 pp.

Lindsay, J.M., Leonard, G.S., Smid, E.R., Hayward, B.W. 2011. Ages of the Auckland Volcanic Field: a review of existing data. *New Zealand Journal of Geology and Geophysics* 54, 379-401.

Linnell, T., Shane, P., Smith, I., Augustinus, P., Cronin, S., Lindsay, J., Maas, R. 2016. Long-lived shield volcanism within a monogenetic basaltic field: the conundrum of Rangitoto volcano, New Zealand. *Geological Society of America Bulletin* 128, 1160-1172.

Lowe, D.J. 2011. Tephrochronology and its application: a review. *Quaternary Geochronology* 6, 107-153.

Lowe, D.J., Pittari, A. 2014. An ashy septingentenarian: the Kaharoa tephra turns 700 (with notes on its volcanological, archaeological, and historical importance). *Geoscience Society of New Zealand Newsletter* 13, 35-46.

Lowe, D.J., Newnham, R.M., McFadgen, B.G., Higham, T.F.G. 2000. Tephras and New Zealand archaeology. *Journal of Archaeological Science* 27, 859-870.

Lowe, D.J., Newnham, R.M., McCraw, J.D. 2002. Volcanism and early Māori society in New Zealand. *In*: Torrence, R., Grattan, J. (editors) *Natural Disasters and Cultural Change*. Routledge, London, pp. 126-161.

Lowe, D.J., Blaauw, M., Hogg, A.G., Newnham, R.M. 2013. Ages of 24 widespread tephras erupted since 30,000 years ago in New Zealand, with re-evaluation of the timing and palaeoclimatic implications of the late-glacial cool episode recorded at Kaipo bog. *Quaternary Science Reviews* 74, 170-194.

Lowe, D.J., Shane, P.A.R., de Lange, P.J., Clarkson, B.D. 2016. Guidebook for Rangitoto Island AQUA field trip, Auckland, 2016. School of Science, University of Waikato, in association with the Australasian Quaternary Association (AQUA) Biennial Conference, Auckland, New Zealand, 5-9 December, 35 pp.

Lowe, D.J., Pearce, N.J.G., Jorgensen, M.A., Kuehn, S.C., Tryon, C.A., Hayward, C.L. 2017. Correlating tephras and cryptotephras using glass compositional analyses and numerical and statistical methods: review and evaluation. *Quaternary Science Reviews* 175, 1-44.

McGee, L.E., Smith, I.E.M. 2016. Interpreting chemical compositions of small scale basaltic systems: a review. *Journal of Volcanology and Geothermal Research* 325, 45-60.

McGee, L.E., Beier, C., Smith, I.E.M., Turner, S.P. 2011. Dynamics of melting beneath a small-scale basaltic system: a U-Th-Ra study from Rangitoto Volcano, Auckland Volcanic Field, New Zealand. *Contributions to Mineralogy and Petrology* 162, 547-563.

McGee, L.E., Smith, I.E.M., Millet, M.-A., Handley, H.K., Lindsay, J.M. 2013. Asthenospheric control of melting processes in a monogenetic basaltic system: a case study of the Auckland volcanic field, New Zea-land. *Journal of Petrology* 54, 2125-2153.

McGlone, M.S., Wilmshurst J.M. 1999. Dating initial Maori environmental impact in New Zealand. *Quaternary International* 59, 5-16.

McWethy, D.B., Whitlock, C., Wilmshurst, J.M., McGlone, M.S., Fromont, M., Li, X., Dieffenbacher-Krall, A., Hobbs, W.O., Fritz, S.C., Cook, E.R. 2010. Rapid landscape transformation in South Island, New Zealand, following initial Polynesian settlement. *Proceedings of the National Academy of Sciences (USA)* 107, 21343-21348.

Merrill, A. 1994. An investigation of the hydrological balance of Rangitoto Island. Unpublished MSc thesis, University of Auckland.

Molloy, C.M. 2008. Tephrostratigraphy of the Auckland maar craters. Unpublished MSc thesis, University of Auckland, Auckland.

Molloy, C., Shane, P., Augustinus, P. 2009. Eruption recurrence rates in a basaltic volcanic field based on tephra layers in maar sediments: implications for hazards in the Auckland volcanic field. *Geological Society of America Bulletin* 121, 1666-1677.

Murdoch, G. (compiler) 1991. He Korero Ta Whito Mo Rangitoto – a brief outline of the Māori historical associations with Rangitoto Island. Unpublished paper, 14 pp.

Needham, A.J., Lindsay, J.M., Smith, I.E.M., Augustinus, P., Shane, P.A. 2011. Sequential eruption of alkaline and sub-alkaline magmas from a small monogenetic volcano in the Auckland Volcanic Field, New Zealand. *Journal of Volcanology and Geothermal Research* 201, 126-142.

Newnham, R.M., Lowe, D.J. 1991. Holocene vegetation and volcanic activity, Auckland Isthmus, New Zealand. *Journal of Quaternary Science* 6, 177-193.

Newnham, R.M., Lowe, D.J., McGlone, M.S., Wilmshurst, J.M., Higham, T.F.G. 1998a. The Kaharoa Tephra as a critical datum for earliest human impact in northern New Zealand. *Journal of Archaeological Science* 25, 533-544.

Newnham, R.M., Lowe, D.J., Matthews, B.W. 1998b. A late Holocene and prehistoric record of environmental change from Lake Waikaremoana, New Zealand. The *Holocene* 8, 443-454.

Newnham, R.M., Lowe, D.J., Alloway, B.V. 1999. Volcanic hazards in Auckland, New Zealand: a preliminary assessment of the threat posed by central North Island silicic volcanism based on the Quaternary tephrostratigraphical record. *Geological Society (London) Special Publication* 161, 27-45.

Newnham, R.M., Lowe, D.J., Giles, T.M., Alloway, B.V. 2007. Vegetation and climate of Auckland, New Zealand, since ca. 32 000 cal. yr ago: support for an extended LGM. *Journal of Quaternary Science* 22, 517-534.

Newnham, R.M., Lowe, D.J., Gehrels, M.J., Augustinus, P.C. 2017. Two-step human-environmental impact history for Auckland, northern New Zealand, linked to late Holocene climate change. Abstracts, Geoscience Society of New Zealand Annual Conference (28 November-1 December). *Geoscience Society of New Zealand Miscellaneous Publication* 147A*,* 1 p.

Nichol, R. 1981. Preliminary report on excavations at the Sunde site, N38/24, Motutapu Island. *New Zealand Archaeological Association Newsletter* 24**,** 237-256.

Nichol, R. 1982. Fossilised human footprints in Rangitoto Ash on Motutapu Island. *Geological Society of New Zealand Newsletter* 51**,** 11-13.

Nichol, R. 1992. The eruption history of Rangitoto: reappraisal of a small New Zealand myth. *Journal of the Royal Society of New Zealand* 22, 159-180.

Nilsson, A., Muscheler, R., Snowball, I., Aldahan, A., Possnert, G., Augustinus, P., Atkin, D., Stephens, T. 2011. Multi-proxy identification of the Laschamp geomagnetic field excursion in Lake Pupuke, New Zealand. *Earth and Planetary Science Letters* 311*,* 155-164.

Perry, G.L.W., Wilmshurst, J.M., McGlone, M.S., McWethy, D.B., Whitlock, C. 2012. Explaining fire-driven landscape transformation during the Initial Burning Period of New Zealand's prehistory. *Global Change Biology* 18, 1609-1621.

Perry, G.L.W., Wilmshurst, J.M., McGlone, M.S. 2014. Ecology and long-term history of fire in New Zealand. *New Zealand Journal of Ecology* 38, 157-176.

Potter, S.H., Jolly, G.E., Neall, V.E., Johnston, D.M., Scott B.J. 2014. Communicating the status of volcanic activity: revising New Zealand's volcanic alert level system. *Journal of Applied Volcanology* 3, 1-16.

Robertson, D.J. 1986. A paleomagnetic study of Rangitoto Island, Auckland, New Zealand. *New Zealand Journal of Geology and Geophysics* 29, 405-411.

Rodgers, K.A., Chisolm, J.E., Davis, R.J., Nelson, C.S. 1977. Motukoreaite, a new hydrated carbonate, sulphate, and hydroxide of Mg and Al from Auckland, New Zealand. *Mineralogical Magazine* 41, 389-390.

Ryan, P.M. 2012. The Raupō Dictionary of Modern Māori, 4th edition. Penguin, North Shore, 811 pp.

Sahetapy-Engel, S., Self, S., Carey, R.J., Nairn, I.A. 2014. Deposition and generation of multiple widespread fall units from the *c*. AD 1314 Kaharoa rhyolitic eruption, Tarawera, New Zealand. *Bulletin of Volcanology* 76, 836.

Sandiford, A., Alloway, B., Shane, P. 2001. A 28,000-6600 cal yr record of local and distal volcanism preserved in a paleolake, Auckland, New Zealand. *New Zealand Journal of Geology and Geophysics* 44, 323-336.

Scott, S.D. 1970. Excavations at the "Sunde site", N38/24, Motutapu Island, New Zealand. *Records of the Auckland Institute and Museum* 7, 13-30.

Shane, P. 2005. Towards a comprehensive distal andesitic tephrostratigraphic framework for New Zealand based on eruptions from Egmont volcano. *Journal of Quaternary Science* 20, 45-57.

Shane, P.A.R., Hoverd, J. 2002. Distal record of multi-sourced tephra in Onepoto Basin, Auckland, New Zealand: implications for volcanic chronology, frequency and hazards. *Bulletin of Volcanology* 64, 441-454.

Shane, P.A.R., Linnell, T. 2015. Earthquake Commission University Post-Graduate Research Programme: Reconstructing Rangitoto volcano from a 150-m-deep drill core (project 14/U684). Final report, University of Auckland, 12 pp.

Shane, P.A.R., Smith, I.E.M.2000. Geochemical fingerprinting of basaltic tephra deposits in the Auckland Volcanic Field. *New Zealand Journal of Geology and Geophysics* 43, 569-577.

Shane, P.A.R., Zawalna-Geer, A. 2011. Correlation of basaltic tephra from Mt Wellington volcano: implications for the penultimate eruption from the Auckland Volcanic Field. *Quaternary International* 246, 374-381.

Shane, P., Gehrels, M., Zawalna-Geer, A., Augustinus, P., Lindsay, J., Chaillou, I. 2013. Longevity of a small shield volcano revealed by crypto-tephra studies (Rangitoto Volcano, New Zealand): change in eruptive behaviour of a basaltic field. *Journal of Volcanology and Geothermal Research* 257,174-183.

Shibuya, H., Cassidy, J., Smith, I.E.M., Itaya, T. 1992. A geomagnetic excursion in the Brunhes epoch recorded in New Zealand basalts. *Earth and Planetary Science Letters* 111, 41-48.

Smith, R.T., Lowe, D.J., Wright, I.C. 2006. Volcanoes. *Te Ara − The Encyclopedia of New Zealand* [Online]. Updated 16 April, 2007. New Zealand Ministry for Culture and Heritage, Wellington. URL: http://www.TeAra.govt.nz/EarthSeaAndSky/NaturalHazardsAndDisasters/Volcanoes/en

Smith, I.E.M., Lindsay, J.M., Nemeth, K. 2012. Intra-conference field guide: Rangitoto, Auckland's newest volcano. *Gesocience Society of New Zealand Miscellaneous Publication* 131D, 27-34.

Soil Survey Staff 2014. Keys to Soil Taxonomy, 12th edition. USDA Natural Resources Conservation Service, 362 pp.
Stephens, T., Atkin, D., Augustinus, P., Shane, P., Lorrey, A., Street-Perrott, A., Nilsson, A., Snowball, I. 2012a. A late glacial Antarctic climate teleconnection and variable Holocene seasonality at Lake Pupuke, Auckland, New Zealand. *Journal of Paleolimnology* 48, 785-800.
Stephens, T., Atkin, D., Cochran, U., Augustinus, P., Reid, M., Lorrey, A., Shane, P., Street-Perrott, A., 2012b. A diatom-inferred record of reduced effective precipitation during the Last Glacial Coldest Phase (28.8–18.0 cal kyr BP) and increasing Holocene seasonality at Lake Pupuke, Auckland, New Zealand. *Journal of Paleolimnology* 48, 801-817.
Stevenson, C.M., Sheppard, P.J., Sutton, D.G. 1996. Advances in the hydration dating of New Zealand obsidian. *Journal of Archaeological Science* 23, 233-242.
Stracke, A., Bizimis, M., Salters, V.J.M. 2003. Recycling oceanic crust: quantitative constraints. *Geochemistry Geophysics Geosystems* 4(3), 8003, doi: 10.1029/2001GC000223.
Stracke, A., Hofmann, A.W., Hart, S.R. 2005. FOZO, HIMU and the rest of the mantle zoo. *Geochemistry Geophysics Geosystems* 6(5), Q05007, doi: 10.1029 /2004GC000824.
Striewski, B., Mayr, C., Flenley, J., Naumann, R., Turner, G., Lücke, A. 2009. Multiproxy evidence of late-Holocene human-induced environmental changes at Lake Pupuke, Auckland (New Zealand). *Quaternary International* 202, 69-83.
Striewski, B., Shulmeister, J., Augustinus, P.C., Soderholm, J. 2013. Late Holocene climate variability from Lake Pupuke maar, Auckland, New Zealand. *Quaternary Science Reviews* 77, 46-54.
Sun, S.S., McDonough, W.F.1989. Chemical and isotopic systematics of oceanic basalts: implications for mantle composition and processes. *Geological Society (London) Special Publication* 42, 313-345.
Sutton, D.G. 1987. A paradigmatic shift in Polynesian prehistory: implications for New Zealand. *New Zealand Journal of Archaeology* 9, 135-155.
Tomsen, E., Lindsay, J., Gahegan, M., Wilson, T., Blake, D. 2014. Auckland Volcanic Field evacuation planning: a spatio-temporal approach for emergency management and transportation network decisions. *Journal of Applied Volcanology* 3, 1-22.
Walker, G.P.L. 1993. Basaltic-volcano systems. *Geological Society (London) Special Publication* 76, 3-38.
Walker, L.R., Wardle, D.A., Bardgett, R.D., Clarkson, B.D. 2010. The use of chronosequences in studies of ecological succession and soil development. *Journal of Ecology* 98, 725-736.
Wilcox, M.D. (editor*)* 2007a. Natural History of Rangitoto Island. Auckland Botanical Society, Epsom, Auckland, 192 pp.
Wilcox, M.D. 2007b. Introduction. *In*: Wilcox, M.D. (editor), Natural History of Rangitoto Island. Auckland Botanical Society, Epsom, Auckland, pp. 10-22.
Wilcox, M.D., Haines, L., Young, M.E., Brown, P.M., Gardner, R.O. 2007. List of vascular plants. *In*: Wilcox, M.D. (editor), Natural History of Rangitoto Island. Auckland Botanical Society, Epsom, Auckland, pp. 101-118.
Wilmshurst, J.M., Higham T.F.G. 2004. Using rat-gnawed seeds to independently date the arrival of Pacific rats and humans to New Zealand. *The Holocene* 14, 801-806.
Wilmshurst, J.M., Anderson, A.J., Higham, T.F.G., Worthy, T.H. 2008. Dating the late prehistoric dispersal of Polynesians to New Zealand using the commmensal Pacific rat. *Proceedings of the National Academy of Sciences of the United States* 105, 7676-7680.
Wilmshurst, J.M., Hunt, T.L., Lipo, C.P. Anderson, A.J. 2011. High-precision radiocarbon dating shows recent and rapid initial human colonization of East Polynesia. *Proceedings of the National Academy of the United States of Americ*a 108, 1815-1820.
Wilmshurst, J.M., Moar, N.T., Wood, J.R., Bellingham, P.J., Findlater, A.M., Robinson, J.J., Stone, C. 2014. Use of pollen and ancient DNA as conservation baselines for offshore islands in New Zealand. *Conservation Biology* 28, 202-212.
Zawalna-Geer, A., Lindsay, J., Davies, S.M., Augustinus, P., Davies, S.J. 2016. Extracting a primary Holocene cryptotephra record from Pupuke maar sediments, Auckland, New Zealand. *Journal of Quaternary Science* 31*,* 442-457.